

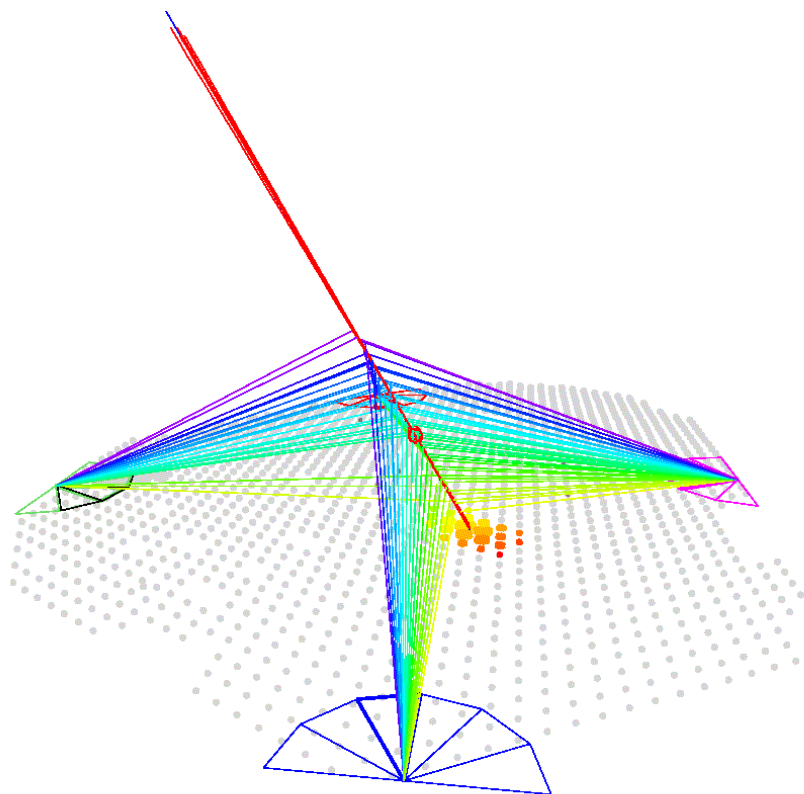
Tecniche di misura con l'Osservatorio Pierre Auger

Lorenzo Perrone

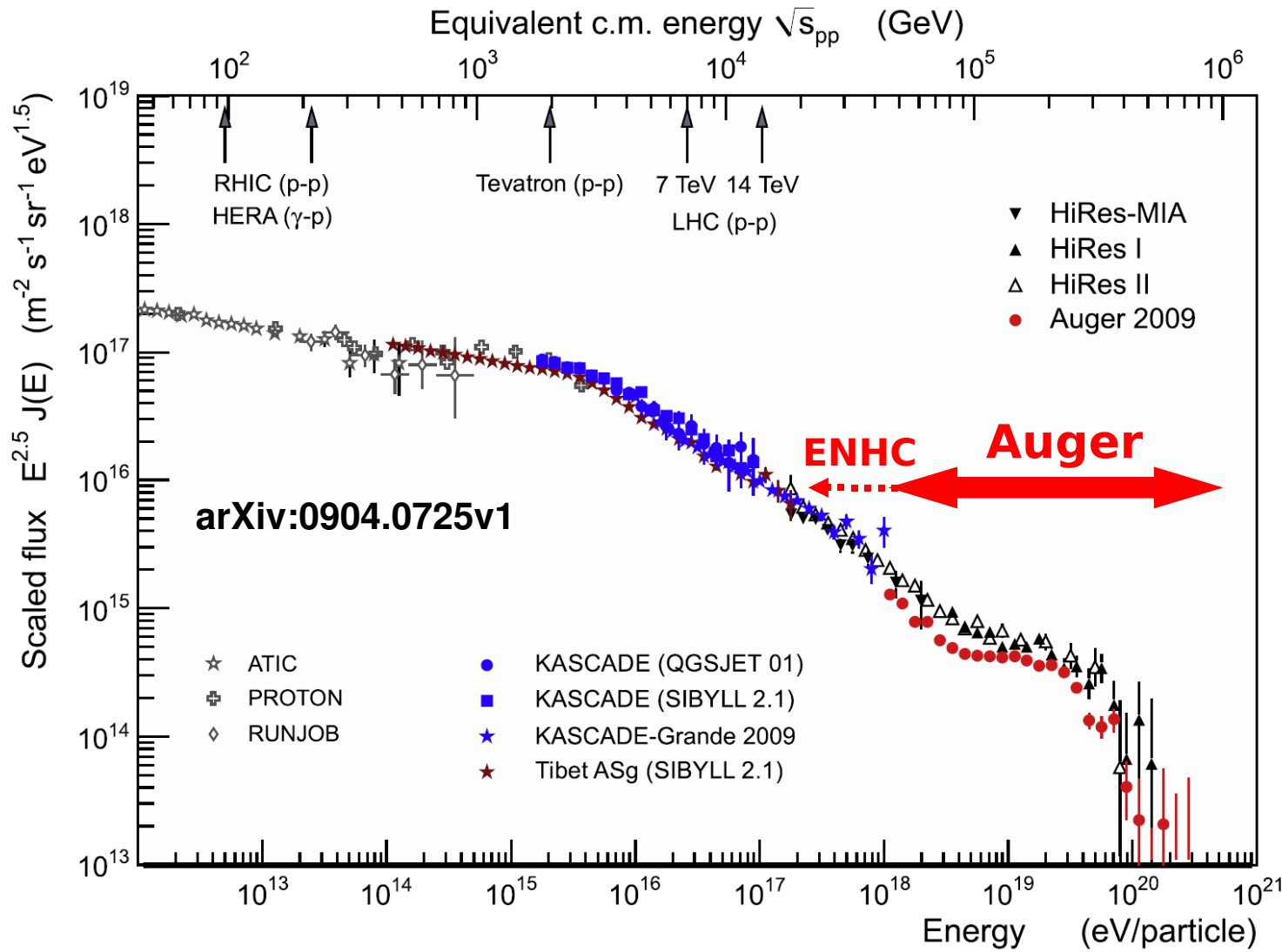
Università del Salento e INFN Lecce (Italy)

Outline

- Physics goals and operation range
- Detector description
- Performance and observables
- Results
- Enhancements



The Pierre Auger Observatory: range of operation



ENHC: Auger low energy extensions

Study of the transition
between galactic and extra-
galactic cosmic rays



The physics case

- Ankle region

- 2nd Knee region (with lower
energies extensions)

End of the spectrum (GZK
region)

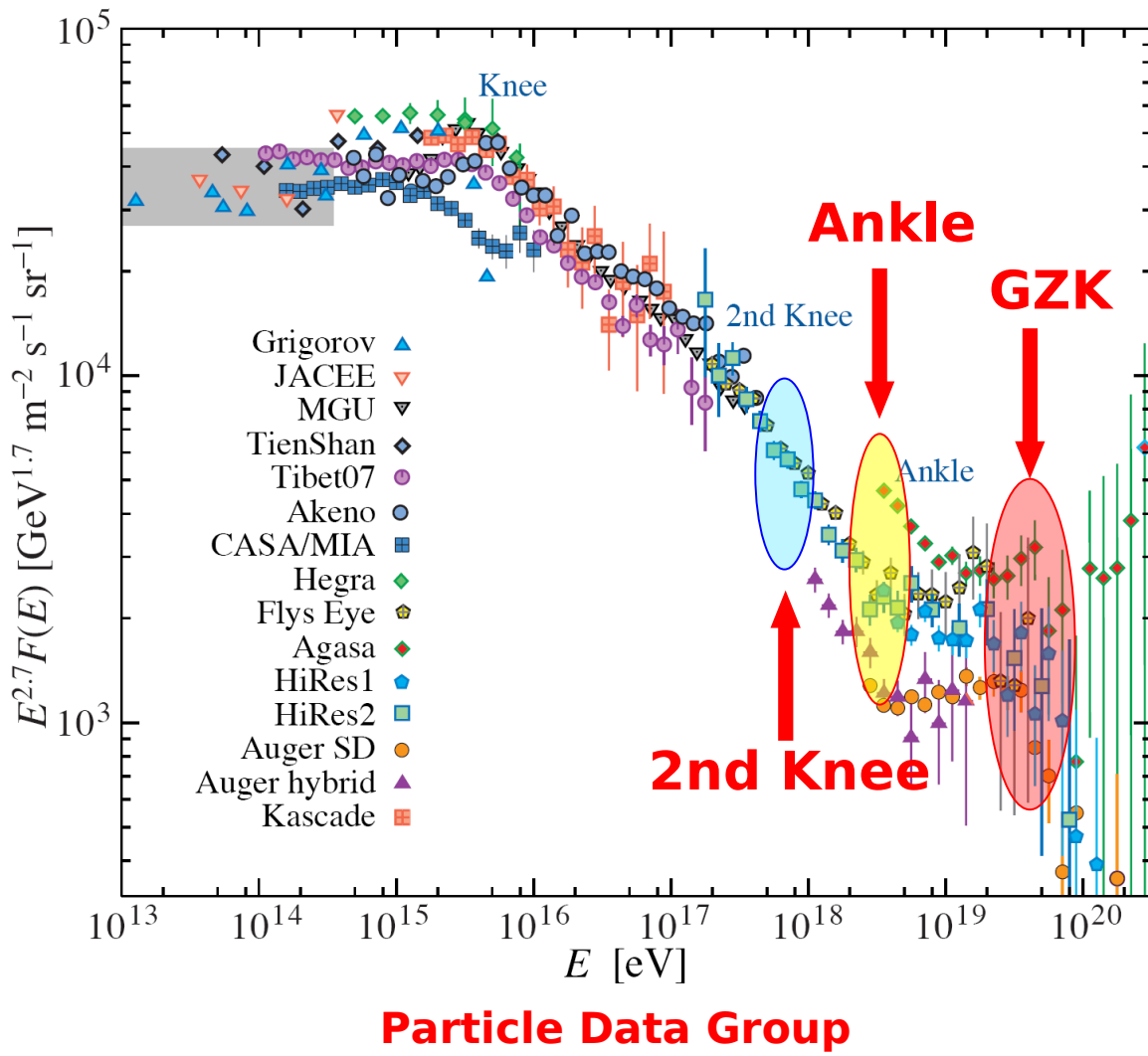
Energy spectrum

Arrival directions

Composition

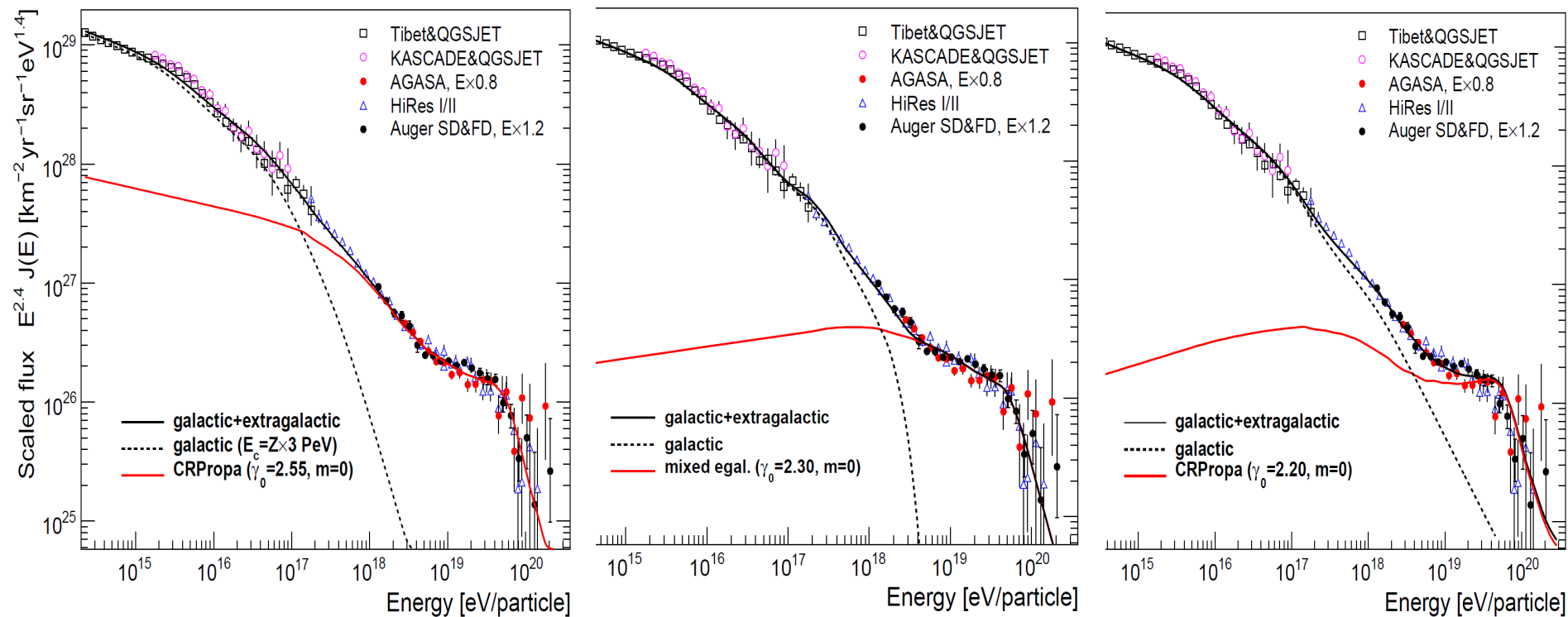
Search for photon and
neutrinos as primary
cosmic rays

Hadronic physics



“the ankle”: models and hypotheses

M.Unger, arXiv:0812.2763 [astro-ph]



$$E_{\text{Gal-ExtraGal}} \sim 10^{17.5} \text{ eV}$$

Dip Model
Extragal. protons
(Berezinsky et al.)

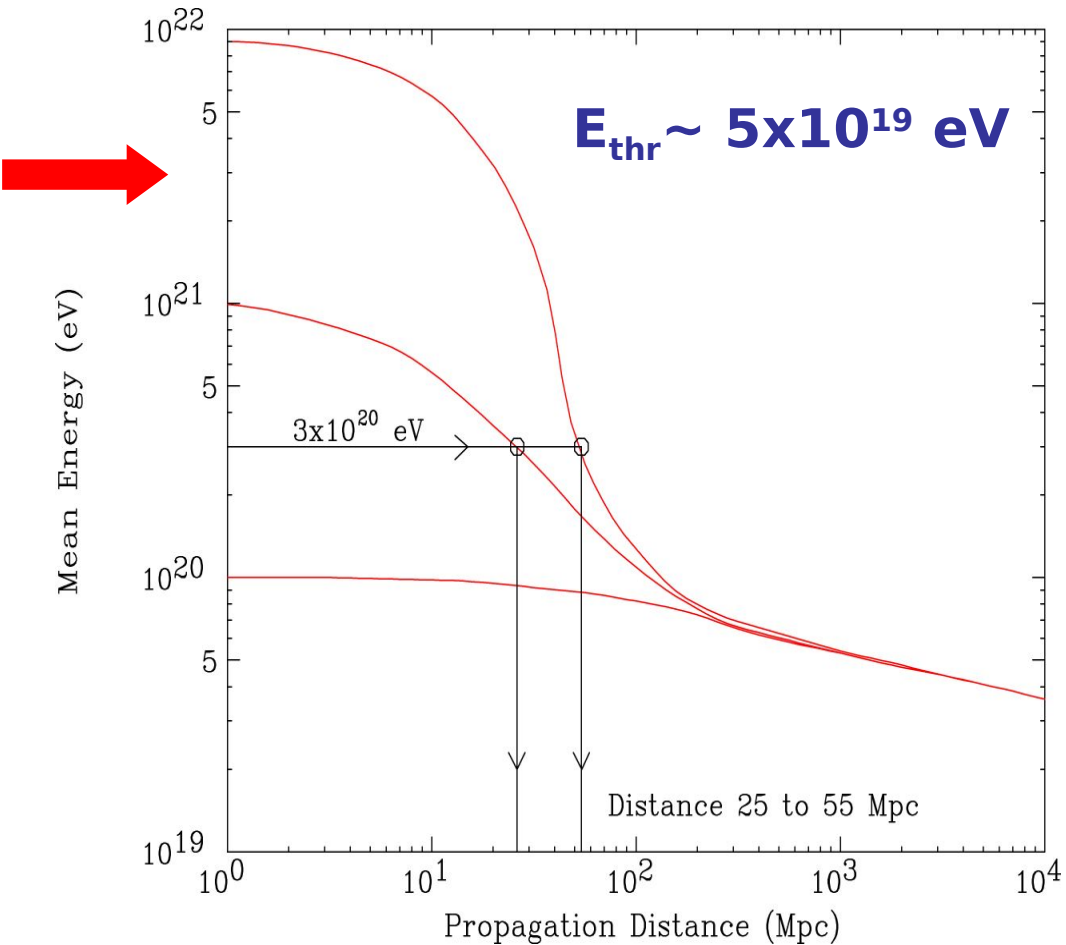
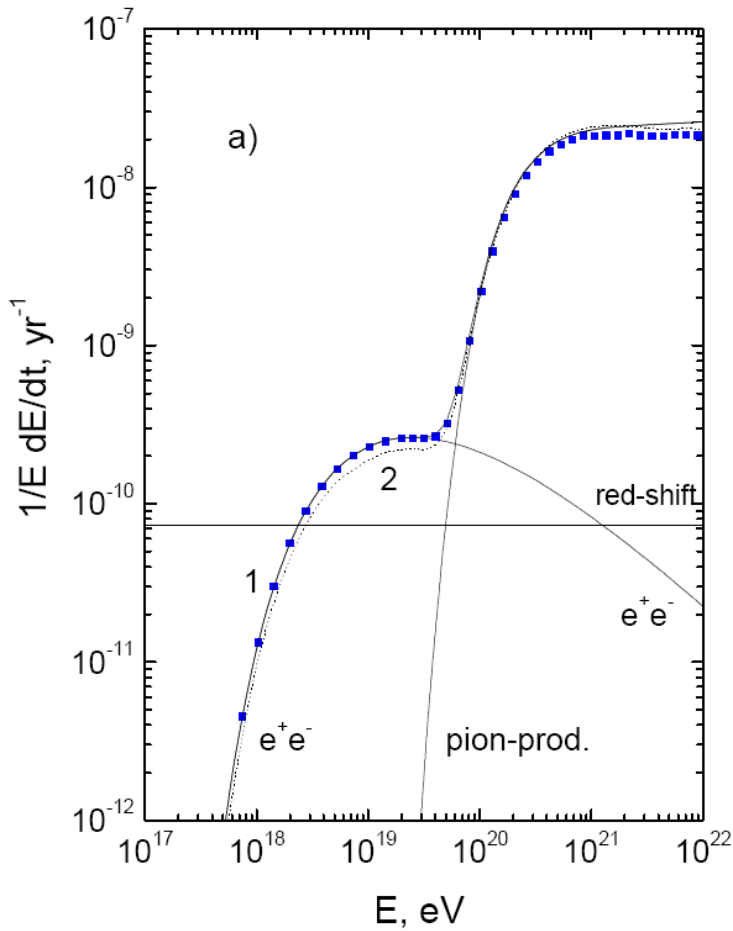
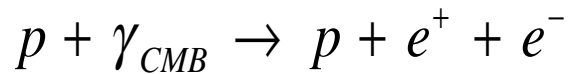
$$E_{\text{Gal-ExtraGal}} \sim 3 \cdot 10^{18} \text{ eV}$$

Mixed comp. of
extragal. component
(Allard et al.)

$$E_{\text{Gal-ExtraGal}} \sim 10^{19} \text{ eV}$$

Extragal. protons
(ankle model)

Propagation of CR: implications

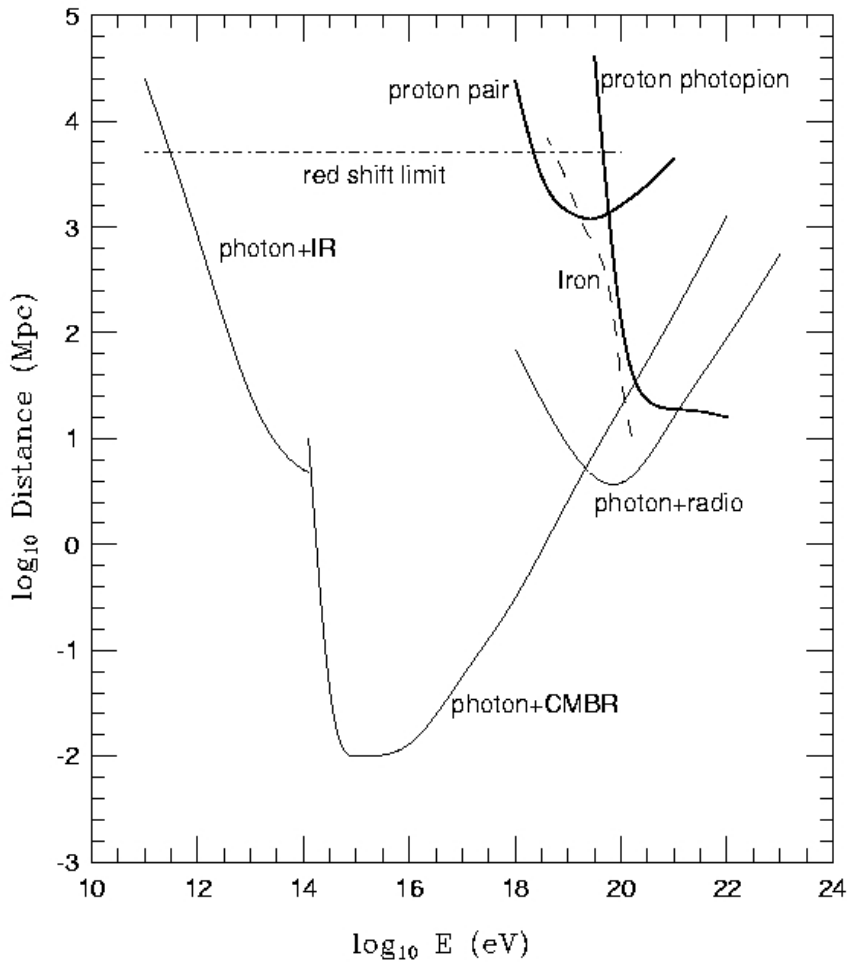


Flux Suppression (GZK cut-off)

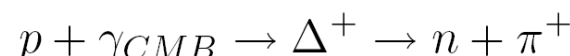
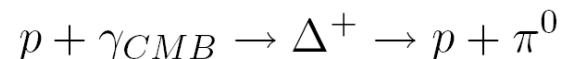
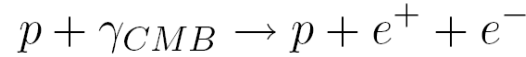
Protons at $E > 10^{20} \text{ eV}$ within 100 Mpc

End to the cosmic ray spectrum?

Greisen Zatsepin Kuz'min effect (1966):
Interaction with the cosmic microwave background (CMB)



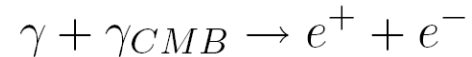
protons:



nuclei: photo-disintegration and pair production on CMB (RB IR)

“horizon” (p and nuclei) ~ 100 Mpc ($\sim 10^{20}$ eV)

photons:



$$E_{thr}(eV) \sim \frac{3 \cdot 10^{14}}{\epsilon_\gamma(eV)}$$

The Pierre Auger Observatory

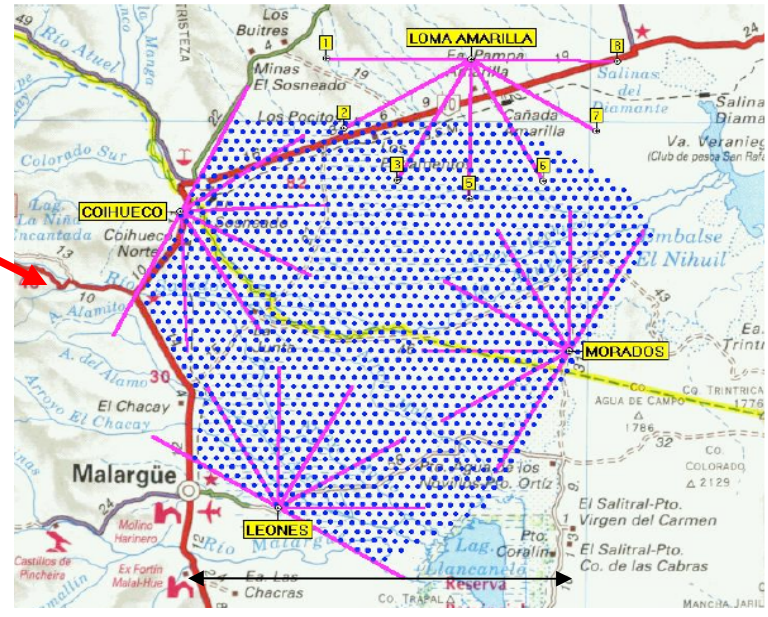
17 Countries, 63 Institutions ~ 350 members



- large and flat region
- low density of population (low background due to artificial light)
- clean and dry atmospheric conditions (small cloud coverage)



Southern hemisphere (3000 km^2)
Malargüe (Mendoza) Argentina



~ 50 km

The Pierre Auger Observatory

- *Surface detector*

an array of 1600 Cherenkov stations on a 1.5 km hexagonal grid ($\sim 3000 \text{ km}^2$)

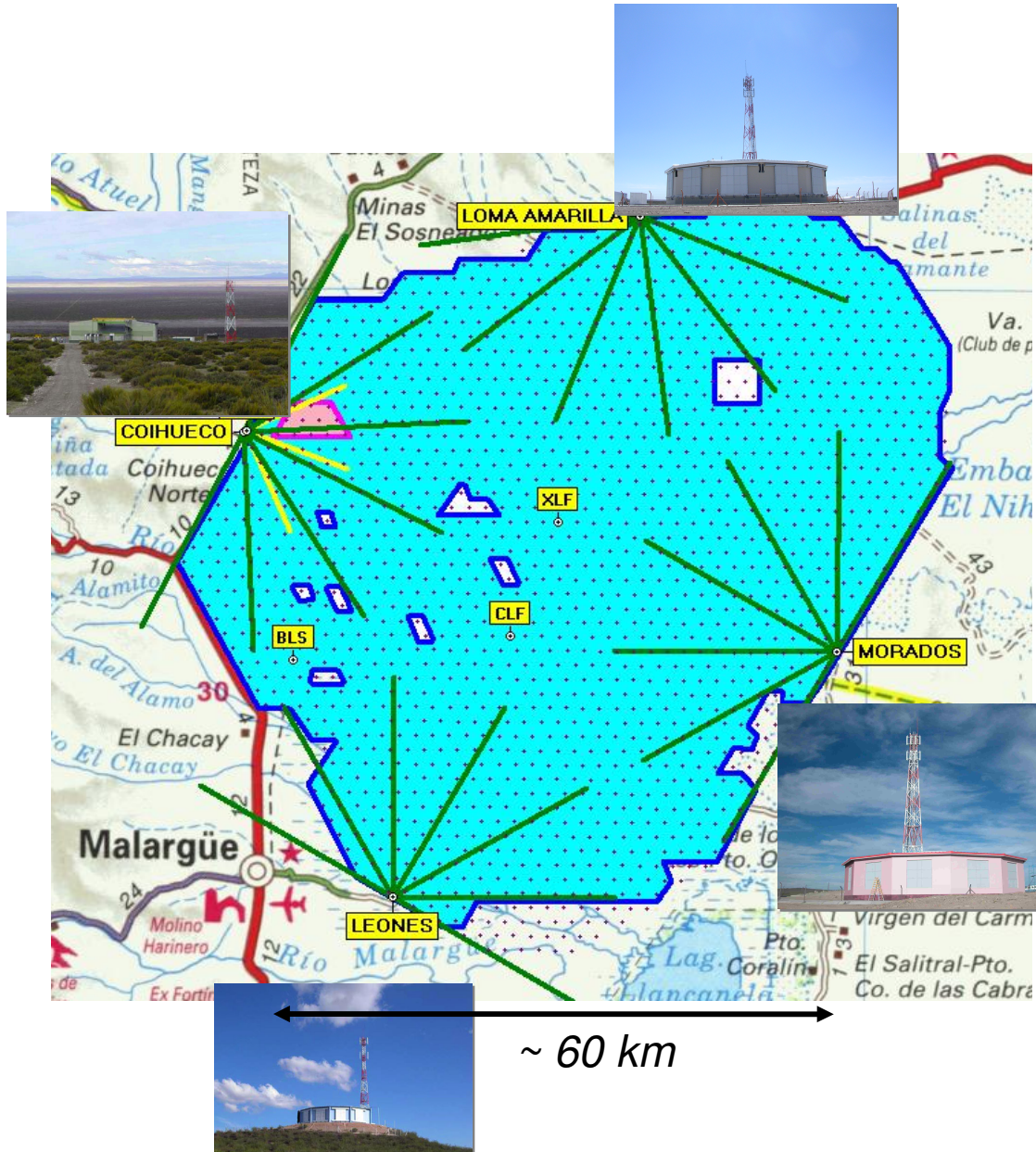
- *Fluorescence detector*

4 buildings overlooking the array

Low energy extensions

AMIGA: dense array plus muon detectors

HEAT: three further high elevation FD telescopes



The Hybrid Concept

Surface Detector Array

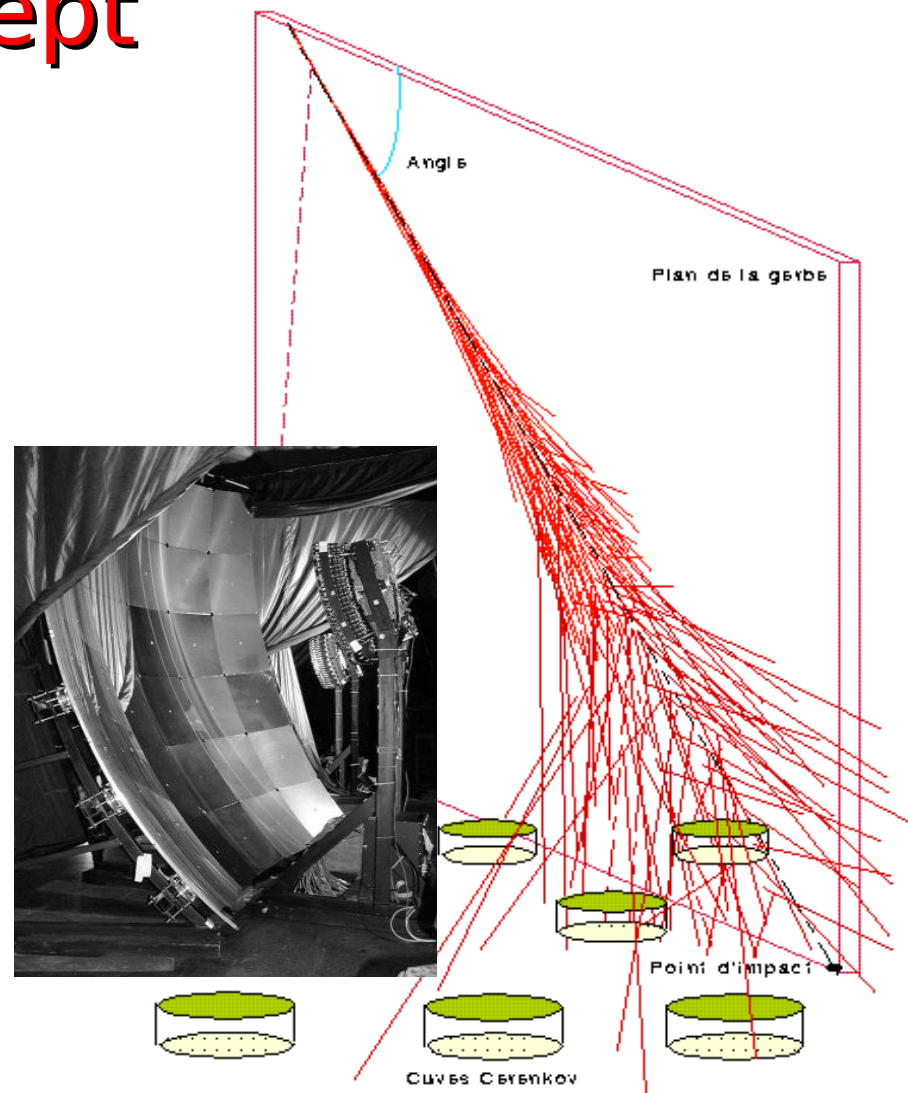
lateral distribution, 100% duty cycle

Air Fluorescence Detectors

Longitudinal profile, calorimetric energy measurement, ~15% duty cycle

accurate energy and direction measurement

mass composition studies in a complementary way

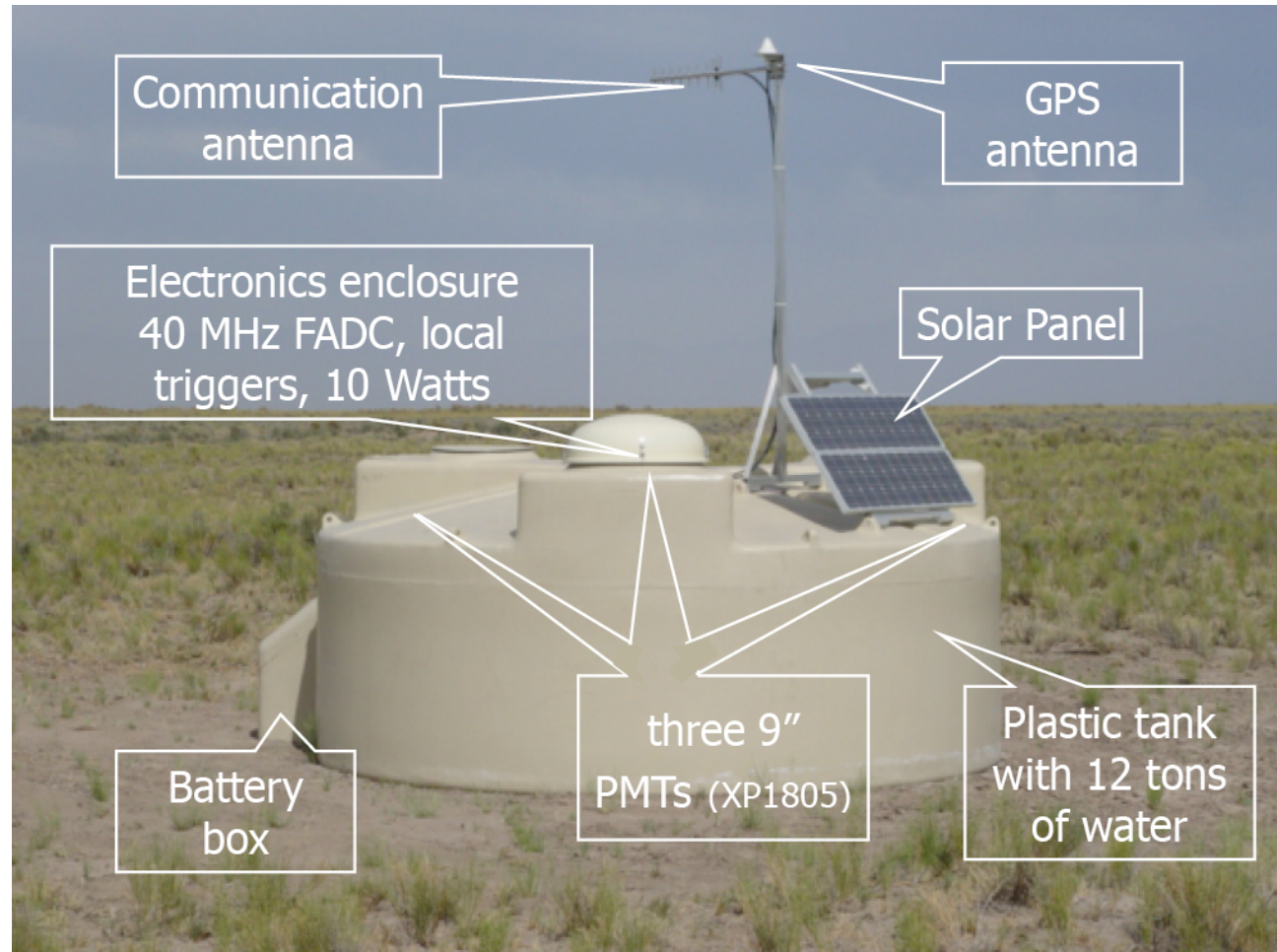


“In order to make further progress, particularly in the field of cosmic rays, it will be necessary to apply all our resources and apparatus simultaneously and side-by-side.”

V.H.Hess, Nobel Lecture, December 1936

A station of the Surface Detector

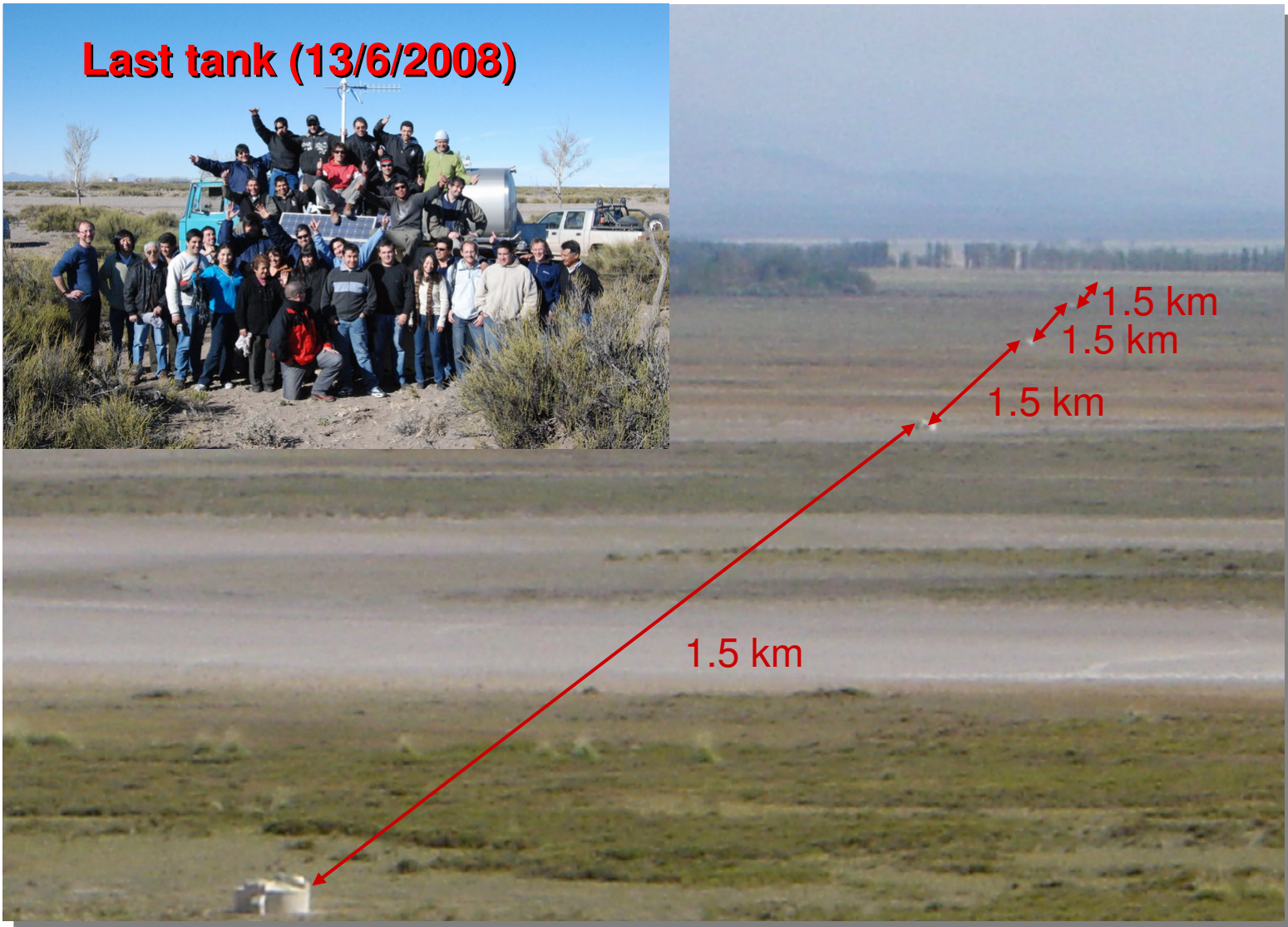
- Plastic Tank
- Ultra-reflective tyvek liner
- 12 m³ purified water
- 3 PMTs (9 inches)
- Independent power supply (solar panels)
- GPS antenna
- Communication antenna



DAQ : 40 MHz FADC sampling (10 bit resolution)

The surface detector (SD)

Last tank (13/6/2008)



Not only muons hit the tank!!!!

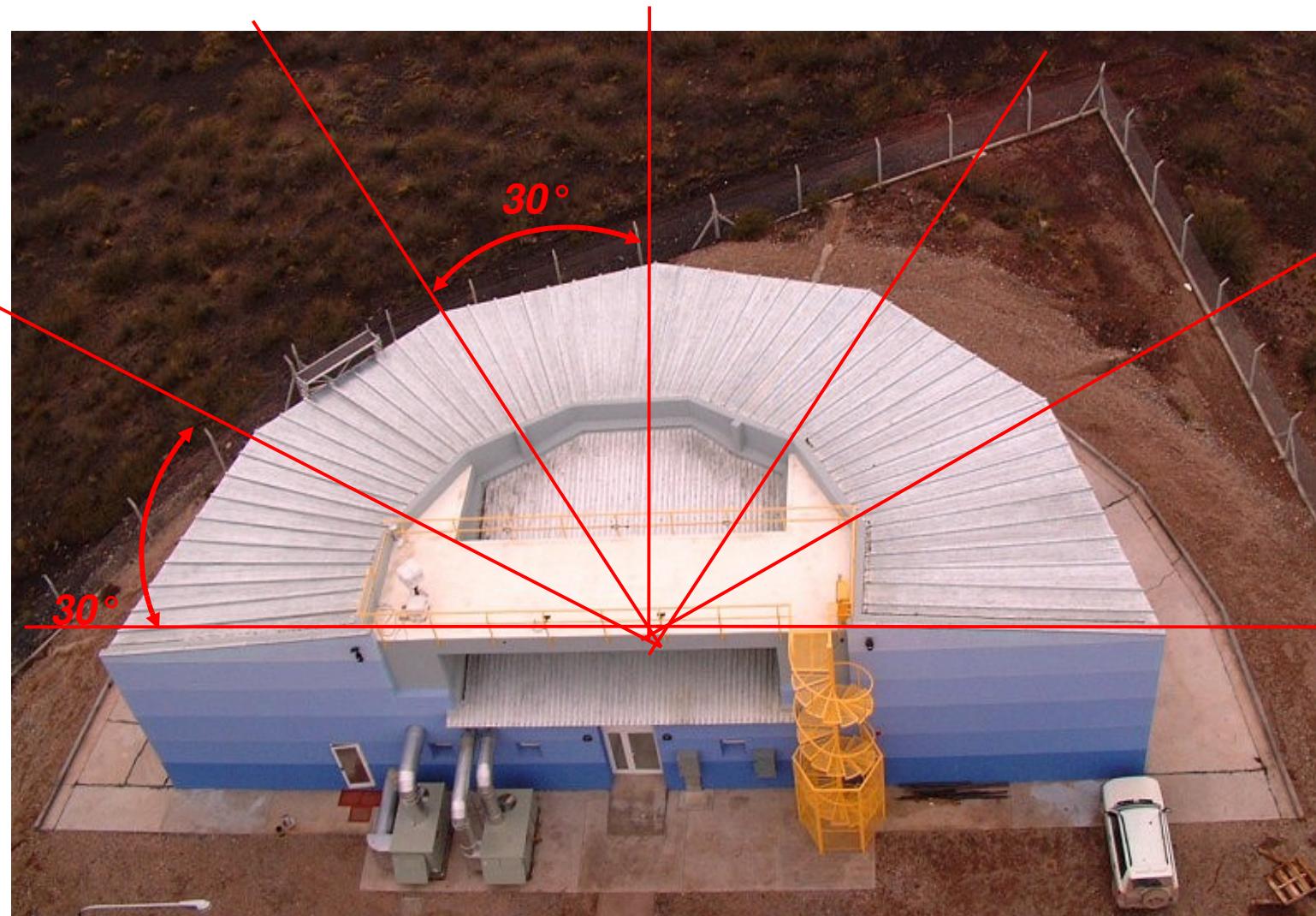


**Bird droppings
together with dry
weather degrade
solar panels.**



**Bird nests behind
solar panels
sometimes catch
fire.**

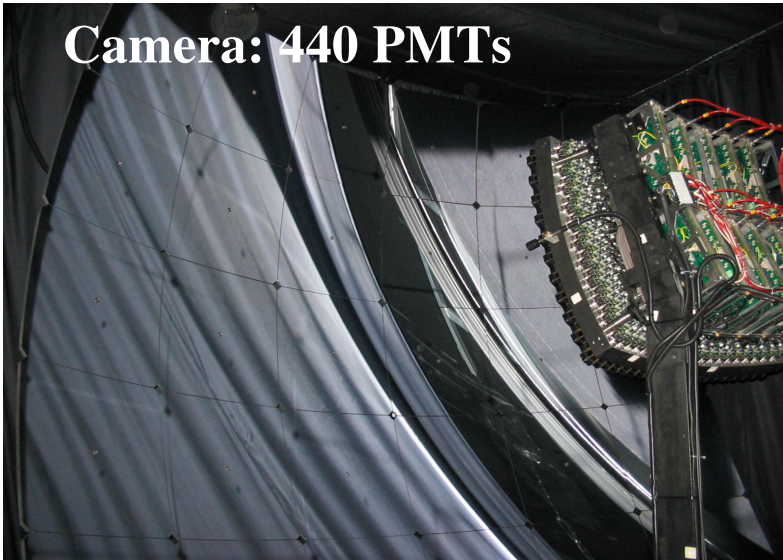
The fluorescence detector (FD)



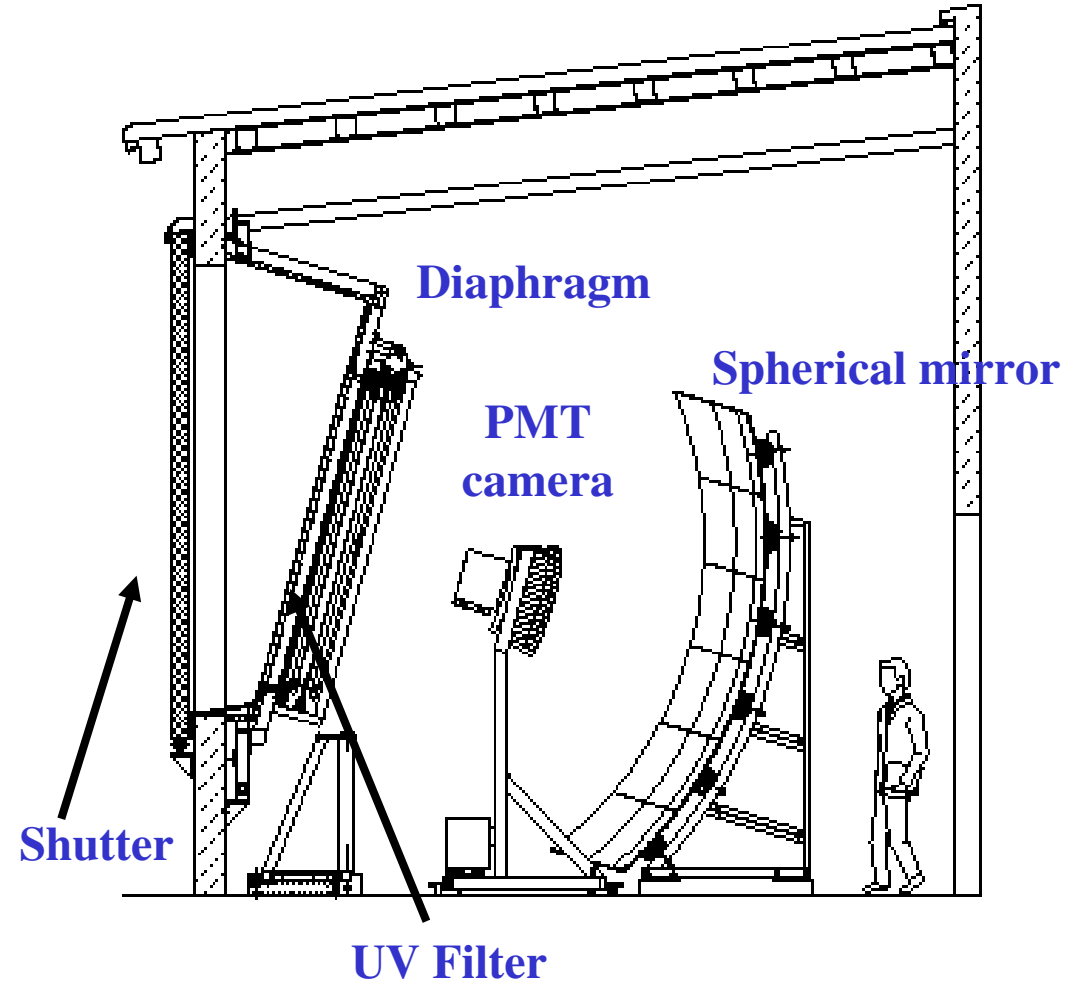
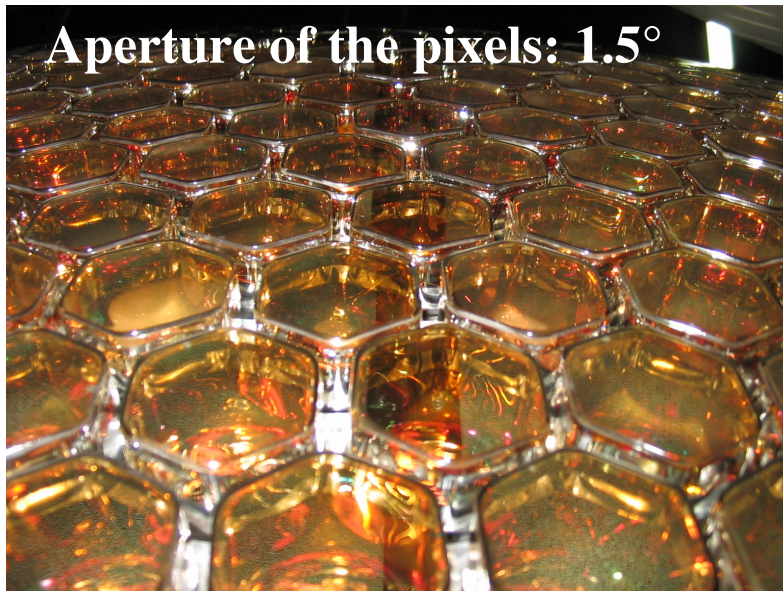
6 telescopes, each with $30^\circ \times 30^\circ$ FOV

The fluorescence detector (FD)

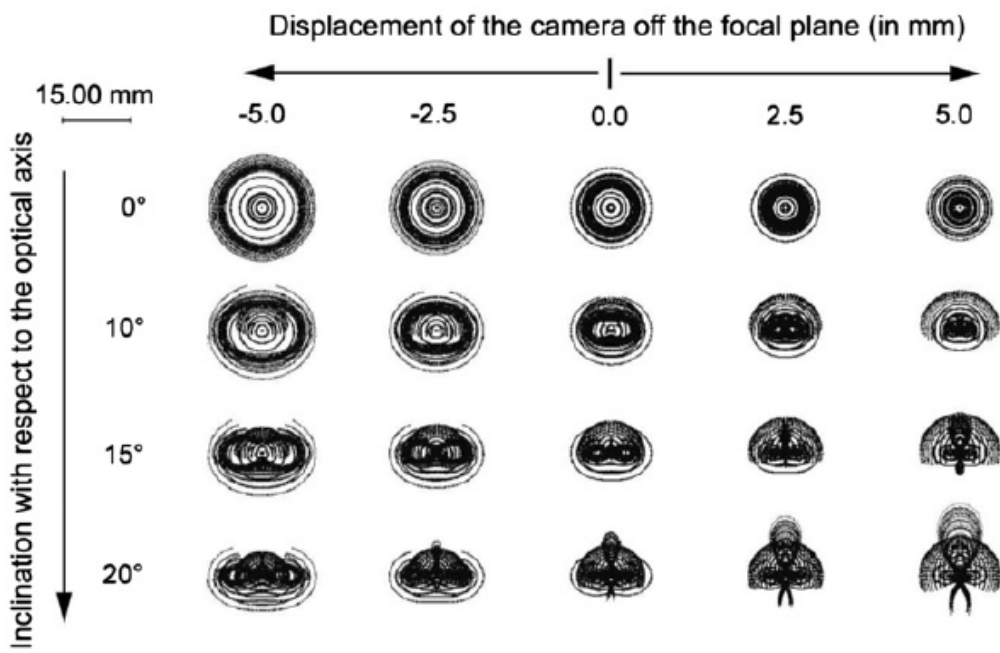
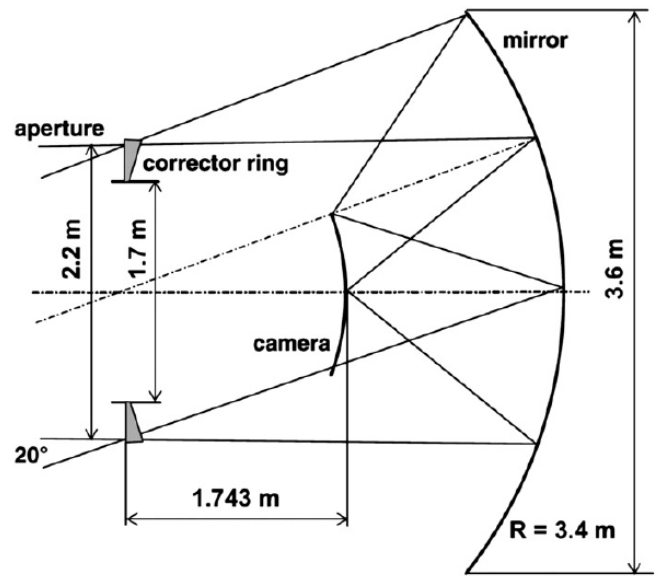
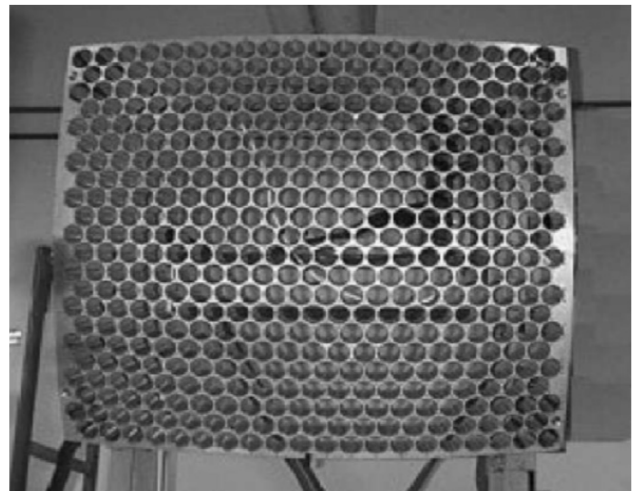
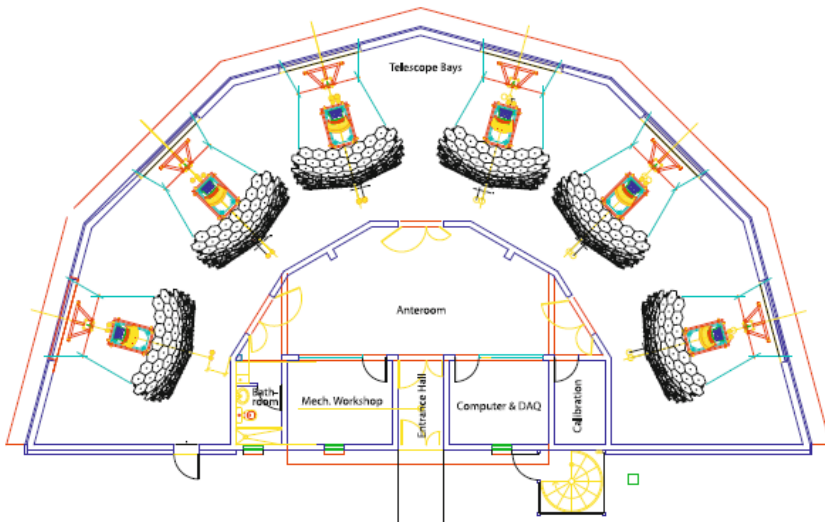
Camera: 440 PMTs



Aperture of the pixels: 1.5°



The fluorescence detector (FD)

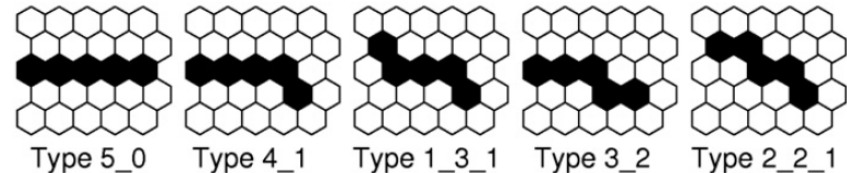


Trigger strategy for FD

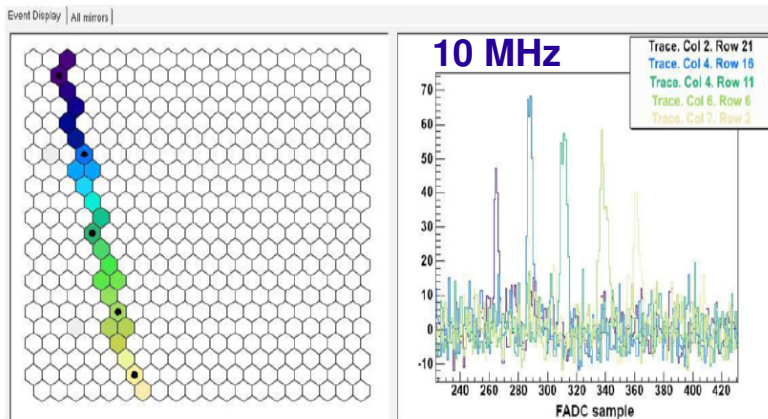
T1 individual pixel above threshold - 100 Hz/pixel

T2 on specific patterns (~40000) - 0.1 Hz/telescope

T3 software trigger (event builder) 0.02 Hz/FD-site

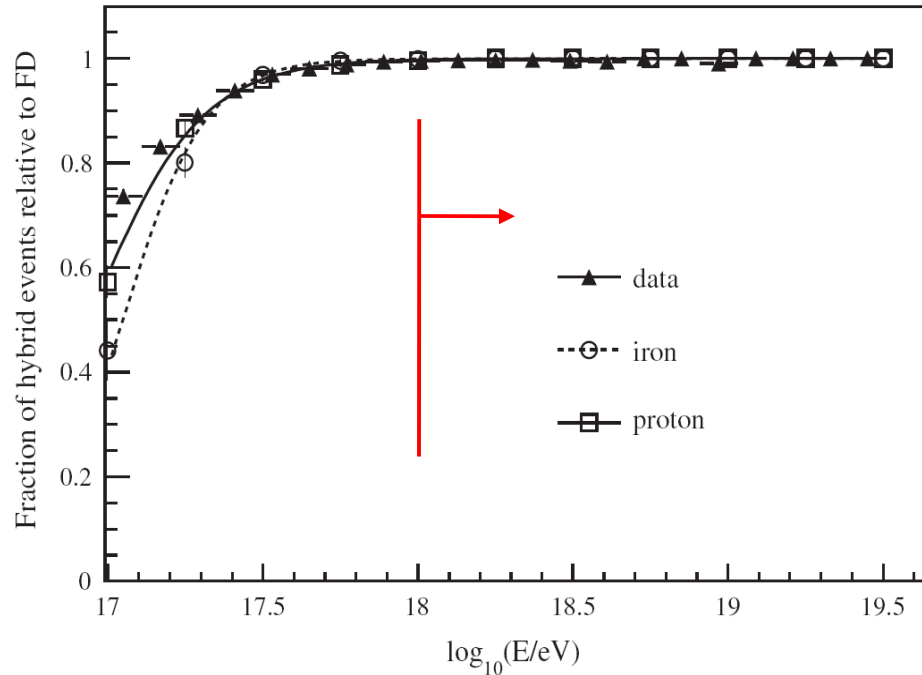


Event Display

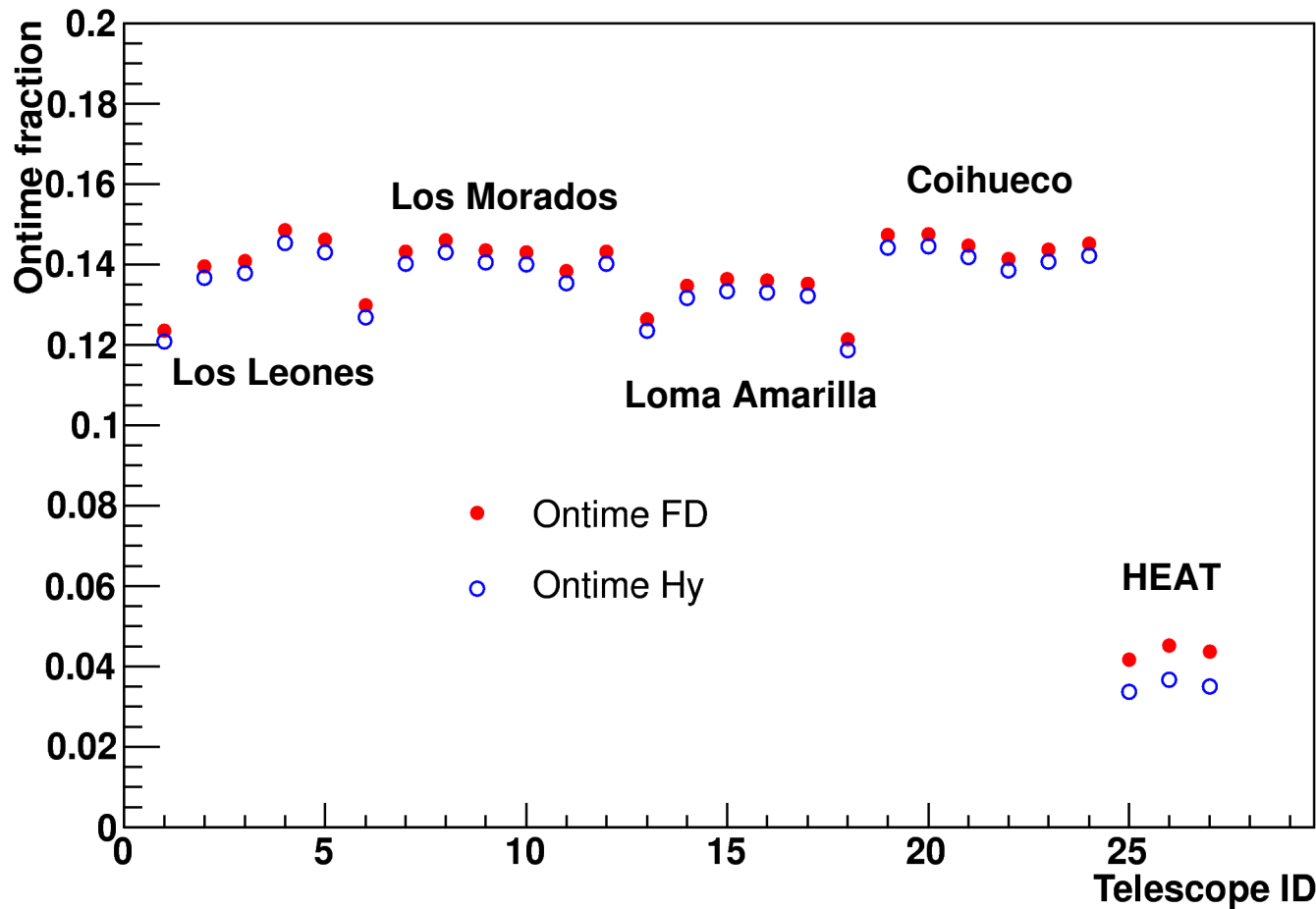


At energy above 10^{18} eV each FD event has at least one station, regardless of its primary mass if hadron

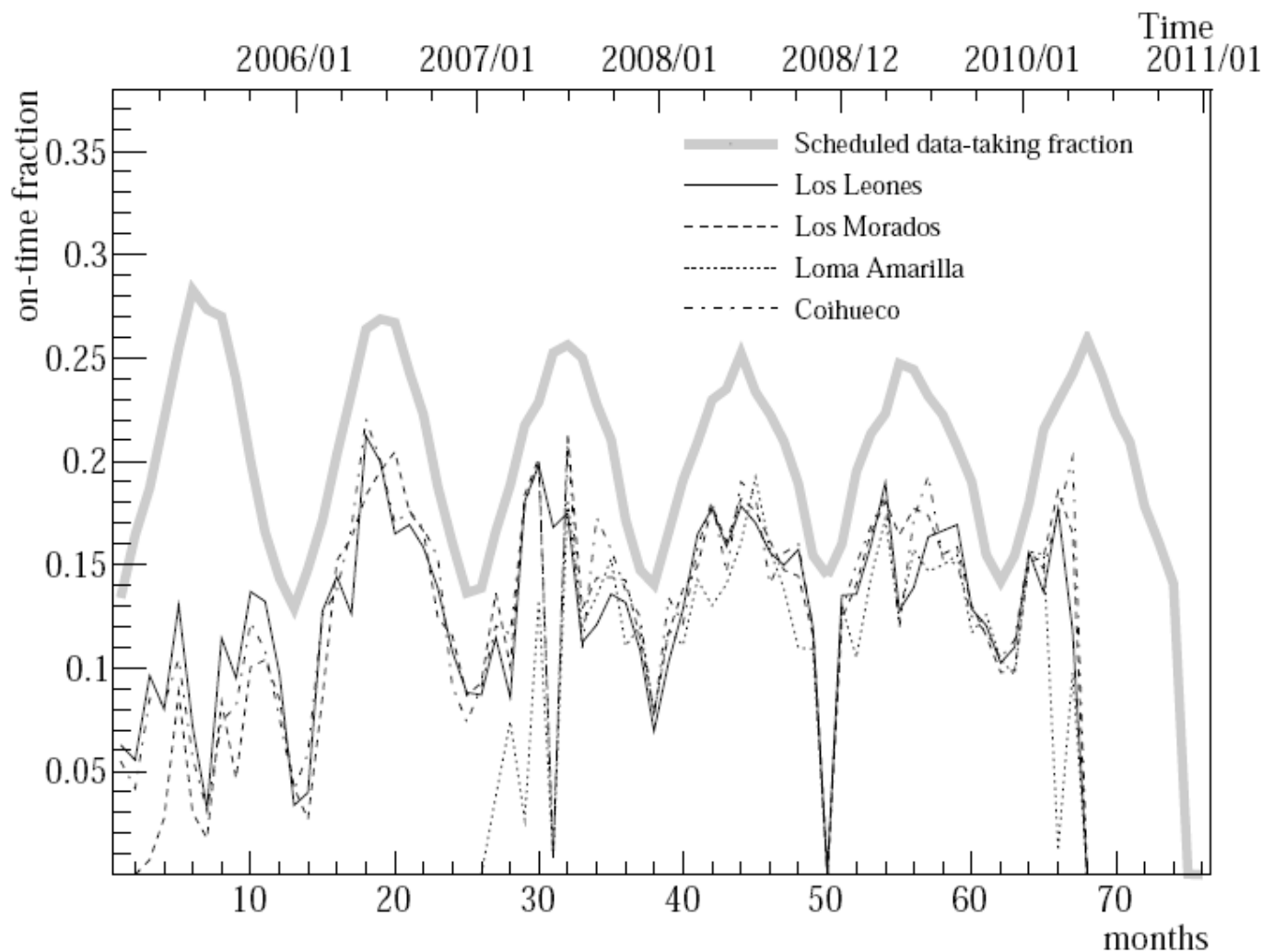
Time and geometrical info of each T3 sent to SD -> **Hybrid trigger!**



FD On-time fraction



FD On-time fraction



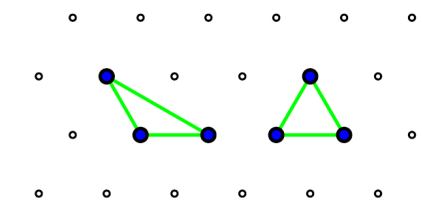
Trigger strategy for SD

Station trigger

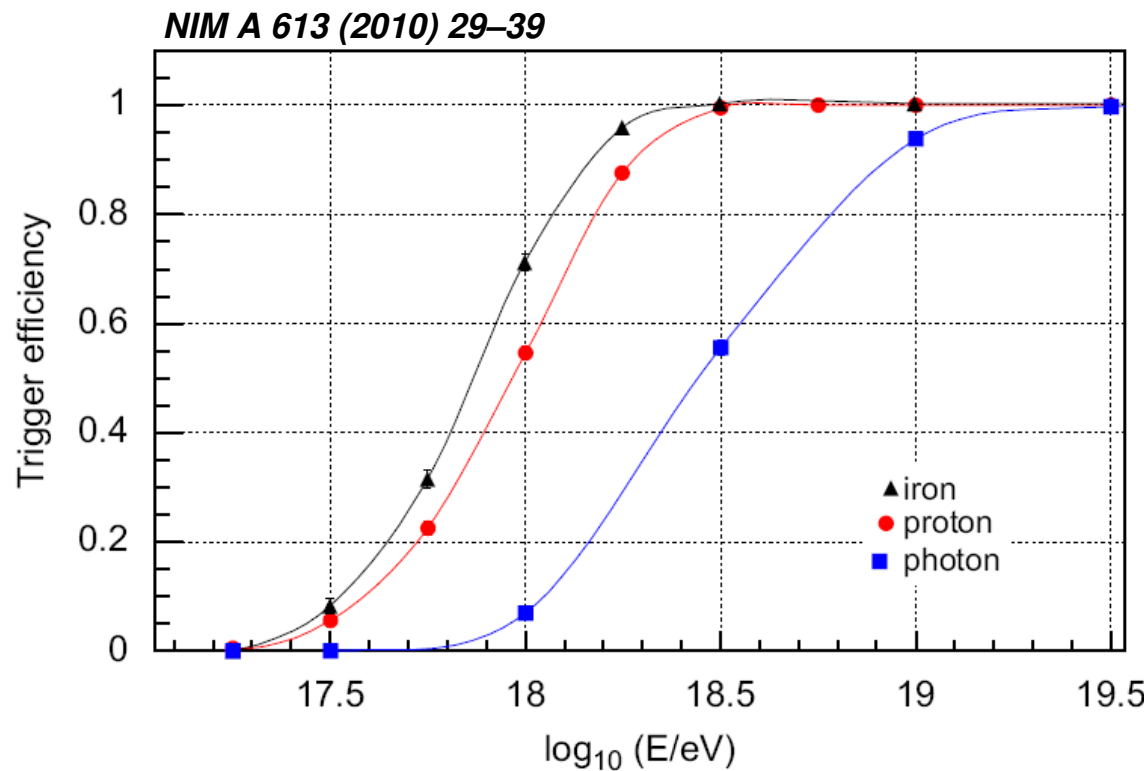
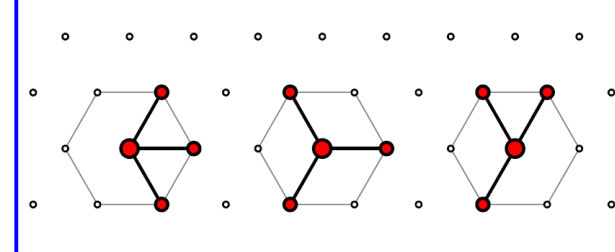
- T1** 3 PMTs above threshold 1.75 VEM – 100 Hz
- ToT** 13 time bins above a threshold of 0.2 VEM in 2 PMTs – 20 Hz
- T2** ToT || threshold above 3.2 VEM in 3 PMTS

Event

3ToT



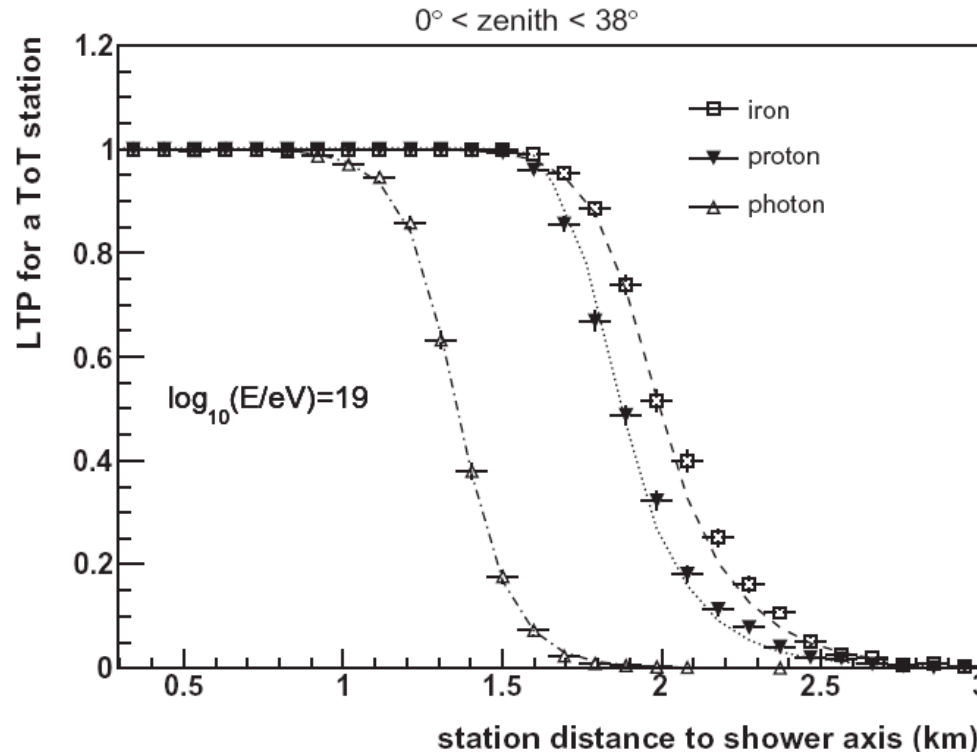
4C1



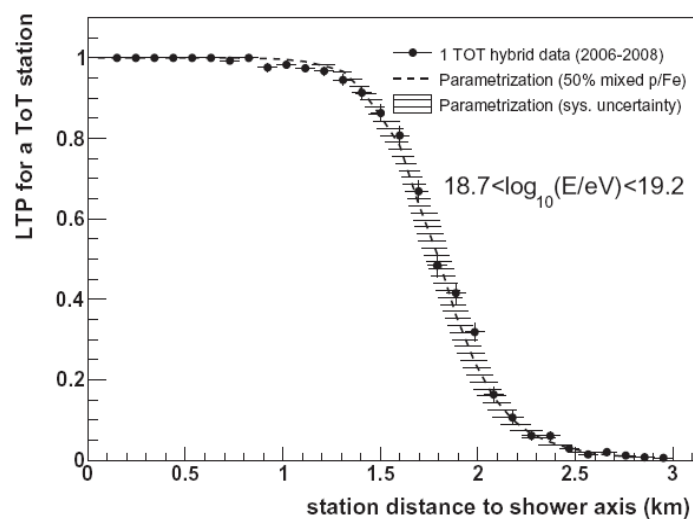
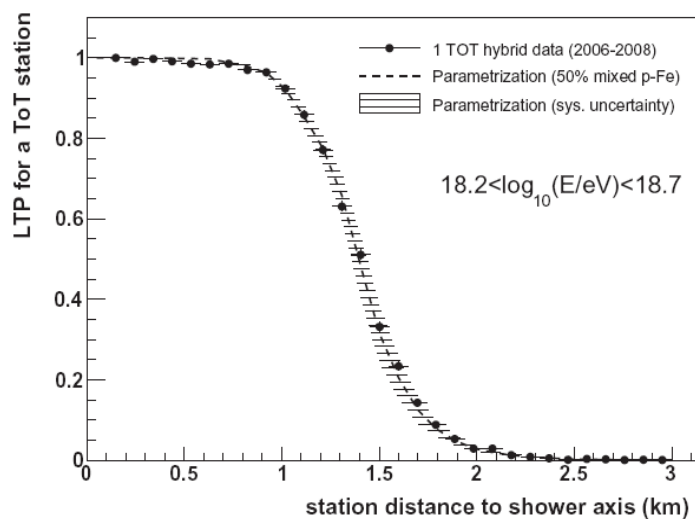
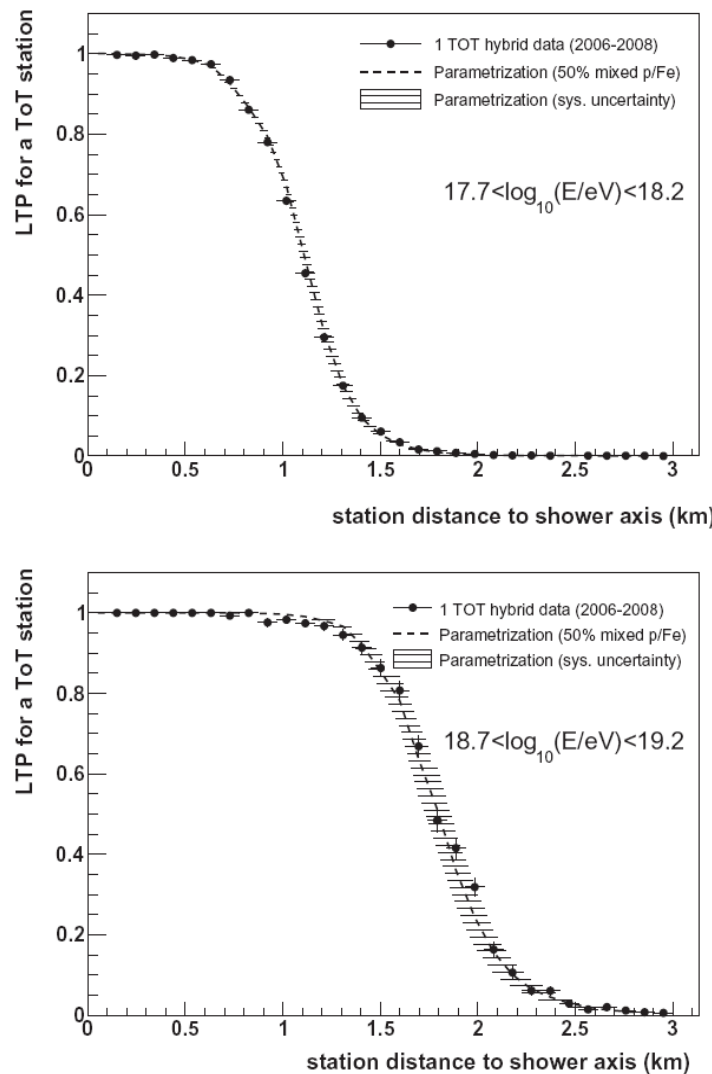
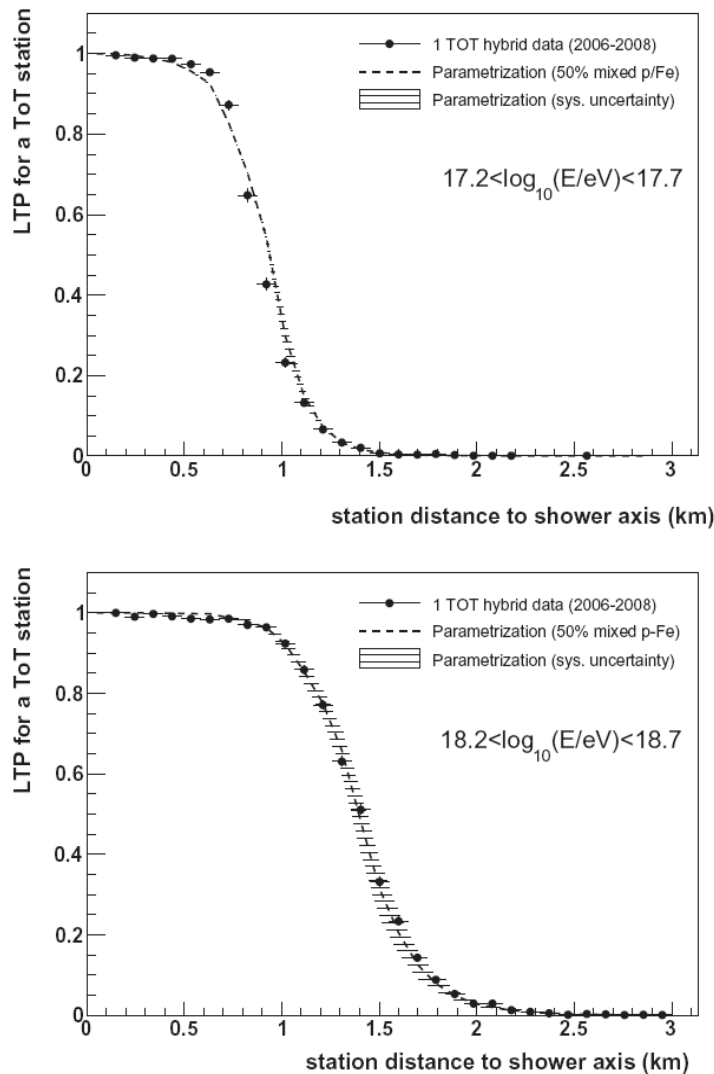
Full efficiency at energy above $10^{18.5}$ eV, regardless of its primary mass if hadron

Lateral Trigger Probability Function

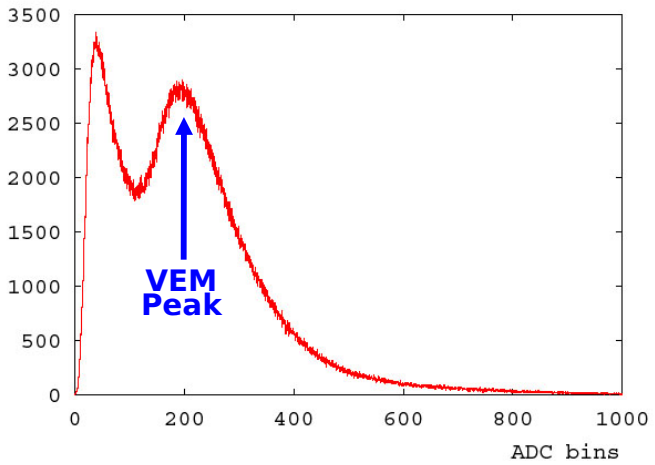
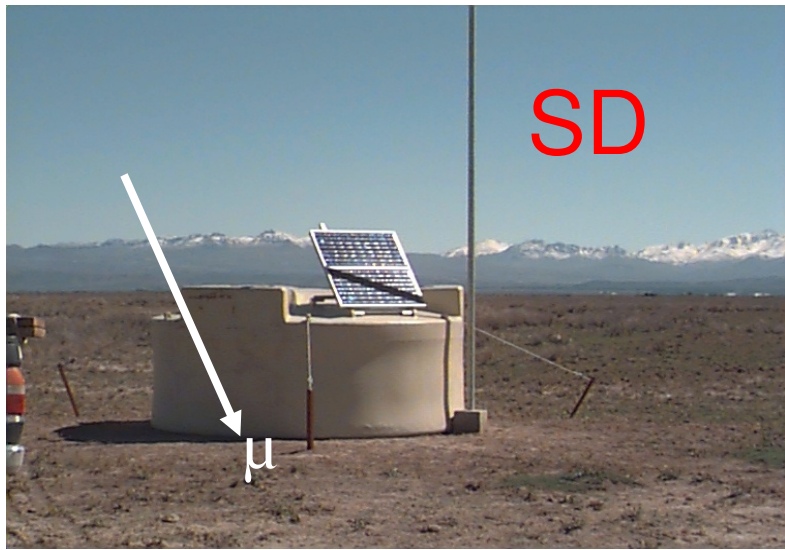
The probability for an Extensive Air Shower to trigger an individual detector of a ground based array as a function of distance to the shower axis, taking into account energy, mass and direction of the primary cosmic ray



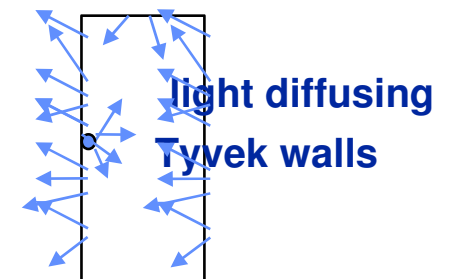
Lateral Trigger Probability Function



SD e FD Calibration



light flux measured
by absolutely
calibrated PMT



Drum: uniform camera illumination

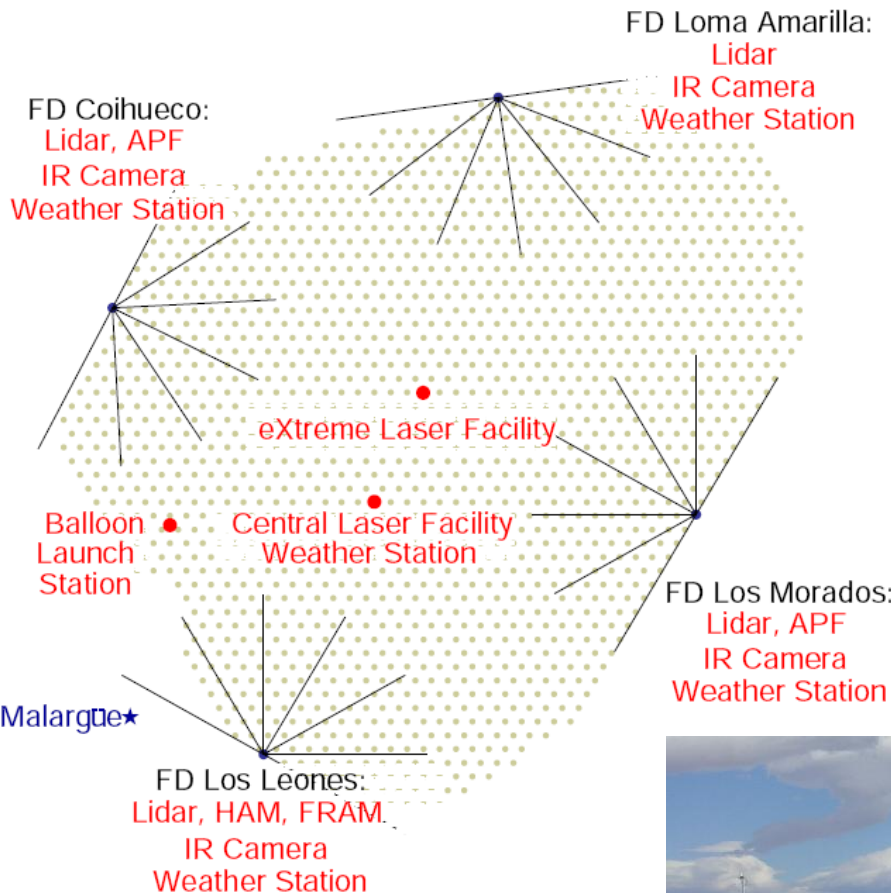
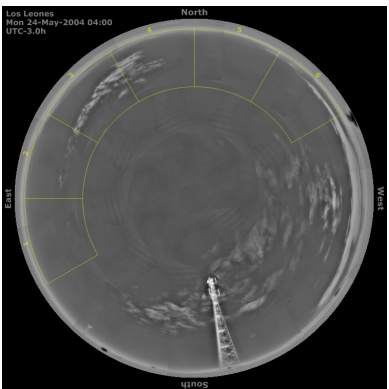
Through-going cosmic muons

Atmospheric monitoring

balloons



IR cloud camera



K. Louedec @ ICRC 2011

backscatter Lidar



Central Laser Facility



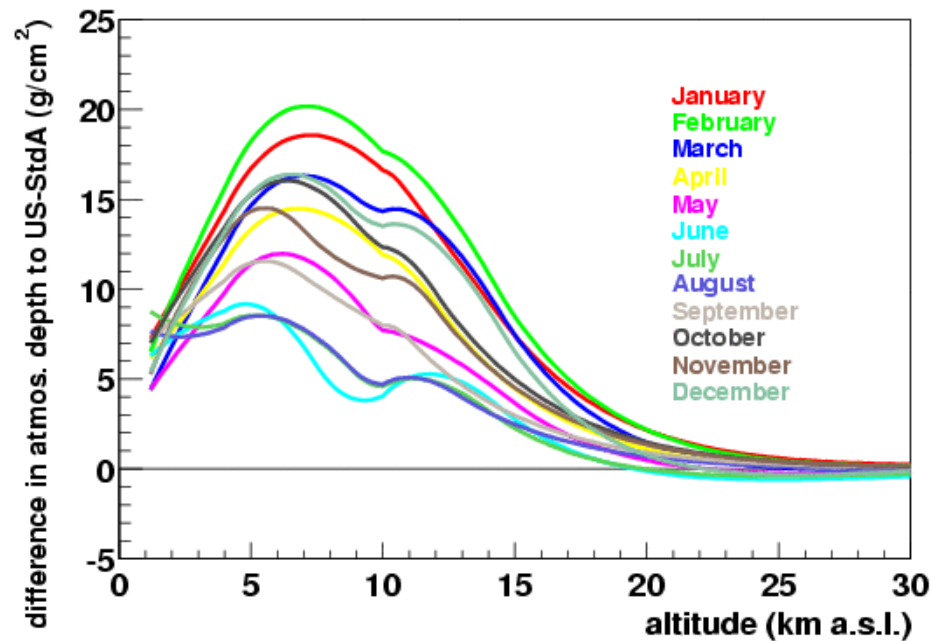
Atmospheric profiles

Local measurements with:

- radio soundes
- ground based weather stations



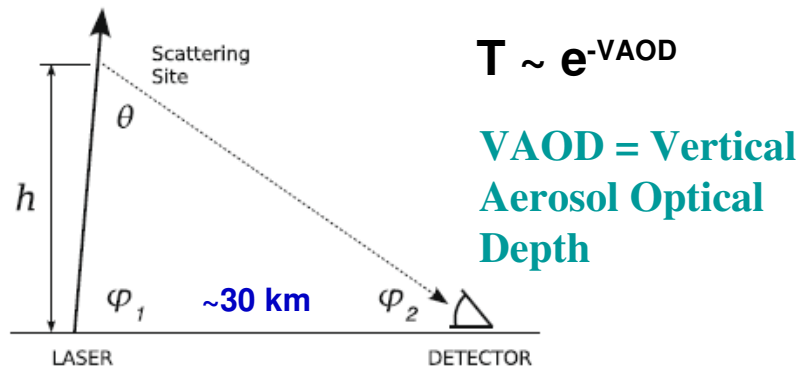
Malargue monthly models



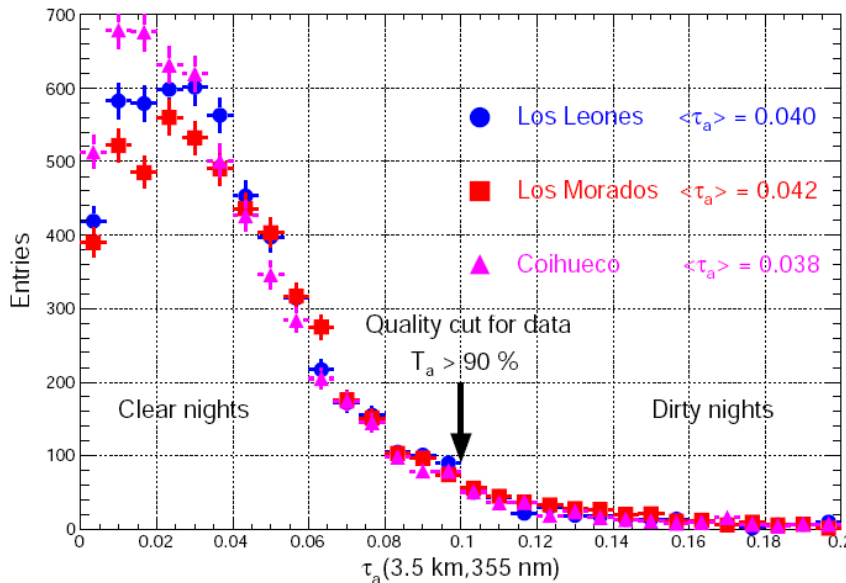
Global Data Assimilation System (GDAS) developed
by the National Oceanic and Atmospheric Administration

M.Will @ ICRC 2011

Central Laser Facility



Aerosol optical depth @ 3.5 km



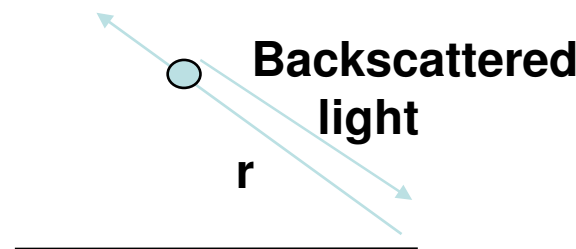
Vertical aerosol optical depth at 3.5 km above the fluorescence Telescopes measured between January 2004 and December 2010. The transmission coefficient is defined as $T = \exp (-\tau_a)$.

Aerosol monitoring

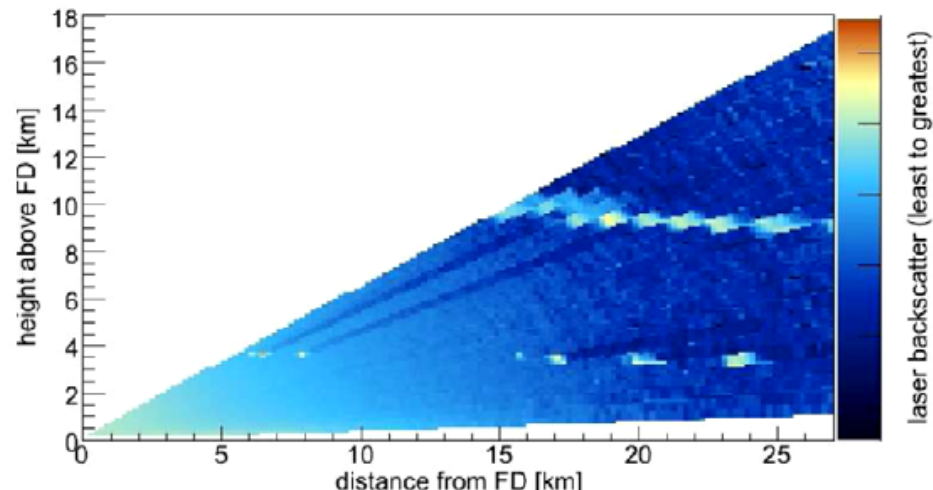
- Aerosols: clouds, dust, smoke and other pollutants

Backscatter Lidars

- 1 steerable laser per eye
- hourly scan of aerosols and
“shoot the shower”



Cloud image

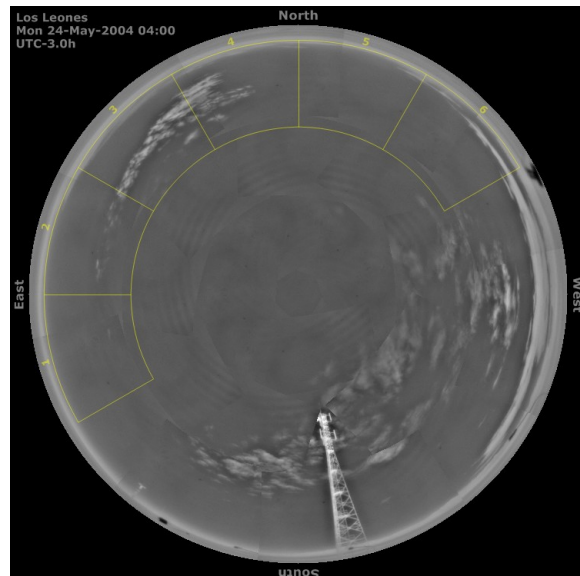


Infrared cloud monitoring

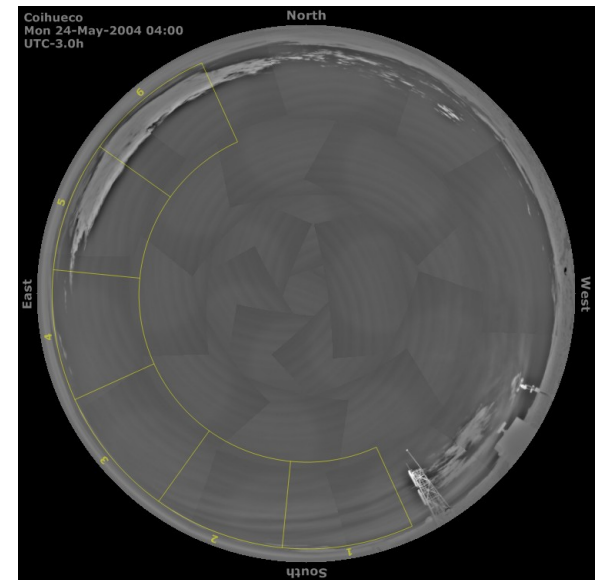


Finely pixelated infrared
Raytheon 2000B camera

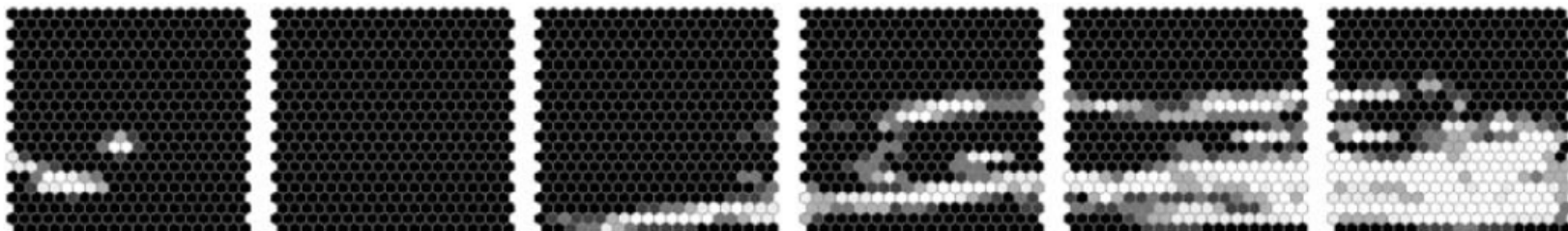
Los Leones



Coihueco



Full sky cloud scan

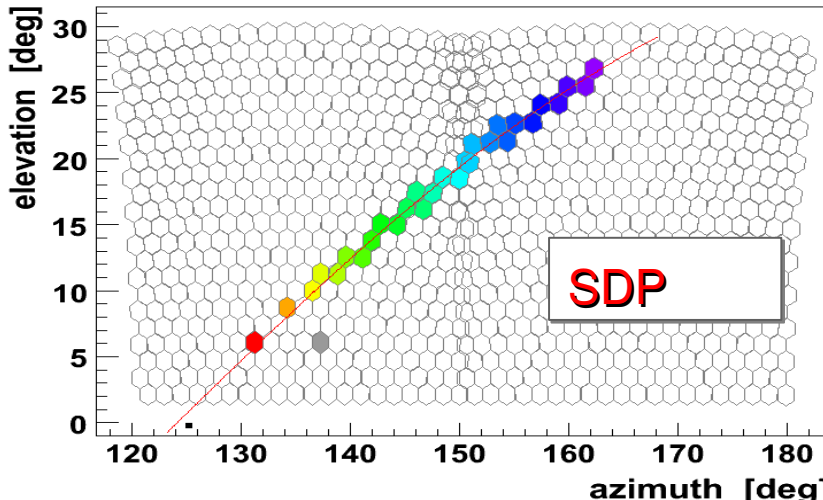


Pixel-wise mask for shower reconstruction

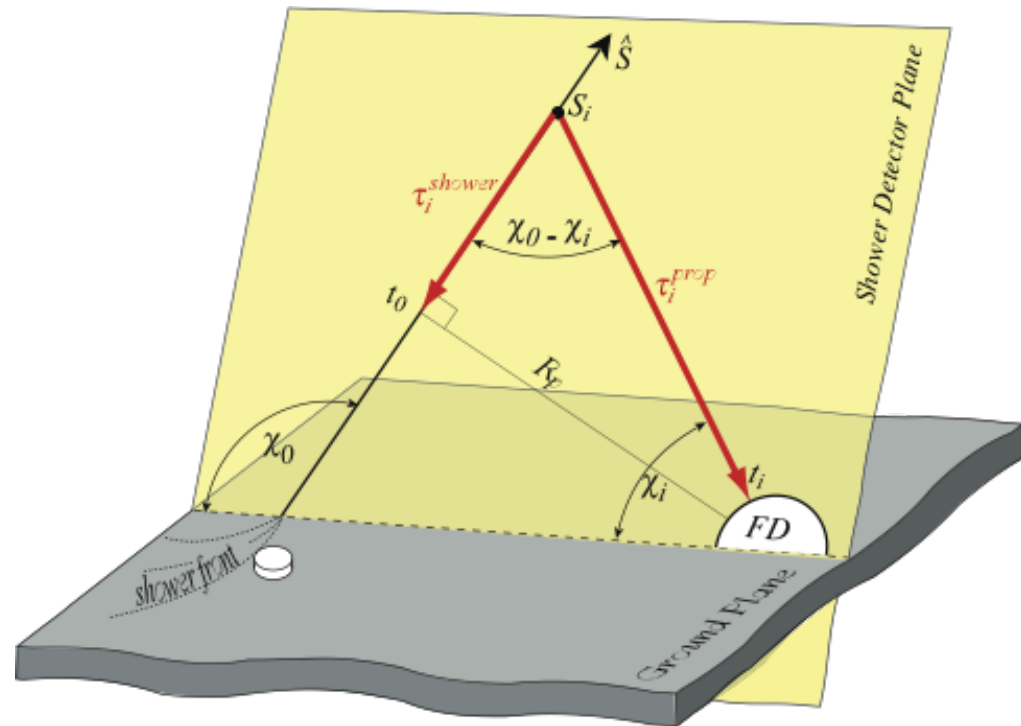
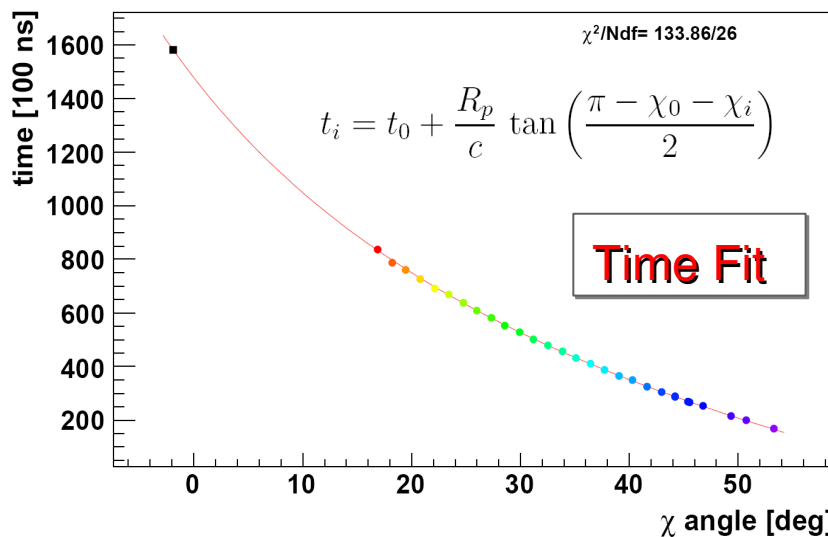
Observables and Detector Performance

- Reconstruction of arrival directions with FD/SD/Hybrid
- Reconstruction of longitudinal profile
- Energy determination

FD-Hybrid geometry reconstruction

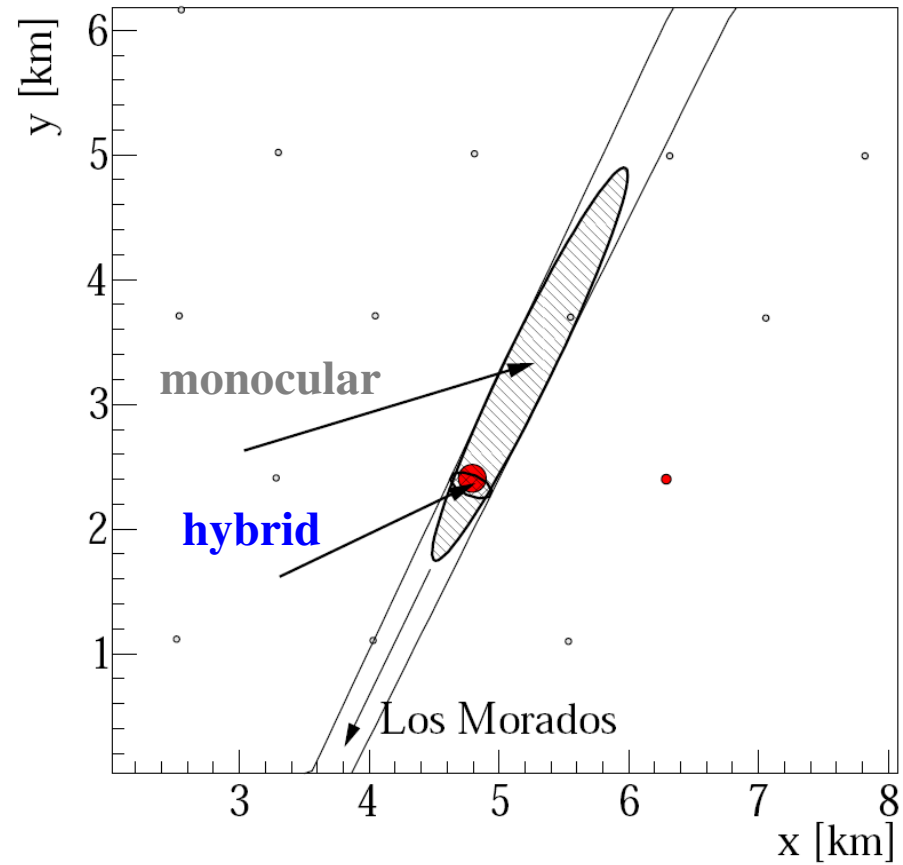
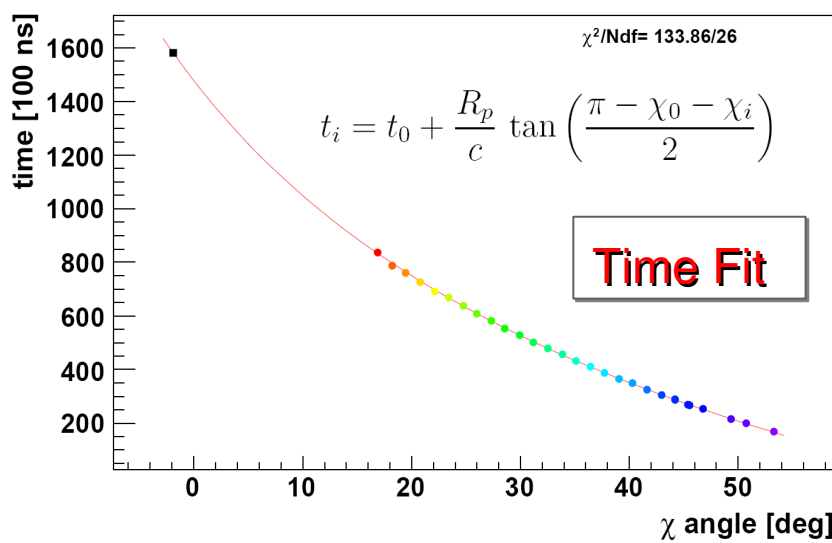
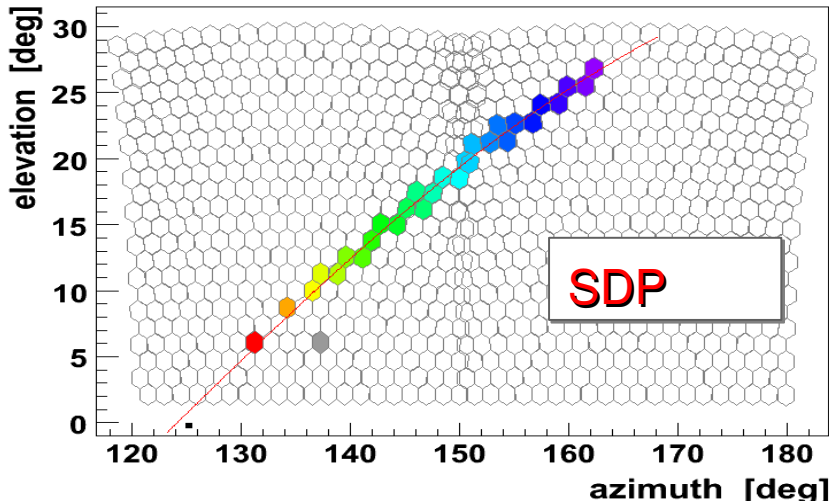


Shower-Detector Plane (SDP) using the directions of the triggered pixels



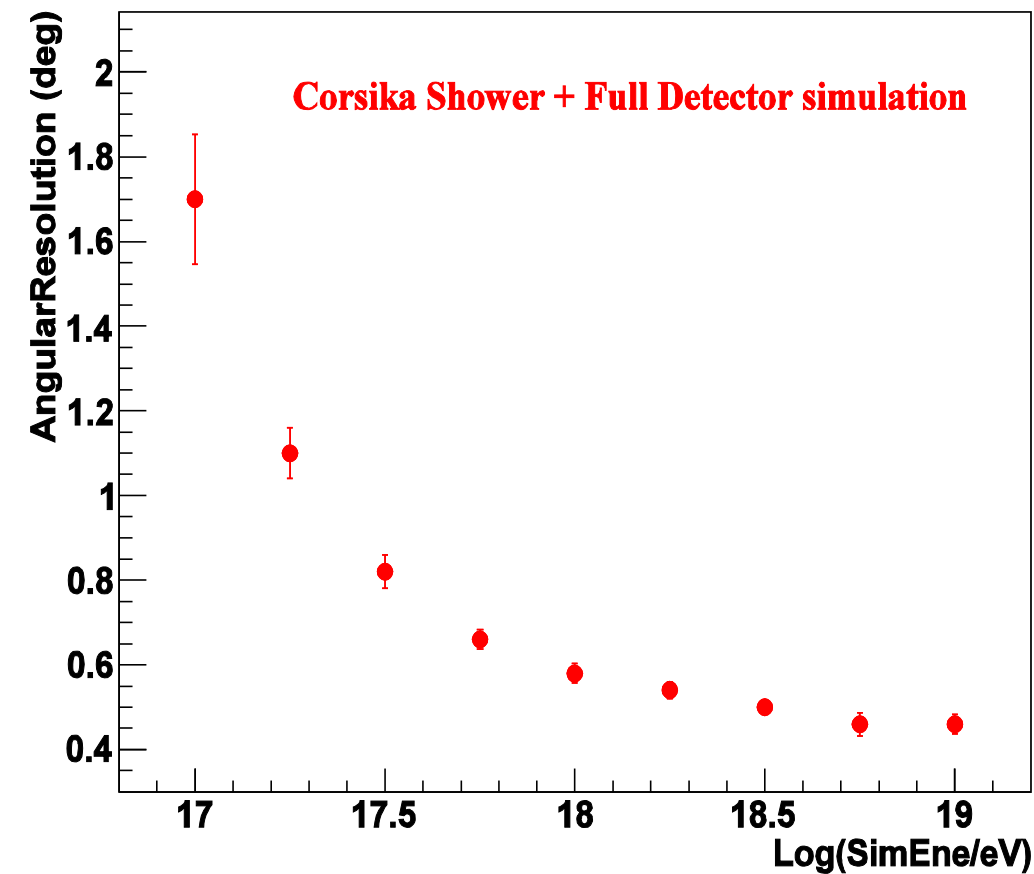
- Shower axis from the time-sequence of triggered FD pixels plus the information from the “hottest” SD station

FD-Hybrid geometry reconstruction



Hybrid angular resolution $\sim 0.6^\circ$
Core resolution about 50 meters

Hybrid Angular resolution



Angular Resolution:

the angular radius that contains 68% of the showers coming from a given point source

Hybrid angular resolution
from simulation

$E \sim 10^{18} \text{ eV}$

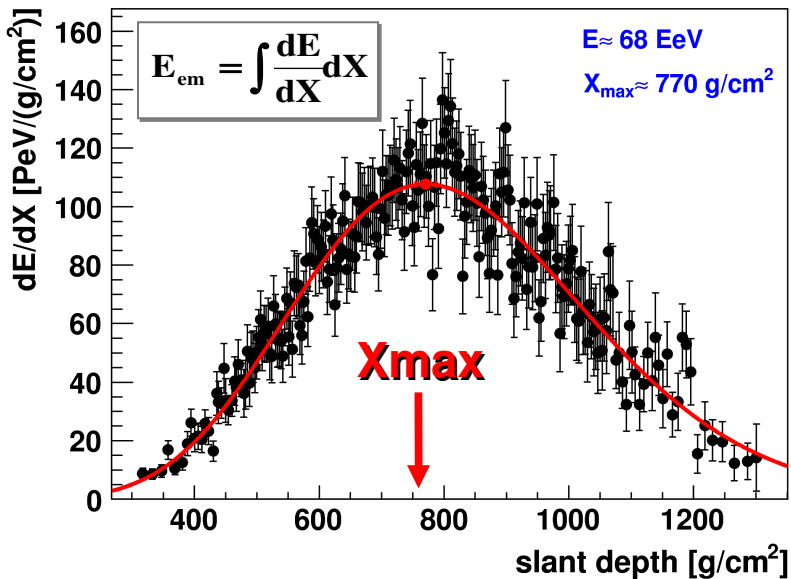
$E > 10^{19} \text{ eV}$

$\text{AR} \sim 0.8^\circ \ (\theta < 60^\circ)$

$\text{AR} \sim 0.5^\circ \ (\theta < 60^\circ)$

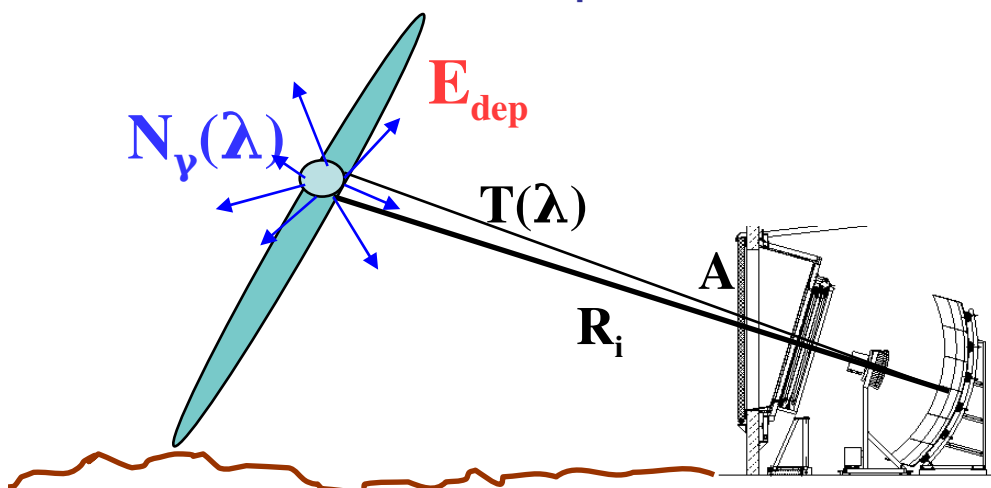
FD: energy determination

Longitudinal Profile



Energy “Calorimetric measurement”

Almost model independent



Fluorescence yield
 (from laboratory
 measurements)

Geometry

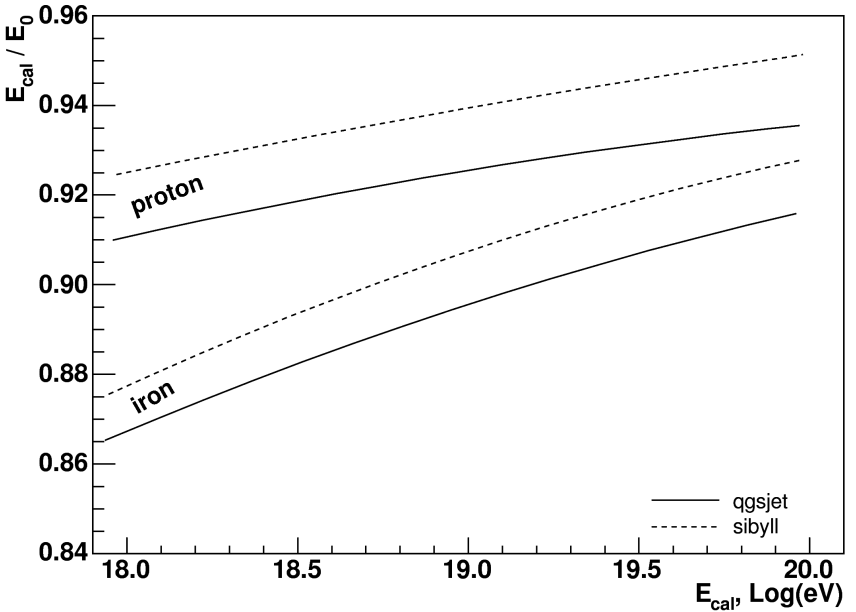
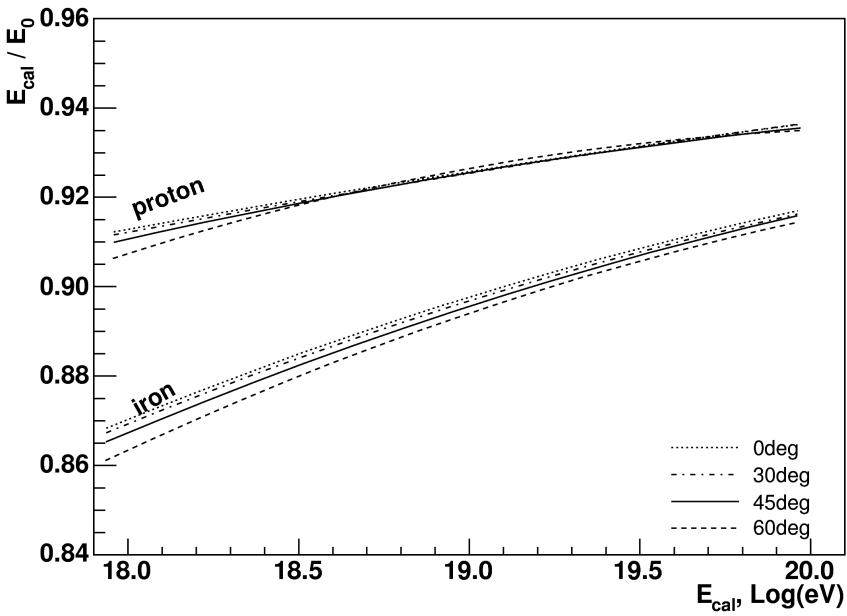
$$\frac{A}{R_i^2}$$

Atmosphere

$$T(\lambda)$$

Detector
 calibration

FD: the invisible energy



The “invisible” energy carried away mainly by muons and neutrinos has to be taken into account to reconstruct the primary energy

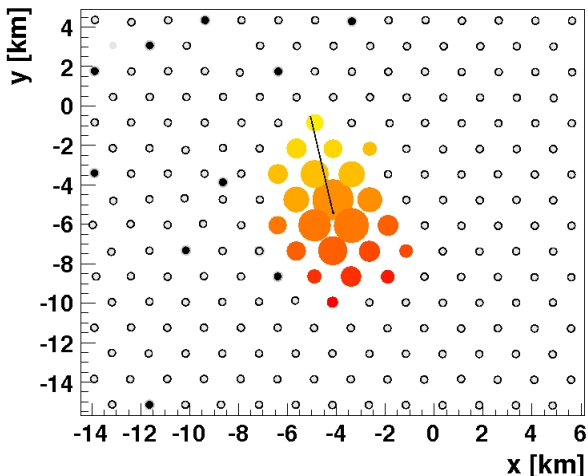
$$E_{\text{FD}} = (1 + f_{\text{inv}}) E_{\text{cal}}$$

This correction is mass and model dependent

SD reconstruction

Direction:

fit to arrival times sequence of particles in shower front



Determination of the arrival direction with χ^2 -method

Determination of the lateral particle density function and LDF with a Likelihood method to fit a NKG-type function

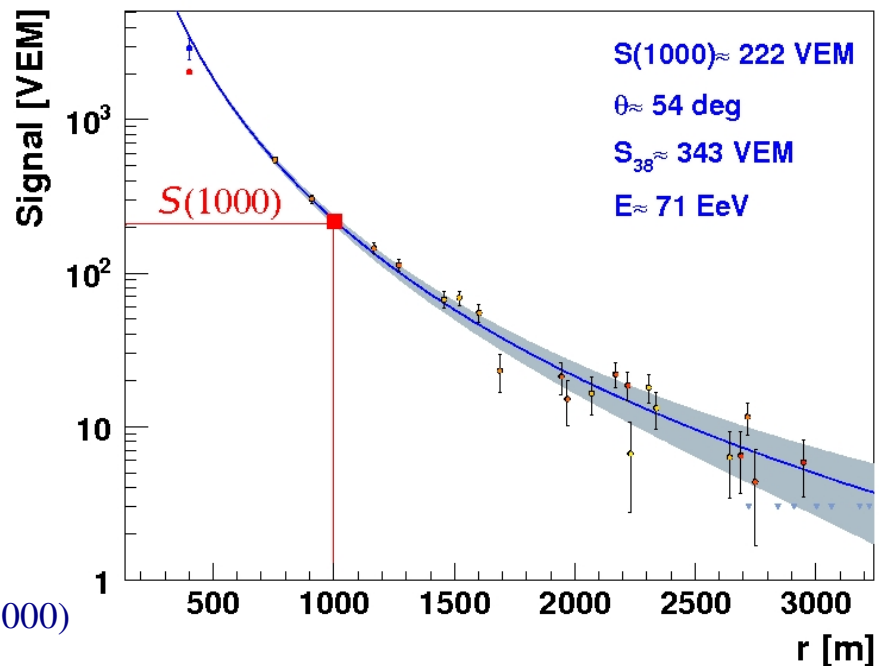
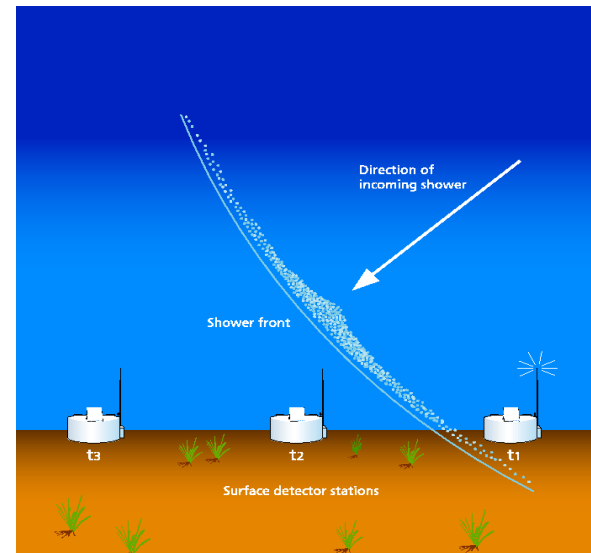
$$S(r) = S(1000) \left(\frac{r}{1000}\right)^{-\beta} \left(\frac{r+700}{1700}\right)^{-\beta}$$

Free parameters: core position and signal at 1000 m, $S(1000)$

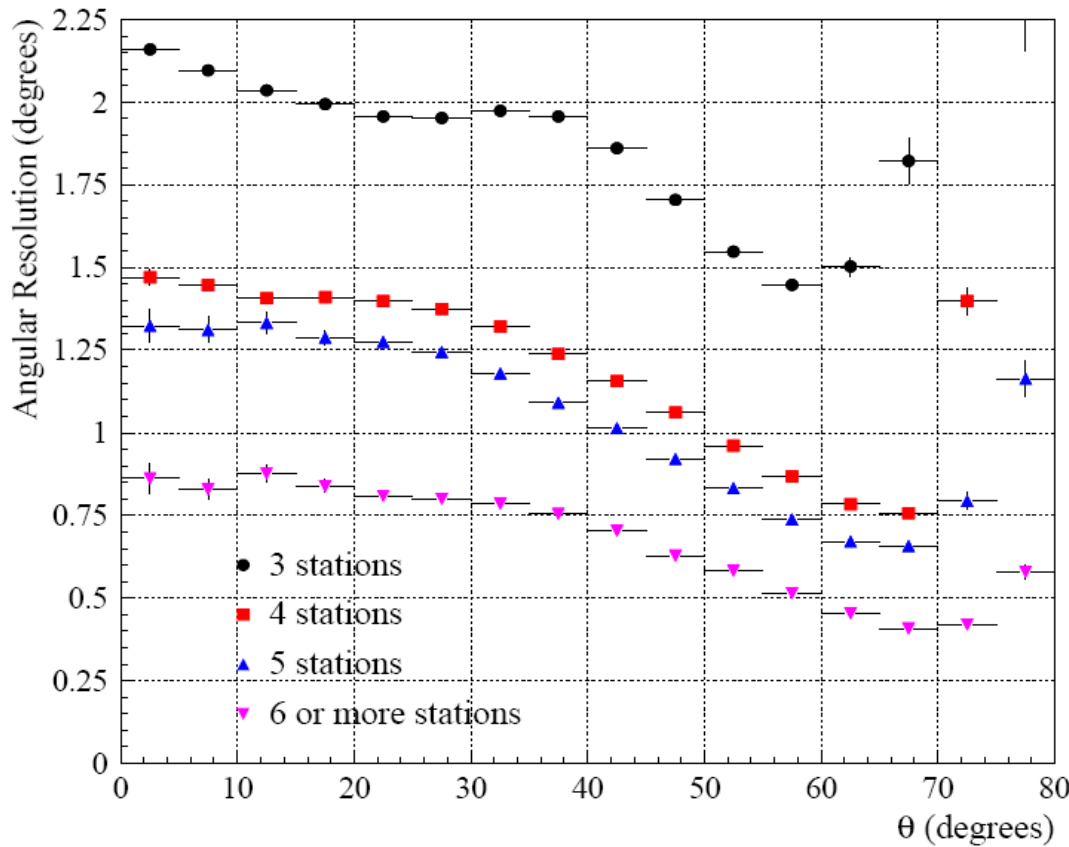
β is parameterized as a function of shower zenith angle and $S(1000)$

Angular resolution

$E > 10^{18} \text{ eV}, \sim 3 \text{ stations}, < 2^\circ$
 $E > 10^{19} \text{ eV}, \sim 6 \text{ stations}, < 1^\circ$



Angular resolution with SD



Using the time variance model
Astropart. Phys. 28 (2008) 523

$$F(\eta) = 1/2 (V[\theta] + \sin^2(\theta) V[\phi])$$

$V[\theta\phi]$ = variances

η = space angle between true and reconstructed angle

$$AR = \sqrt{-2 \ln(0.32) F(\eta)}$$

SD angular resolution from data

3-fold $E < 4 \times 10^{18}$ eV $AR < 2.2^\circ$ ($\theta < 60^\circ$)

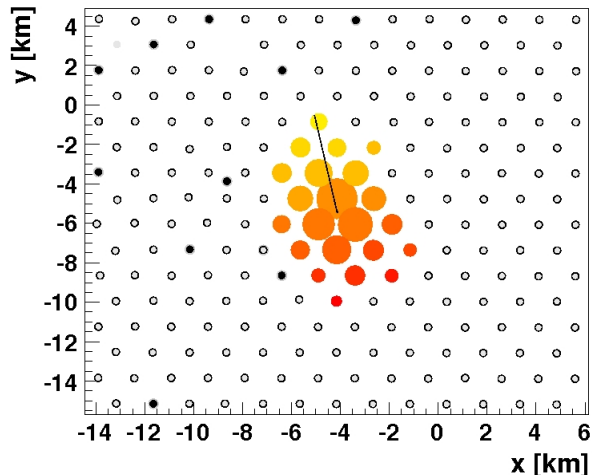
4/5-fold $3 \times 10^{18} < E < 10^{19}$ eV $AR < 1.5^\circ$ ($\theta < 60^\circ$)

More fold $E > 10^{19}$ eV $AR < 1^\circ$ ($\theta < 60^\circ$)

SD reconstruction

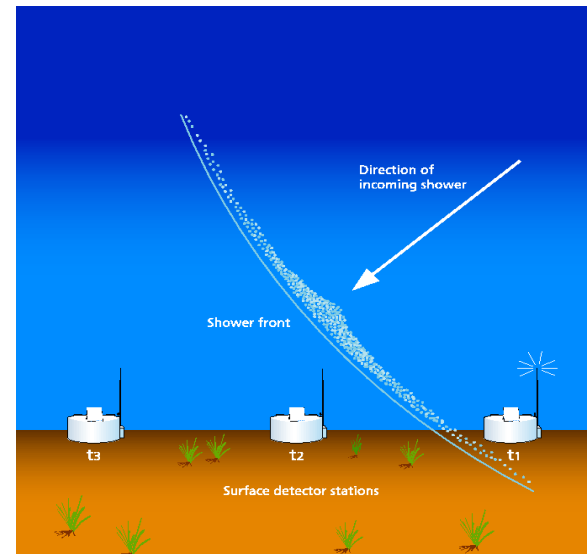
Direction:

fit to arrival times sequence of particles in shower front



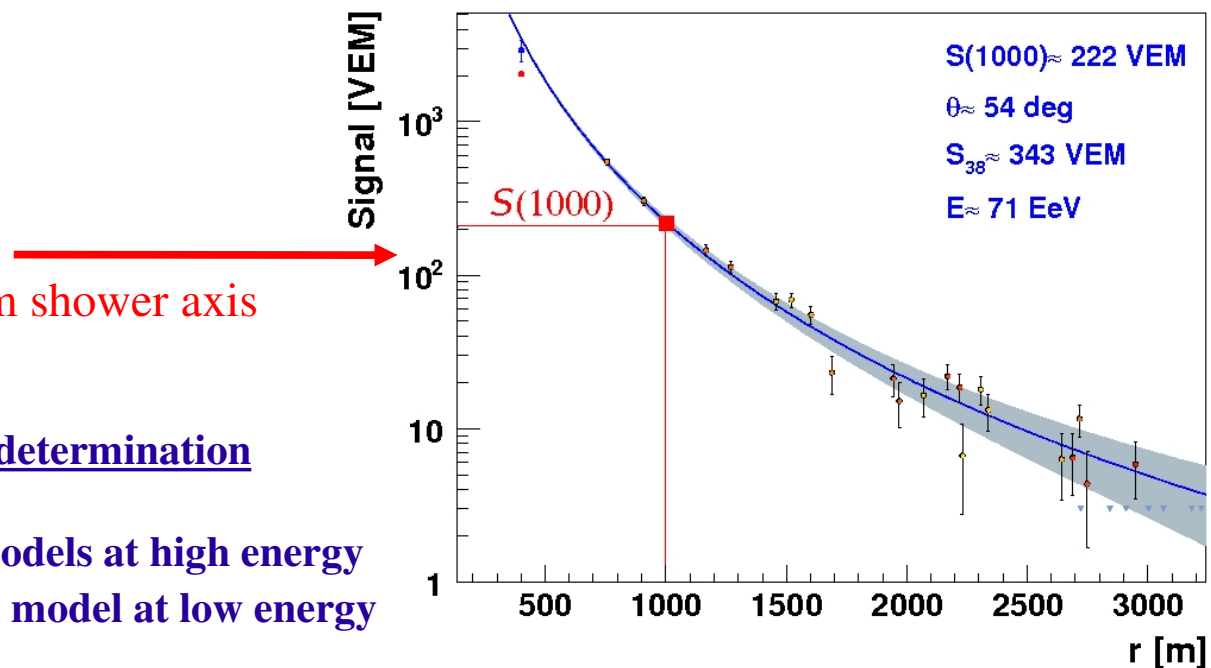
Angular resolution

$E > 10^{18}$ eV, ~ 3 stations, $< 2^\circ$
 $E > 10^{19}$ eV, ~ 6 stations, $< 1^\circ$



Energy estimator: S(1000)

particle density at 1000 m from shower axis

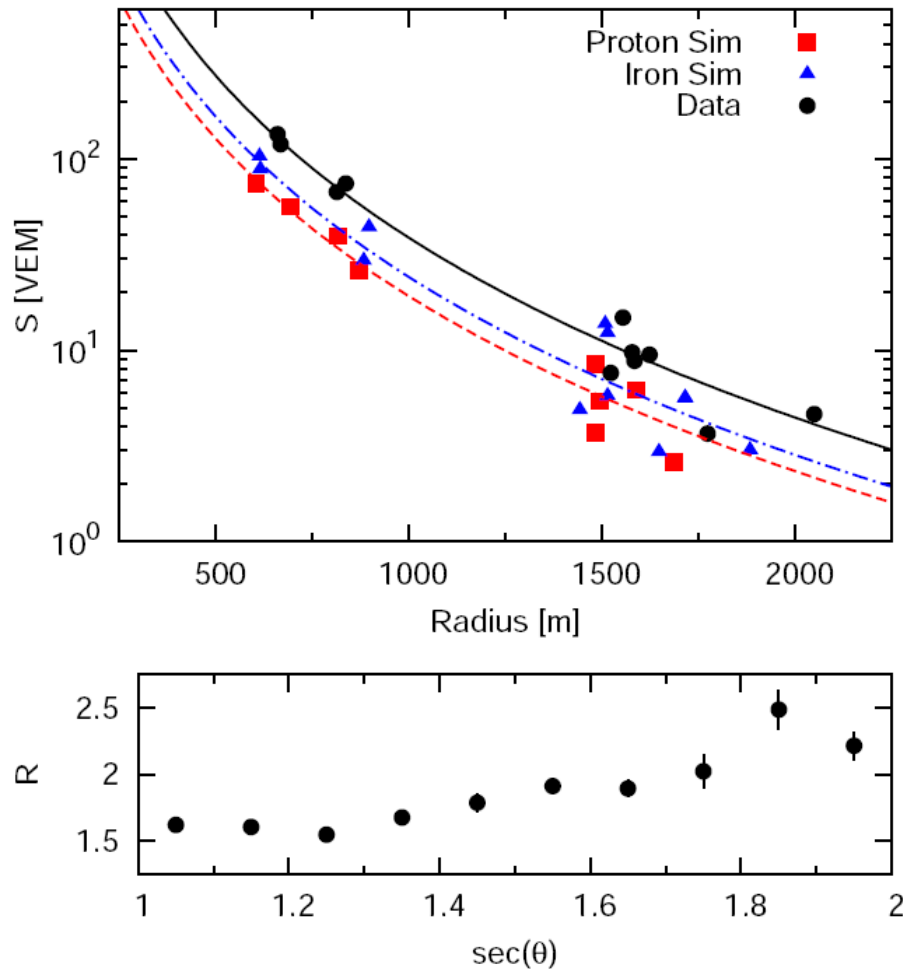


Systematic uncertainties on energy determination

- 30% from hadronic interaction models at high energy
- 10-20% from hadronic interaction model at low energy

Muon puzzle....

J.Allen @ ICRC 2011



More muons in data than in simulation!

Not easy to reproduce with models these measurements

SD energy based on LDF systematically overestimated with respect to FD calorimetric measurements.

FD-SD-Hybrid

	SD-only	FD-only	Hybrid
Duty-cycle	~100% (high stat)	~10-15%	~10-15%
Angular Res.	1-2 deg	~3 deg	~ 0.5 deg (>1 EeV)
Energy	relies on MC and composition	missing energy geometry bias	missing energy
Energy Range	$\sim >10^{18.5}$ eV	$\sim >10^{17.5}$ eV	$\sim >10^{18}$ eV

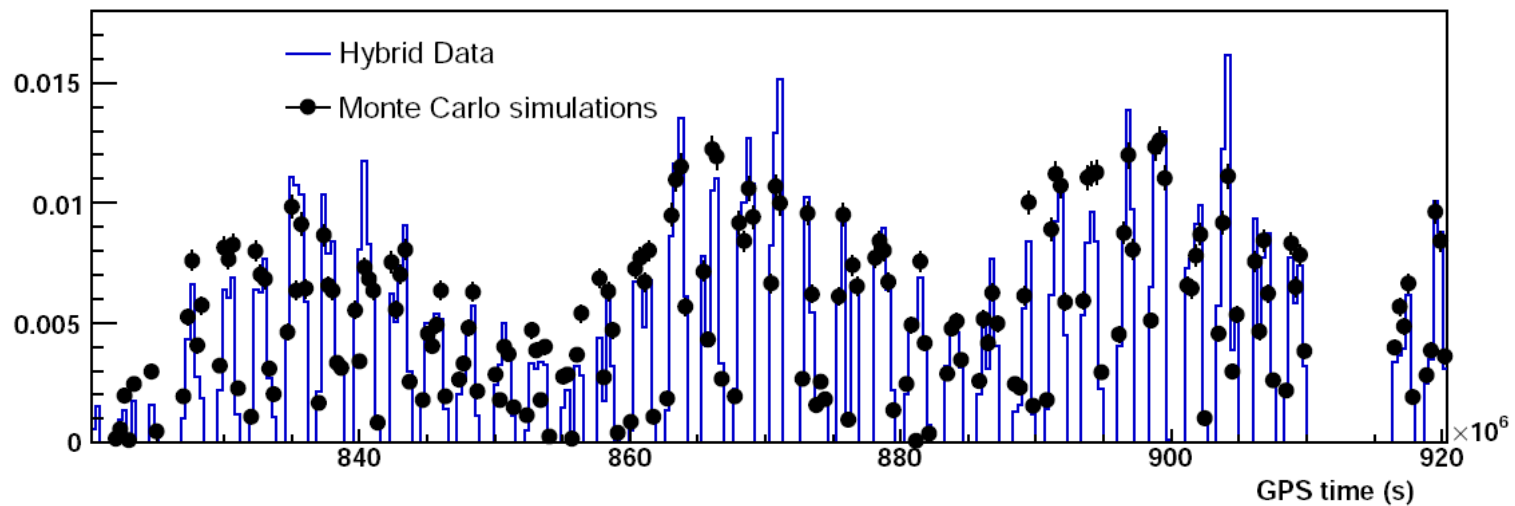
Results

- **Energy spectrum**
- Mass composition
- Hadronic interactions
- Astrophysics
- Search for photons and neutrinos

Hybrid Exposure

$$\mathcal{E}(E) = \int_T \int_{\Omega} \int_{A_{gen}} \varepsilon(E, t, \theta, \phi, x, y) \cos \theta \, dS \, d\Omega \, dt$$

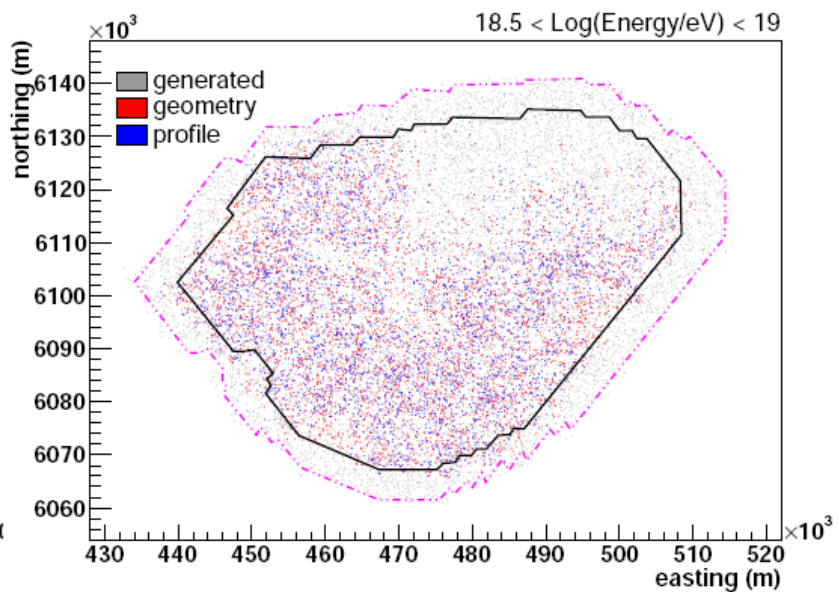
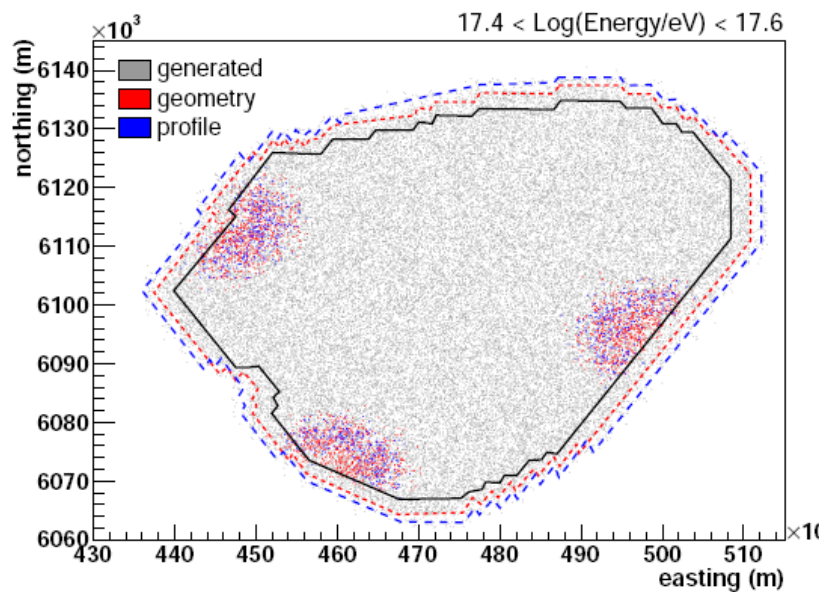
Time dependent simulations



FD on-time and SD stations status reproduced according to the actual data taking conditions along the considered time window

Efficiency

Simulations taking into account the FD and SD
detector status plus the atmospheric conditions



Time period with only 3 FD sites, for two different energy ranges

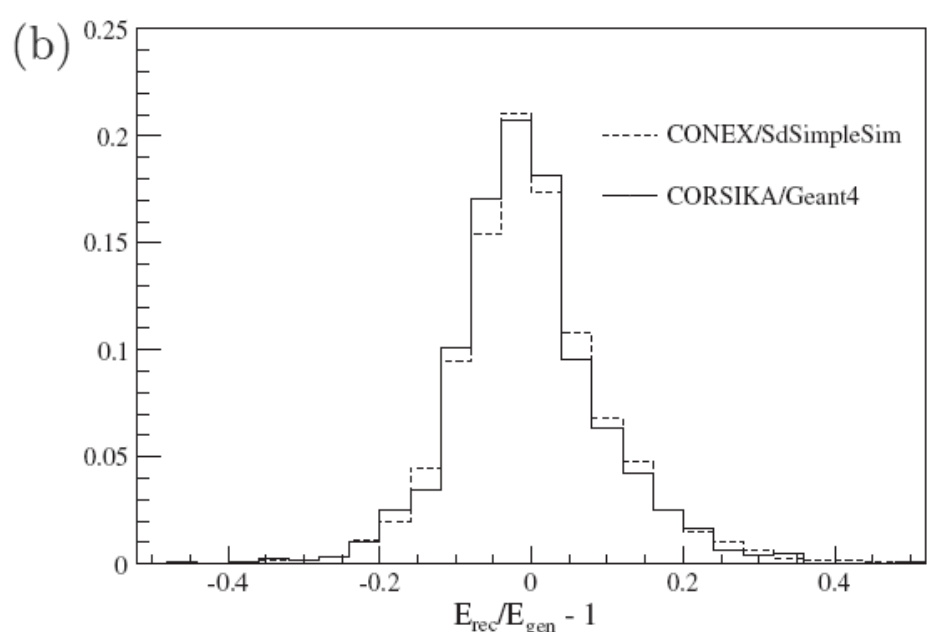
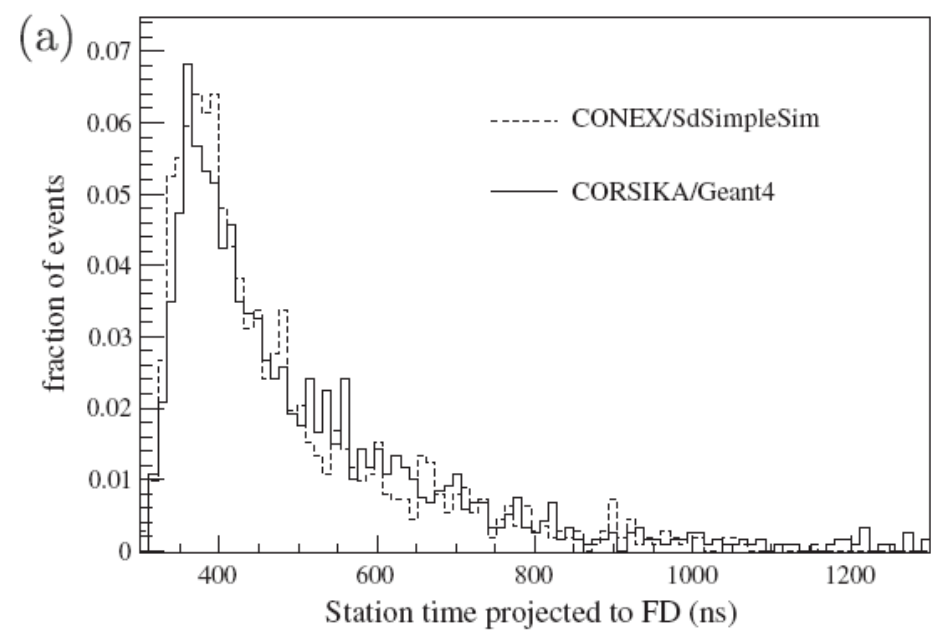
Hybrid Exposure

First Method : Conex profiles + LTPs (large statistics, no signal in the stations)
Second Method : Corsika+Geant4 (less statistics, signal in the stations)

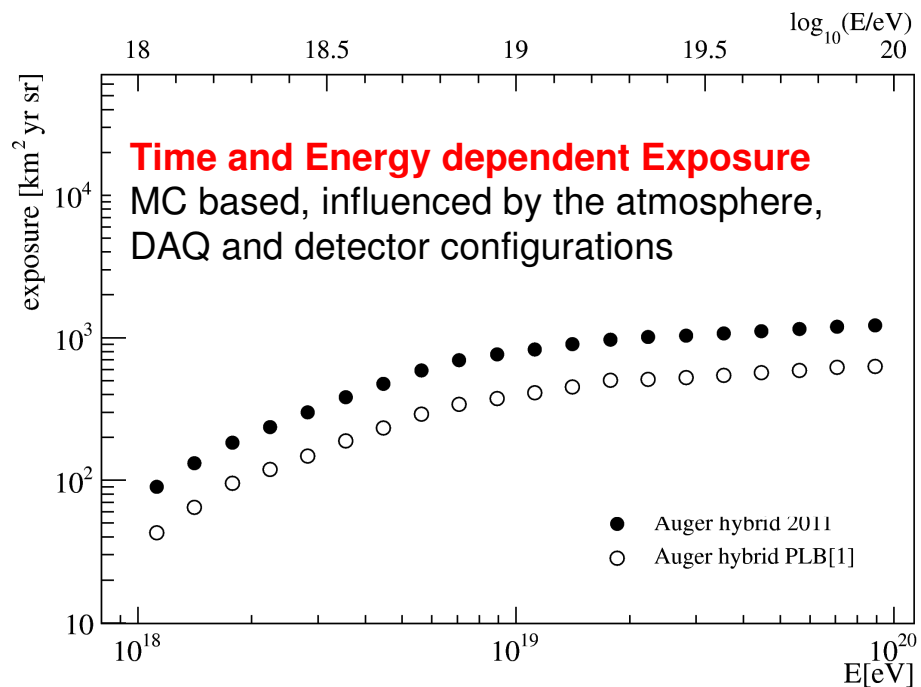
First method validated with method two



**Astroparticle Physics
34 (2011) 368**



Hybrid Spectrum

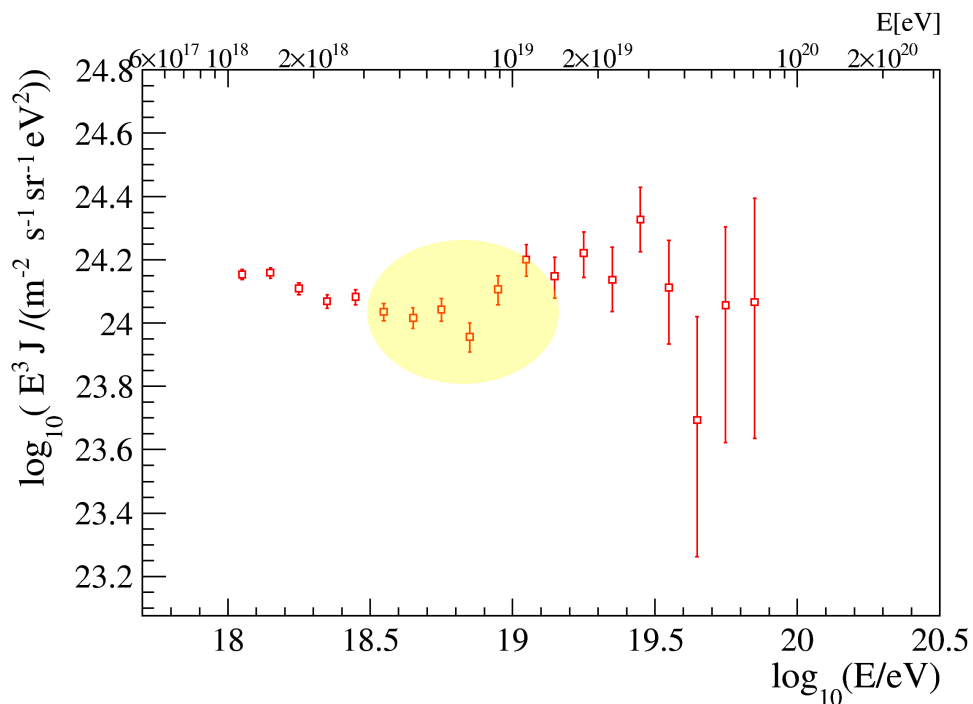


- + Full efficiency at 10^{18} eV (ankle region)
- + Calorimetric measurement
- + Energy Resolution of 8%
- Limited duty cycle (~13%)

Data: Nov. 2005 – Sept. 2010

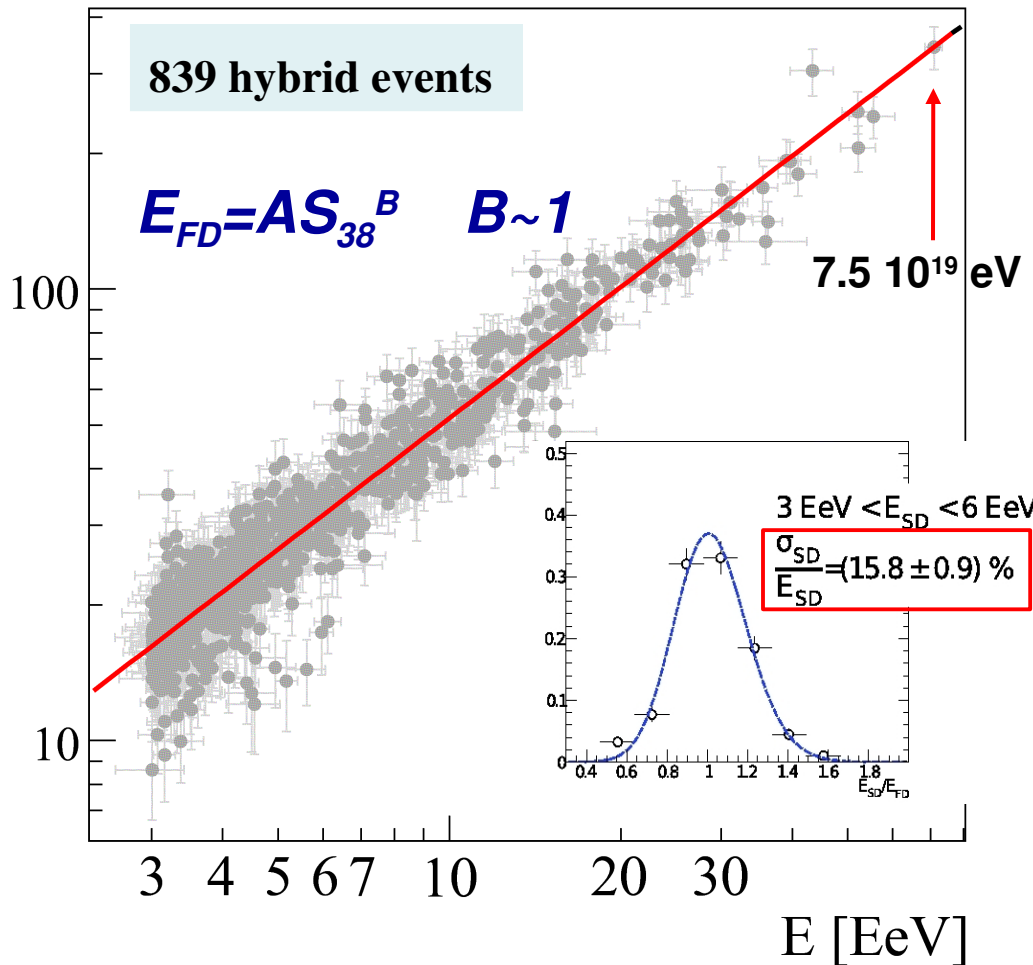
Systematic uncertainty on exposure
10% (6%) $E \sim 10^{18}$ eV ($>10^{19}$ eV)

Clear indication of the ankle



Energy calibration

R.Pesce @ ICRC 2011



Jan 2004 – Sept 2010
 $E > 3 \text{ EeV}$ - zenith $< 60^\circ$

Using hybrid events, the SD energy estimator is calibrated without relying on Monte Carlo

Method Systematic Uncertainties
7% a 10^{19} eV
15% a 10^{20} eV

FD Energy Systematics

- fluorescence yield 14%
 - FD absolute calibration 9.5%
 - invisible energy 4%
 - reconstruction 10%
 - atmospheric effects 8%
- TOTAL: 22%**

$S_{38} \rightarrow S1000$ that a shower would have produced had it arrived with a zenith angle of 38°

The attenuation curve

R.Pesce @ ICRC 2011

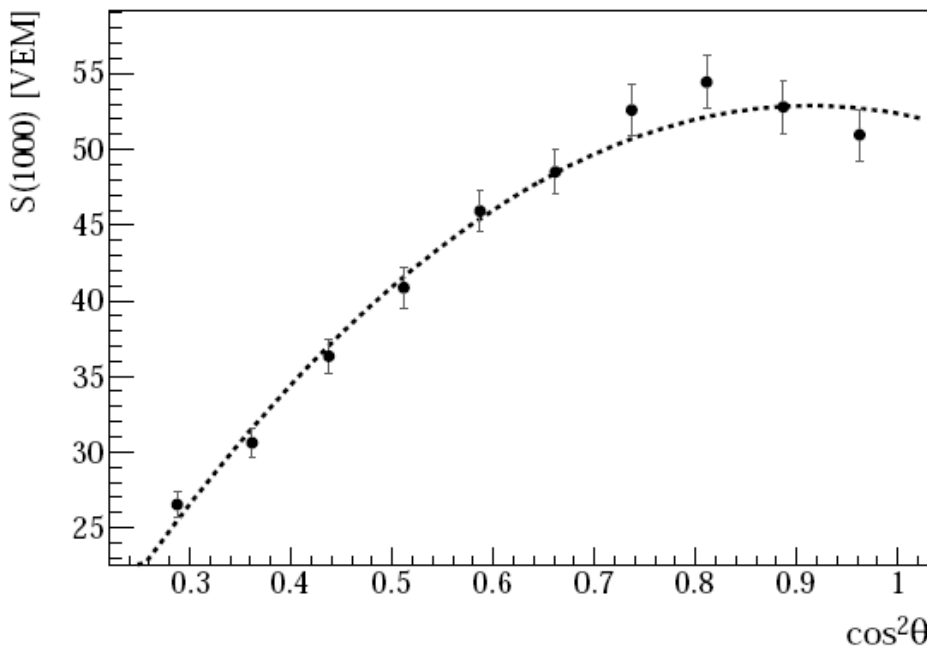
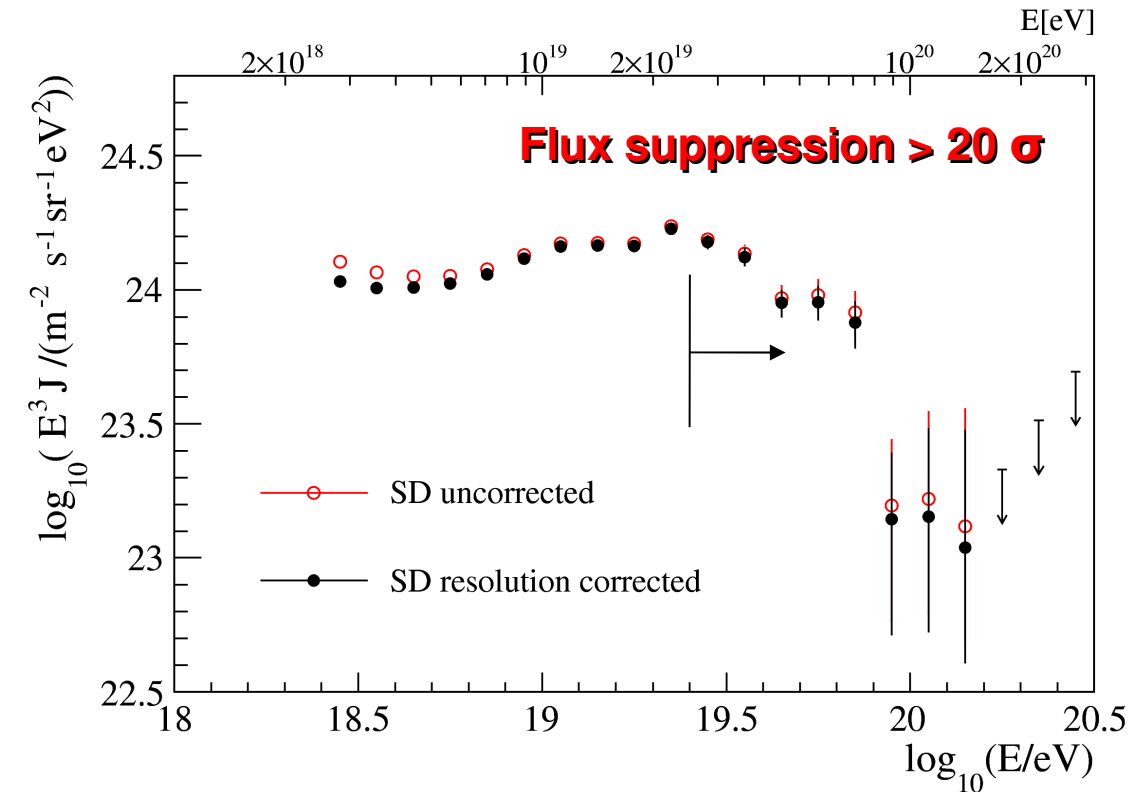


Figure 1: Attenuation curve, $CIC(\theta)$ fitted with a second degree polynomial in $x = \cos^2 \theta - \cos^2 \bar{\theta}$.

$$S_{38} \equiv S(1000)/CIC(\theta)$$

SD Energy spectrum



SD Exposure

- $E > 3 \text{ EeV}$ and zenith $< 60^\circ$
- $20905 \text{ km}^2 \text{ sr yr}$ (Jan 04 - Dec 10)
- geometrical, counting active hexagons. Not relying on simulations, full efficiency
- independent of primary mass
- 3% systematic uncertainty

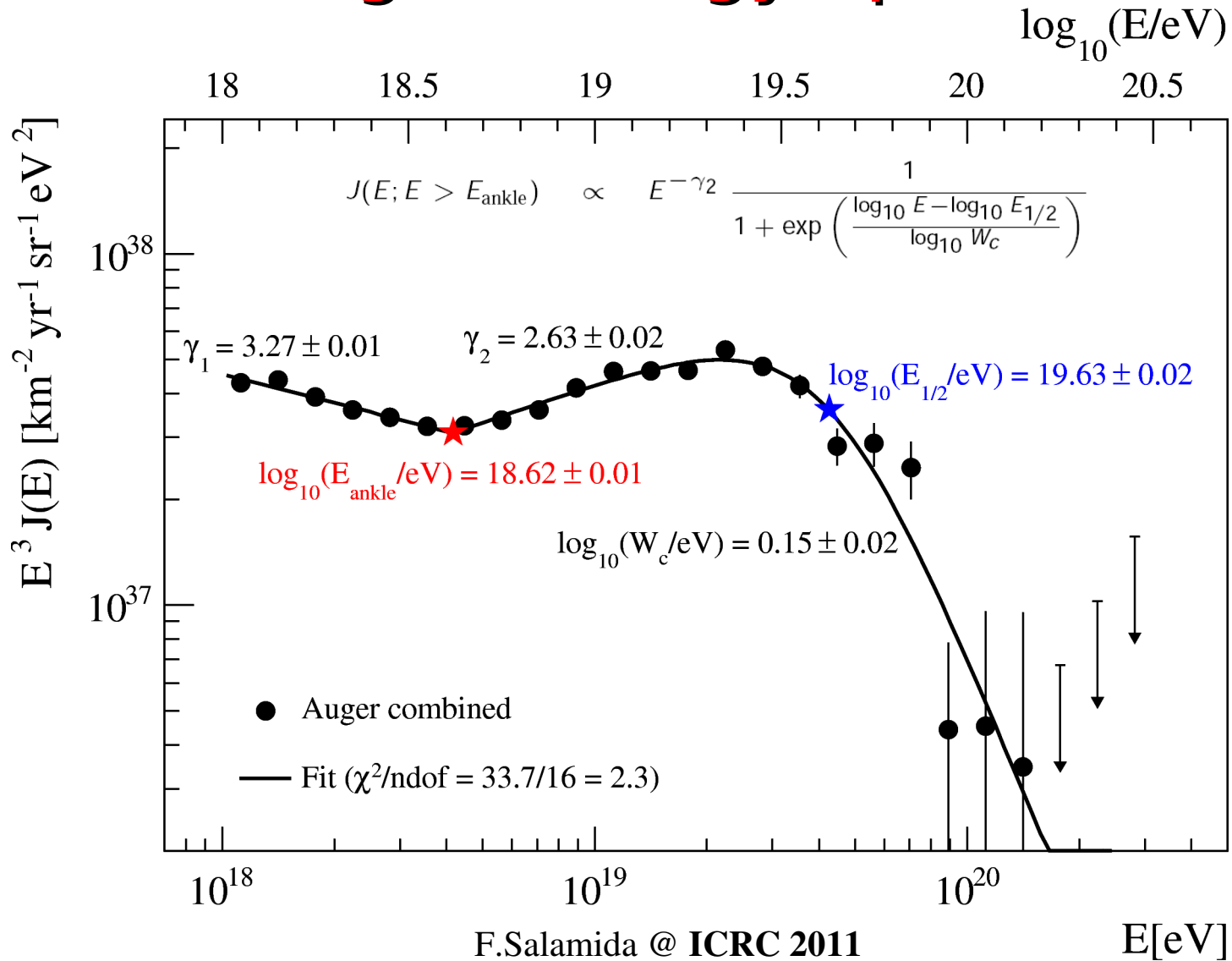
64000 (5000) events $E > 3 \times 10^{18} \text{ eV} (> 10^{19} \text{ eV})$

Energy scale from FD

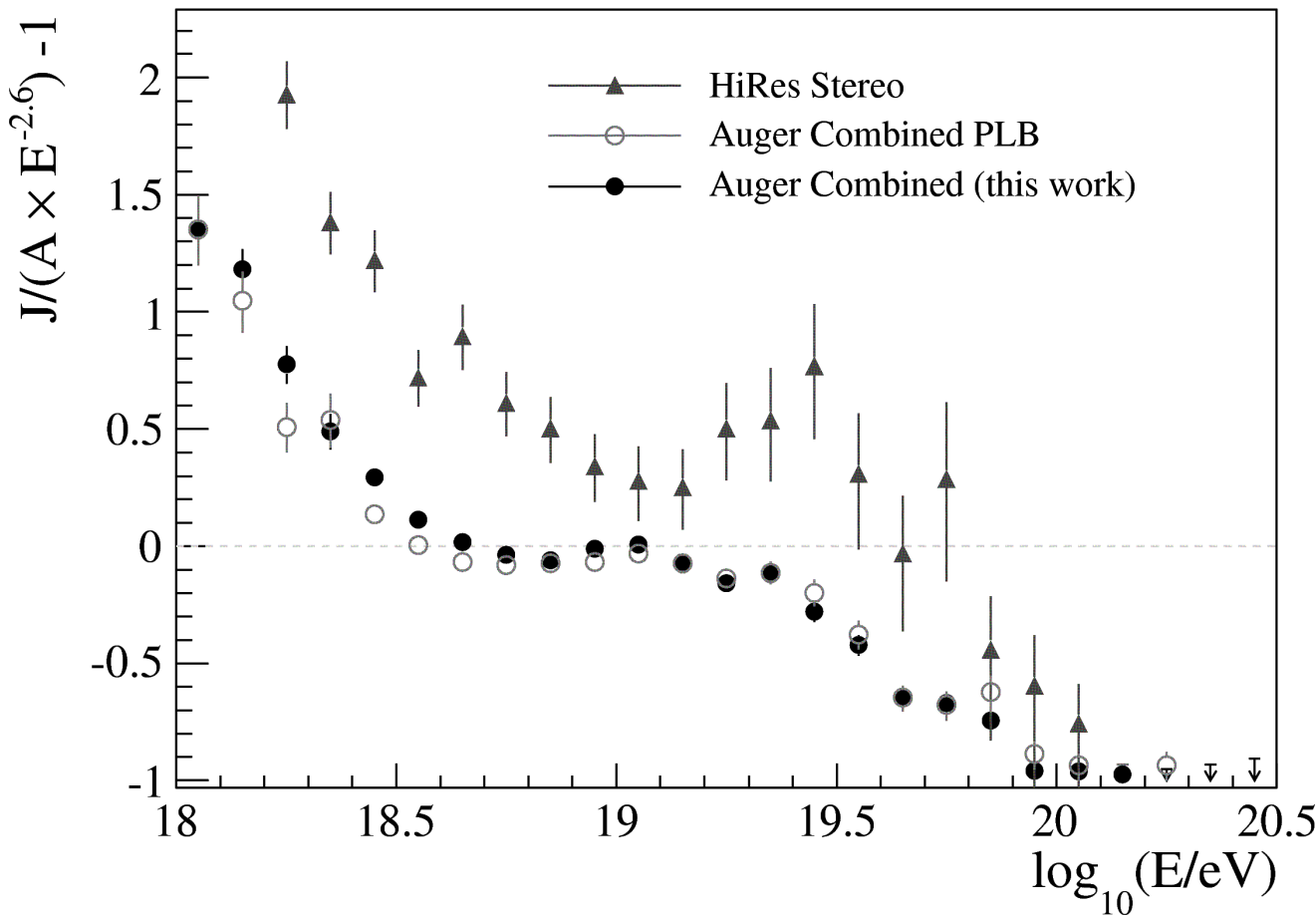
Energy resolution ~ 15%
forward folding method to correct
for the bin-to-bin migration

Total systematic uncertainty on flux ~ 6%
22% on the energy scale

The Auger Energy spectrum

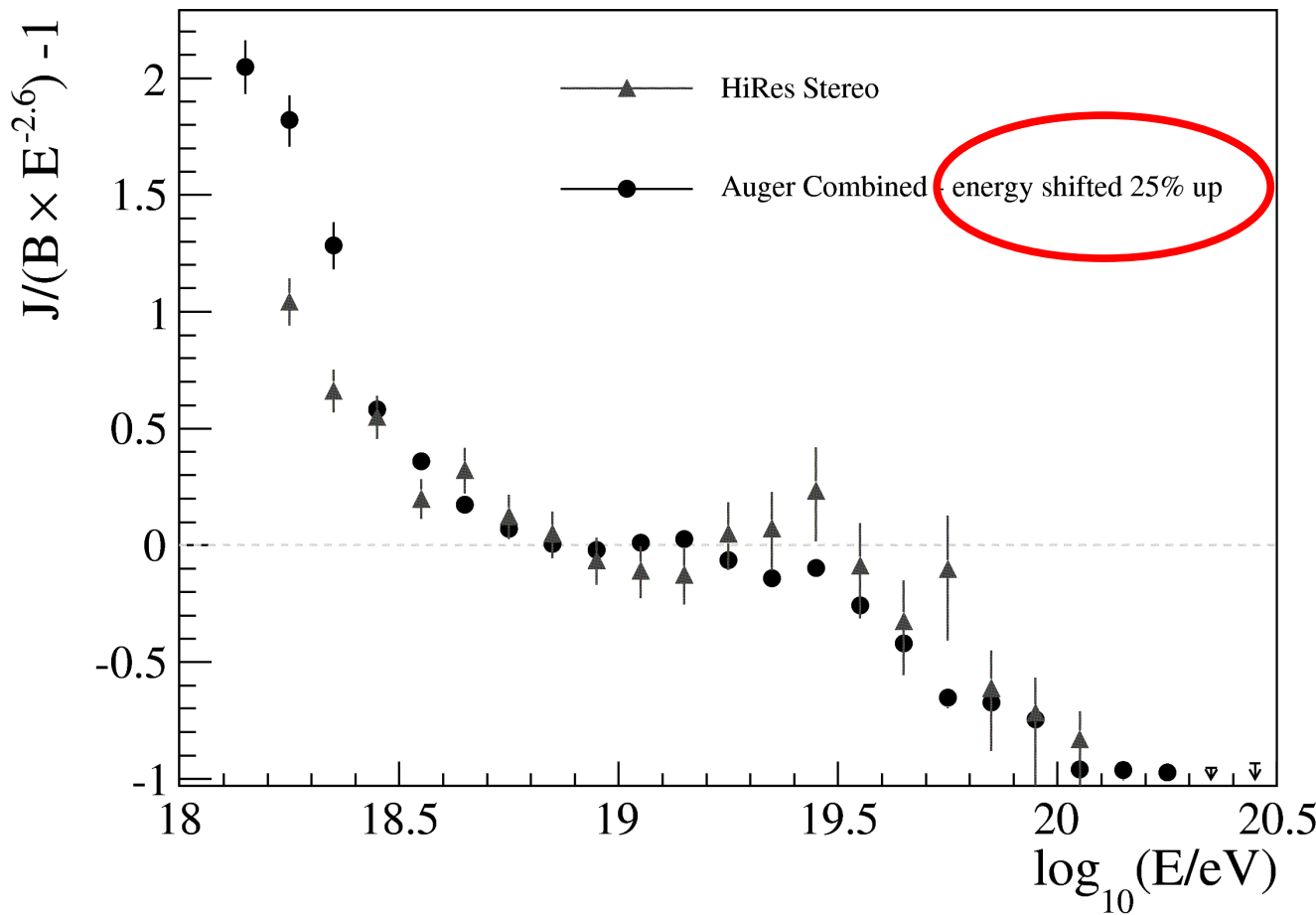


Energy spectrum: Auger vs HiRes



- Difference with respect to PLB 2010 due to changes of calibration curve
- Spectral features very well defined
- Compatible with HiRes within the energy scale systematic uncertainty

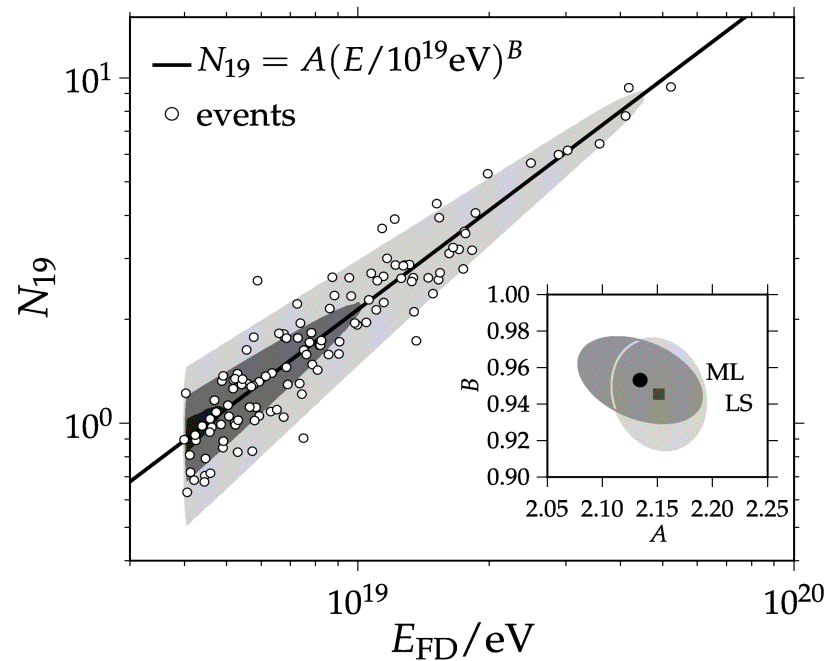
Energy spectrum: Auger vs HiRes



- Auger Energy Scale shifted of 25%
- Main spectrum features observed by both experiments

Spectrum with inclined events

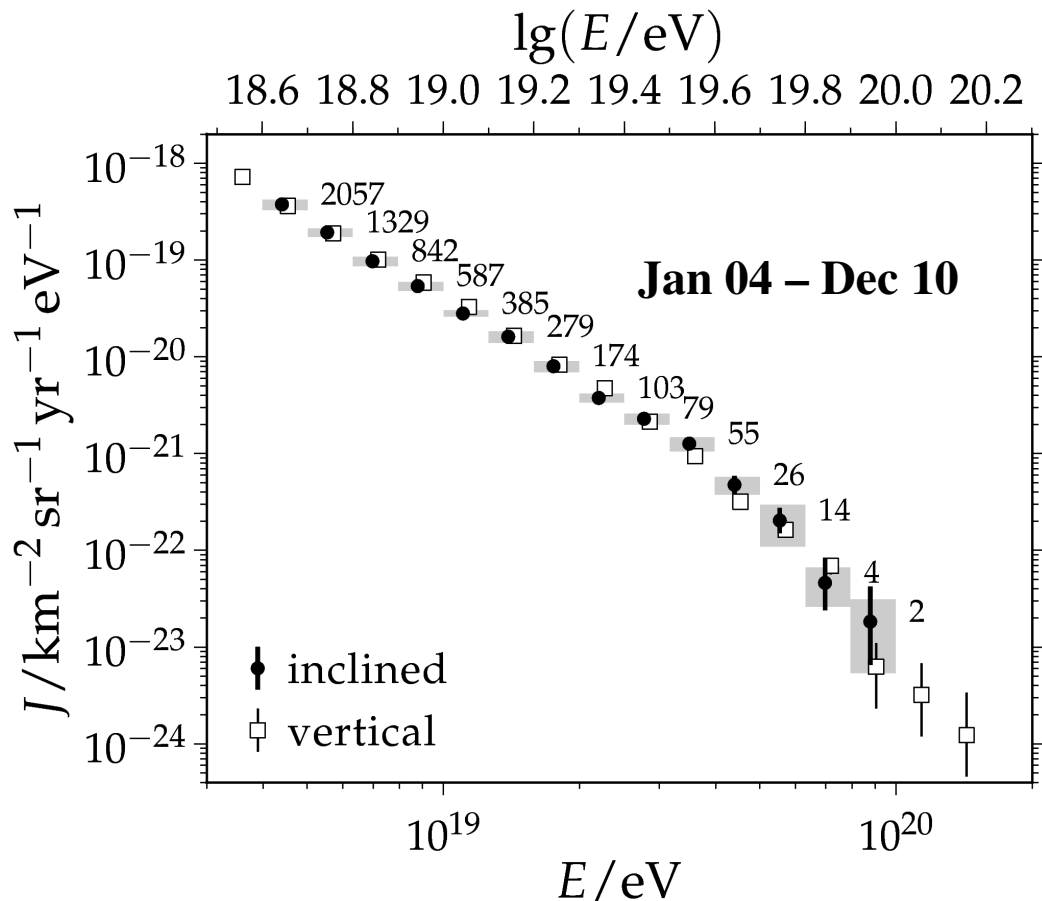
Energy Calibration with FD energy



Energy estimator:
 $N_{19} \rightarrow$ lateral muon density

- Energy $> 4 \cdot 10^{18}$ eV

- $62^\circ < \text{Zenith} < 80^\circ$



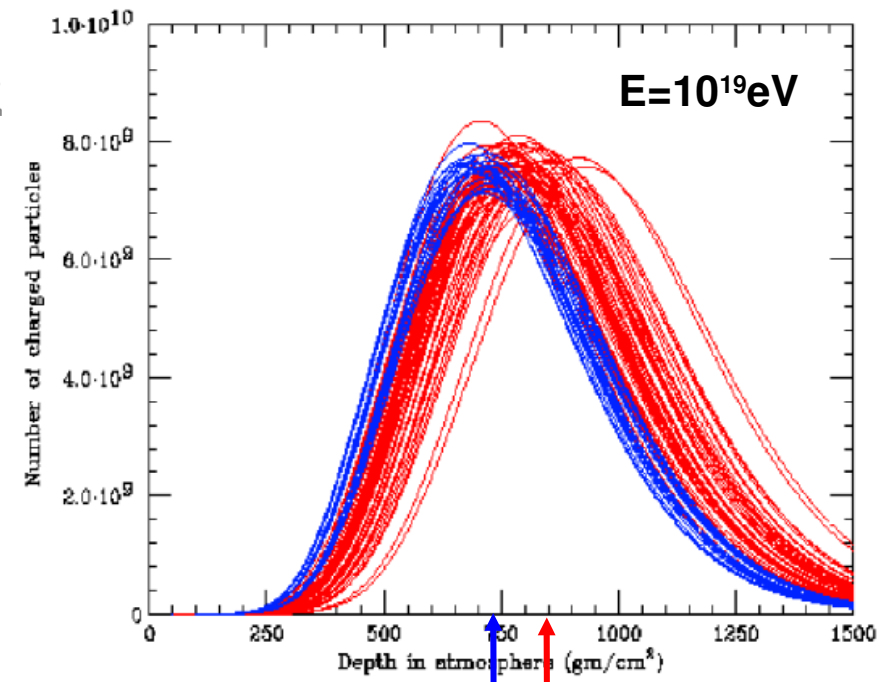
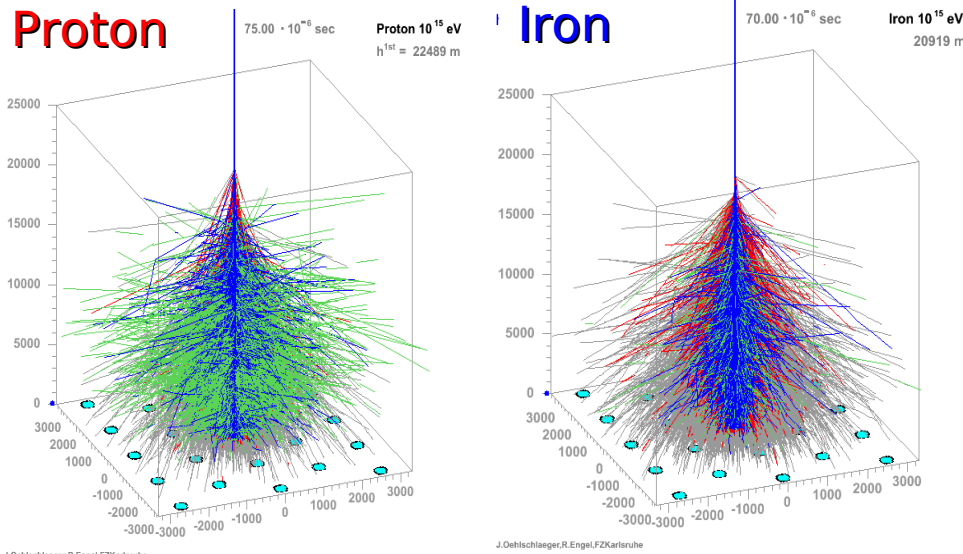
Full agreement with
flux from vertical showers

Results

- Energy spectrum
- **Mass composition**
- Astrophysics
- Search for photons and neutrinos
- Hadronic interactions

X_{\max} as indicator of mass composition

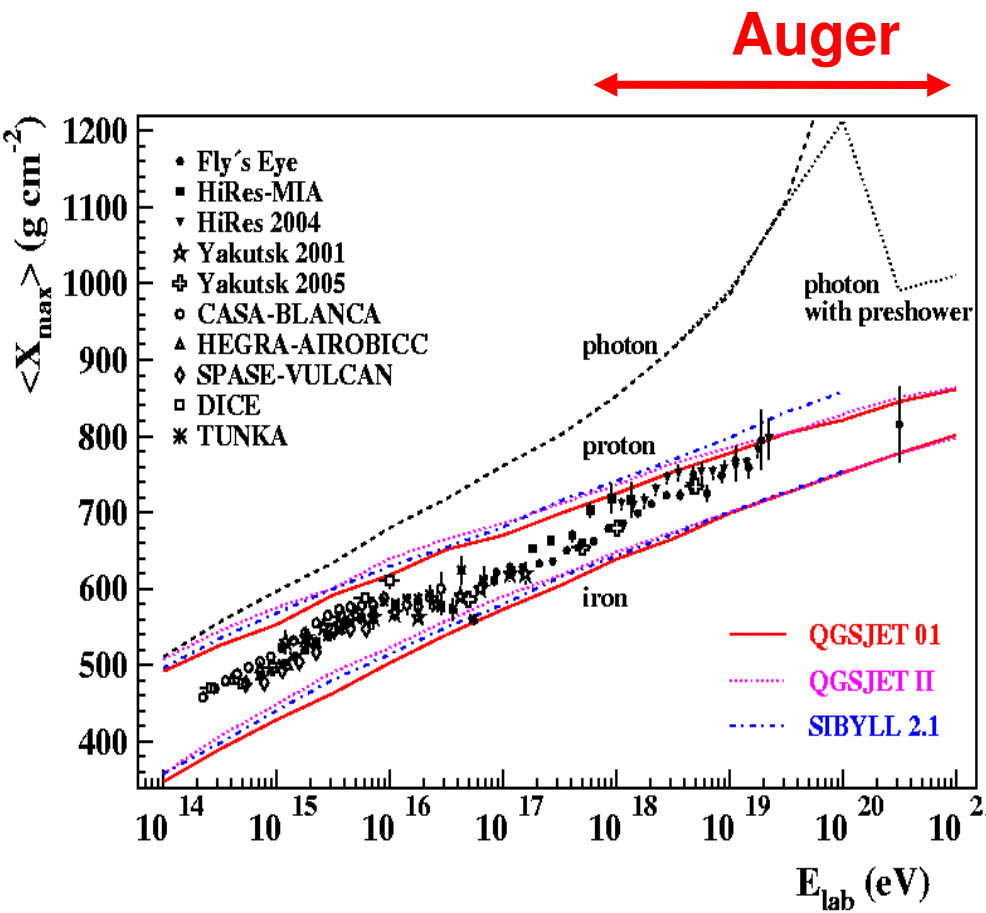
Atmospheric depth of shower maximum correlated with primary type
(Example: proton showers develop deeper than iron , $X_{\max,pr} > X_{\max,Fe}$)



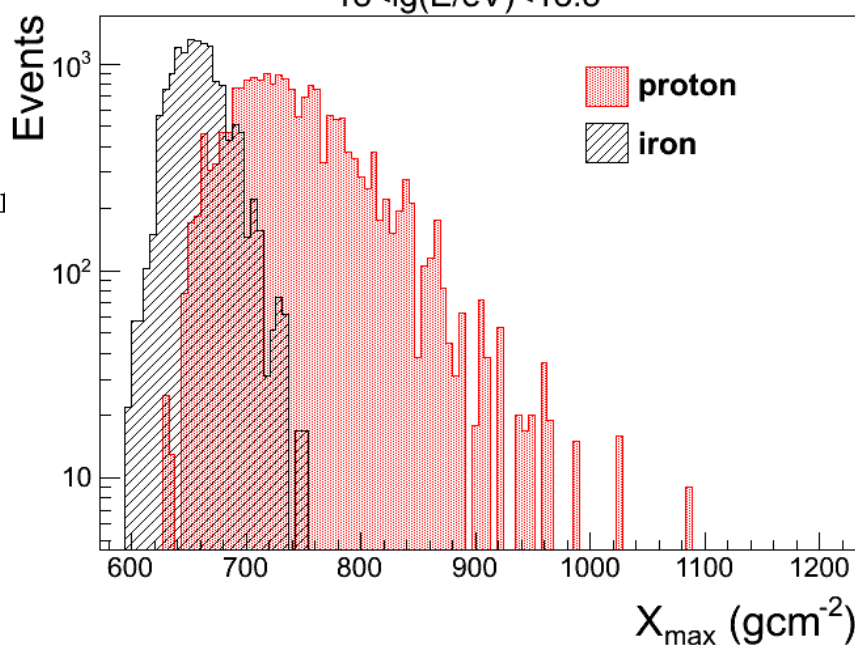
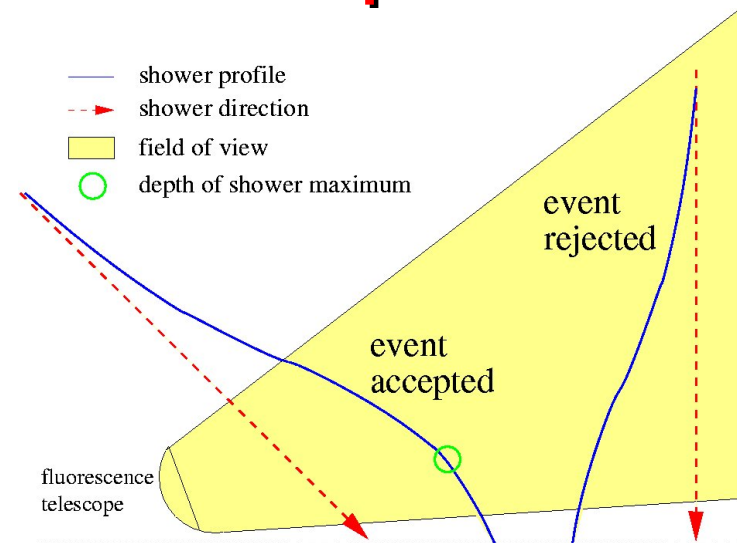
hadrons muons electrs neutrals

<http://www-ik.fzk.de/corsika>

Observation of longitudinal profile



$$\langle X_{\max} \rangle = \alpha(\ln E - \langle \ln A \rangle) + \beta$$

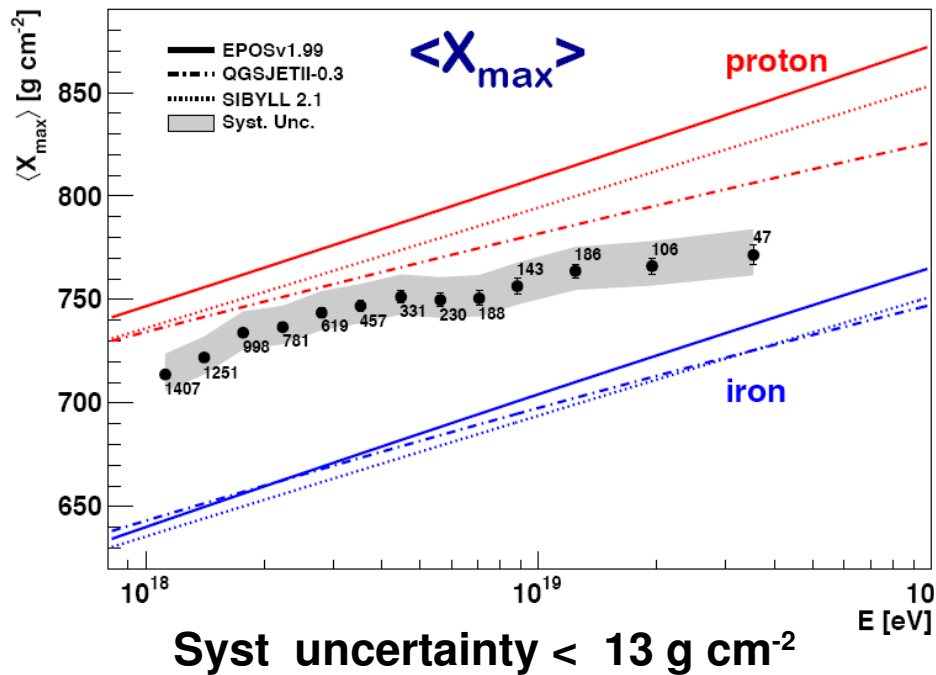


$\langle X_{\max} \rangle$ and its RMS

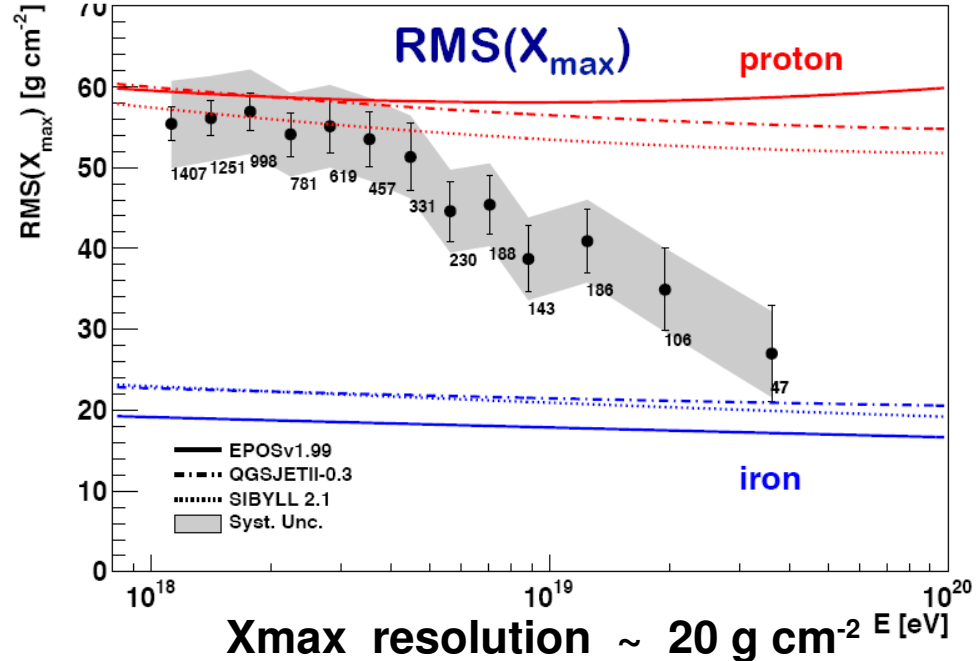
- sensitive to mass composition
- key observables for composition studies

Mass Composition: mean X_{\max} and its RMS

G. Pinto, P.Facal @ ICRC 2011



Syst uncertainty < 13 g cm⁻²



Xmax resolution ~ 20 g cm⁻²

6744 hybrid events (Dec 2004 – Sept 2010) $E > 10^{18}$ eV

- interpretation depends on hadronic interaction models
- increase of the mean mass with the energy
- Open issue: HiRes (and first results of TA) suggest a lighter composition

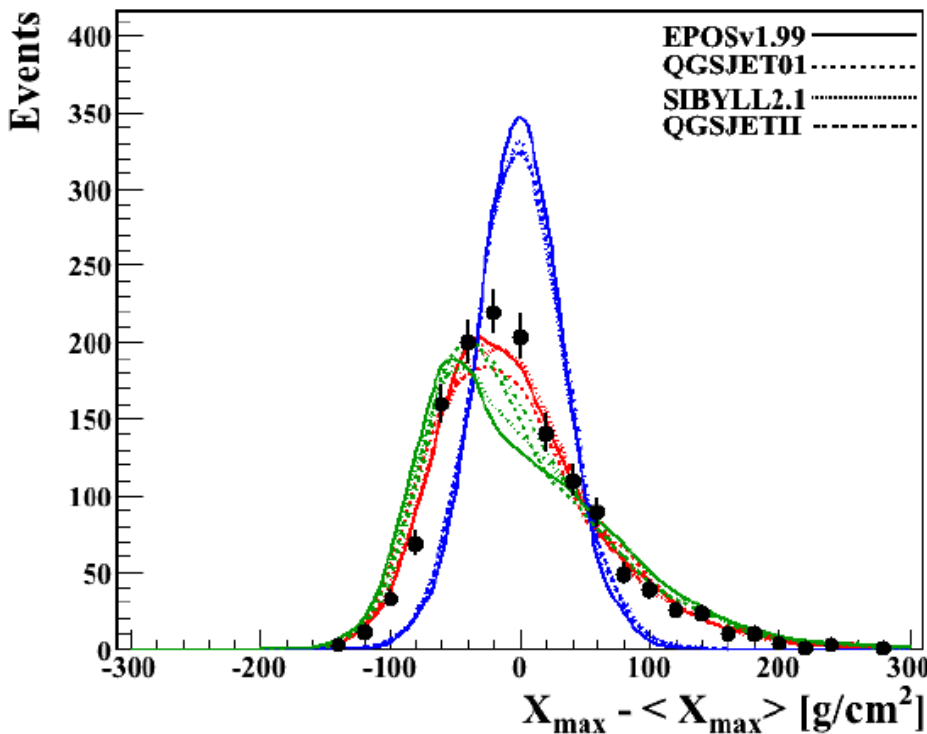
Distributions – Shape

p Fe Mixed

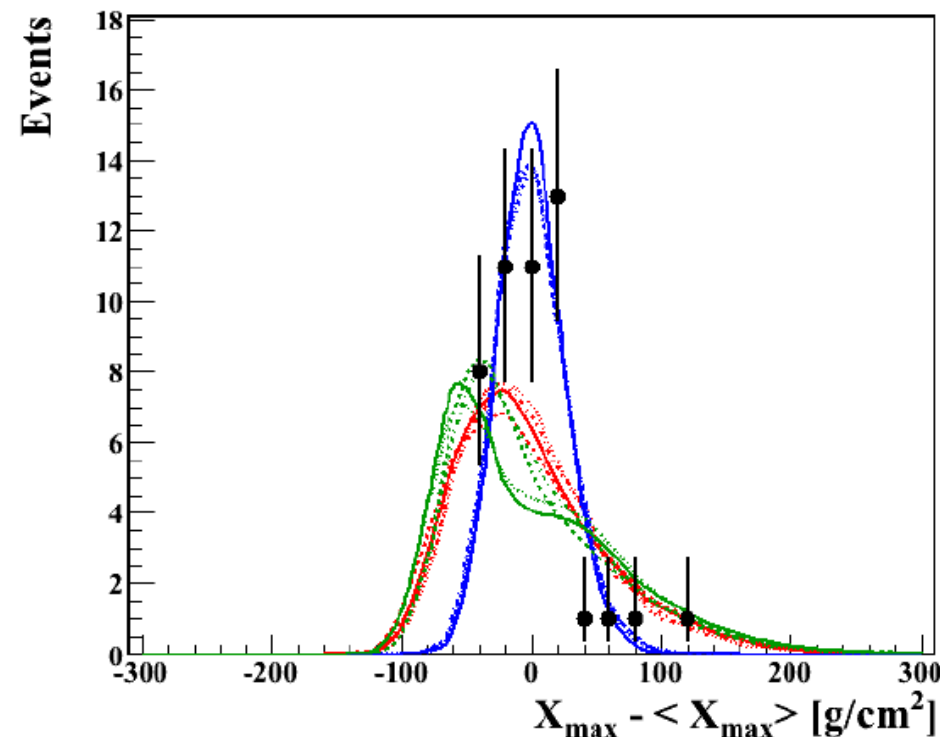
Subtract $\langle X_{\max} \rangle$ to each of the distributions and compare only the shapes

Mixed: 50% p + 50% Fe

$18.1 > \log(E) > 18.0$

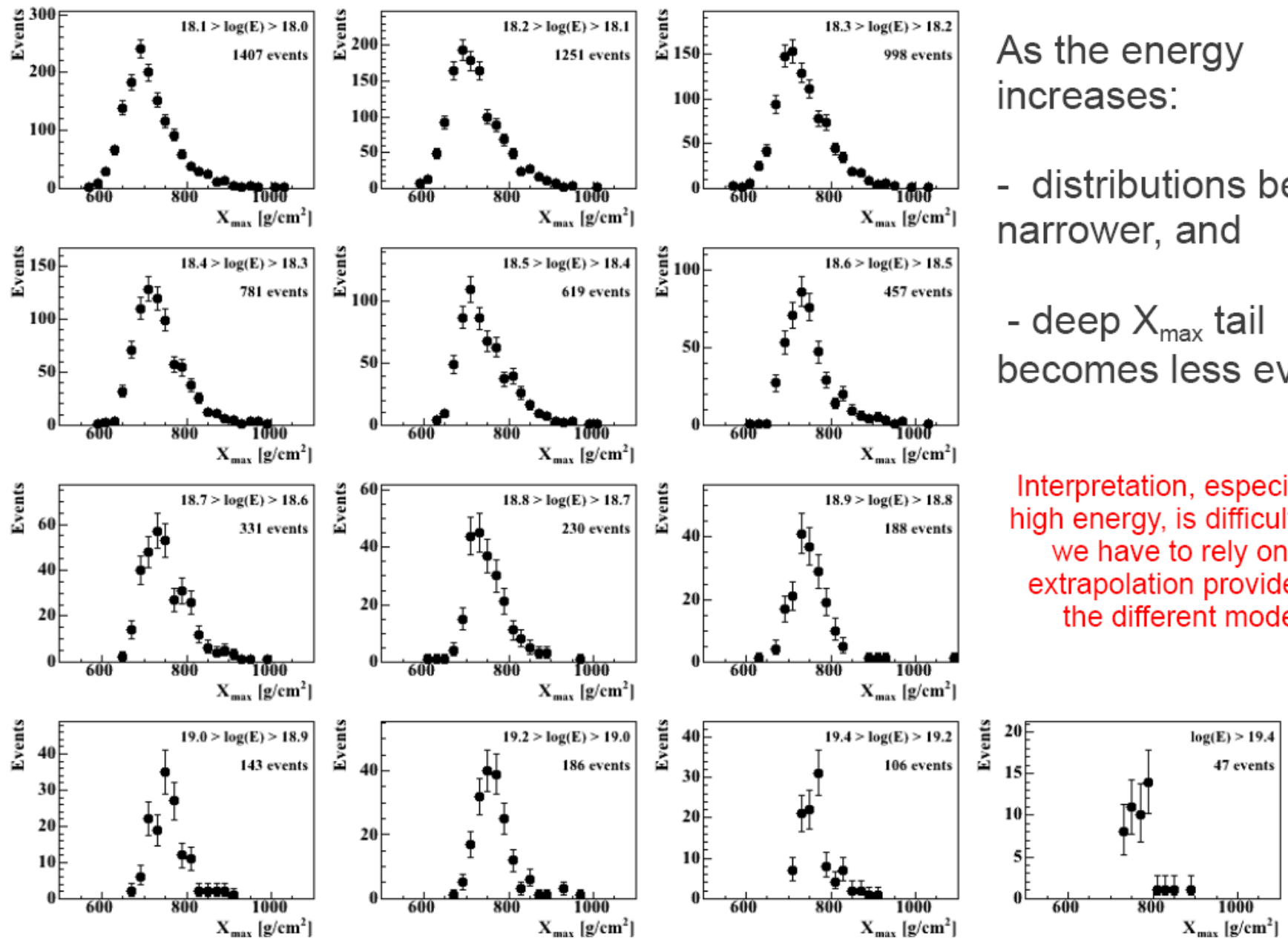


$\log(E) > 19.4$



Fits light to heavier

X_{\max} distributions



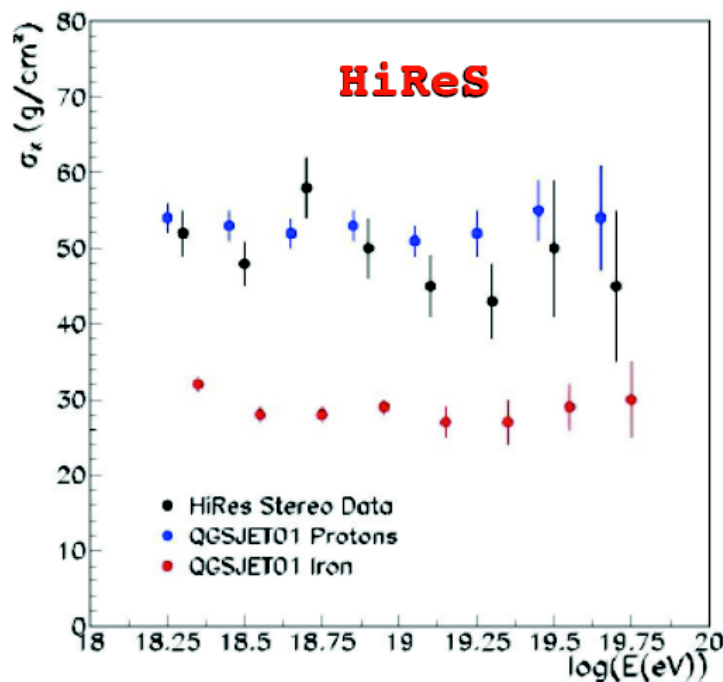
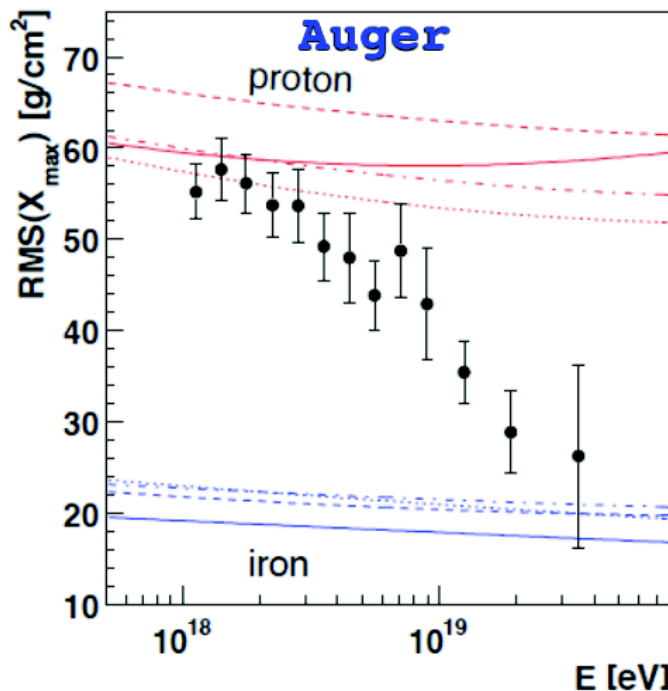
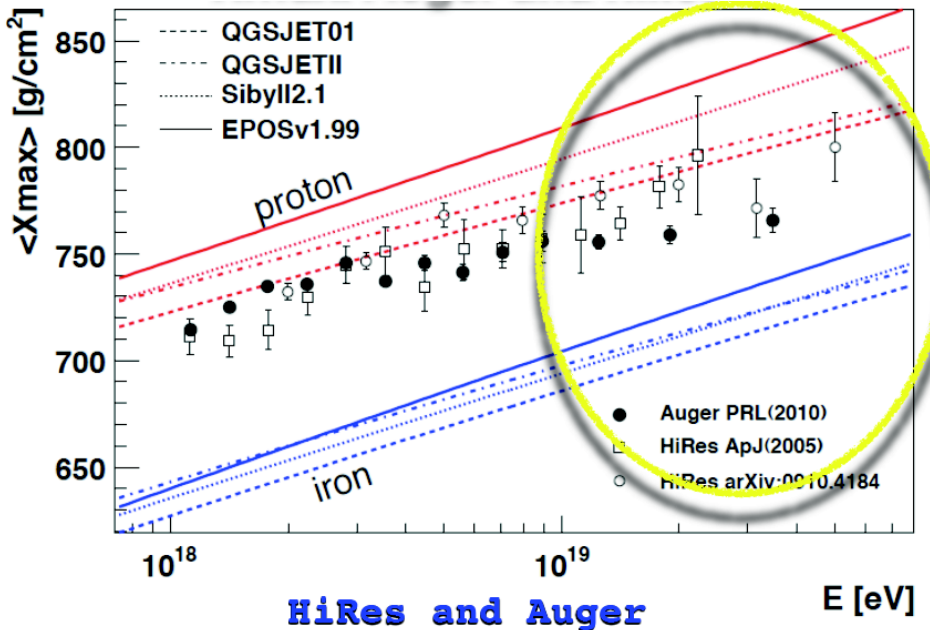
As the energy increases:

- distributions become narrower, and
- deep X_{\max} tail becomes less evident

Interpretation, especially at high energy, is difficult since we have to rely on the extrapolation provided by the different models

HiRes vs Auger

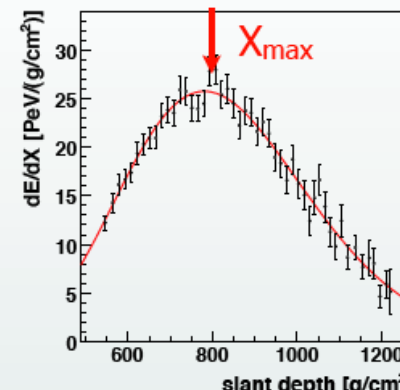
Mass composition



Measurement of Longitudinal Shower Development

From the Fluorescence Detector:

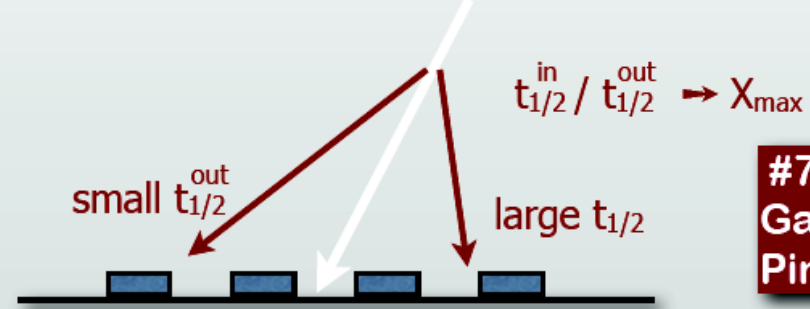
- $\langle X_{\max} \rangle$
- full X_{\max} -distribution
- RMS(X_{\max})



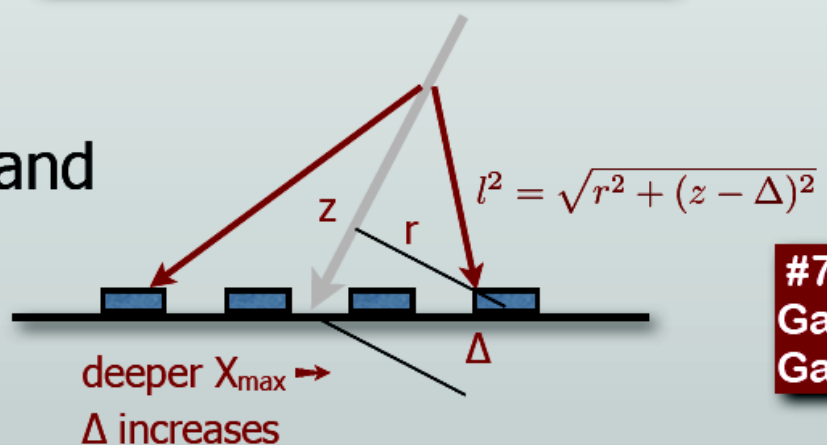
#725:
Facal

From the Surface Detector:

- azimuthal asymmetry of the signal risetime: Θ_{\max}
- time difference between μ and shower plane $\rightarrow \langle X_{\max}^{\mu} \rangle$



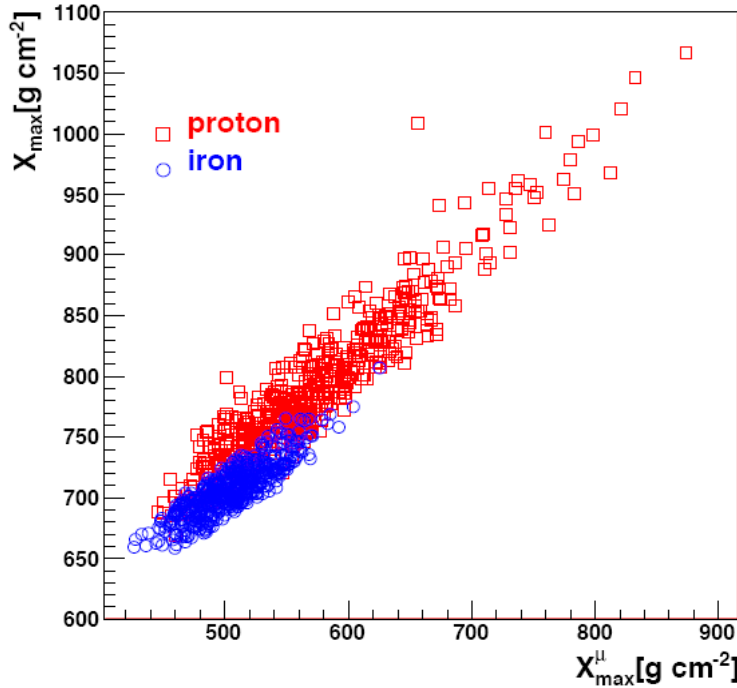
#709:
Garcia
Pinto



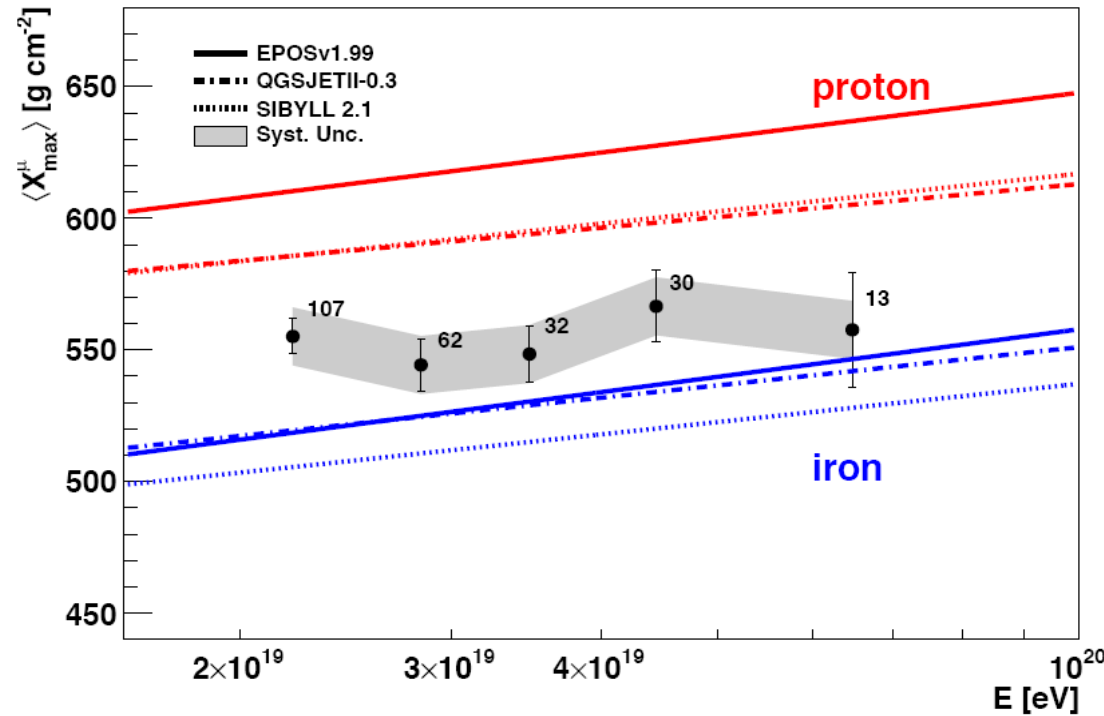
#735:
Garcia
Gamez

Mass Composition: X_{\max}^{μ}

X_{\max}^{μ} vs X_{\max}



$\langle X_{\max}^{\mu} \rangle$ vs E

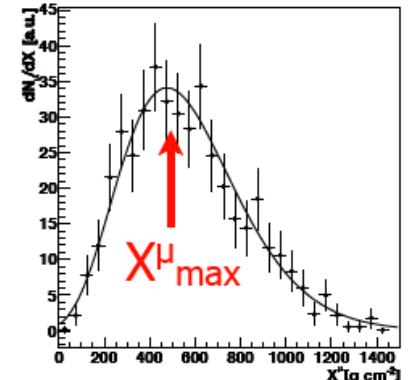


- MC hybrid events
- Correlation with X_{\max}

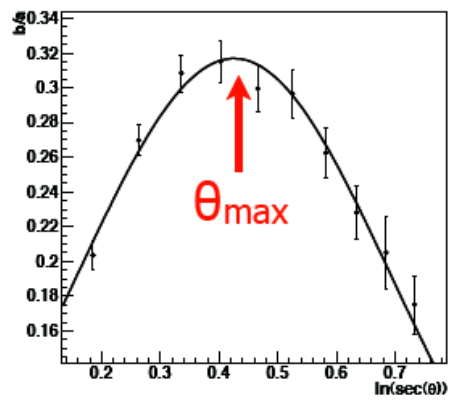
- 244 SD events (Jan 2004 – Dec 2010)
- $E > 20$ EeV $55^\circ < \theta < 65^\circ$

Comparison of Methods

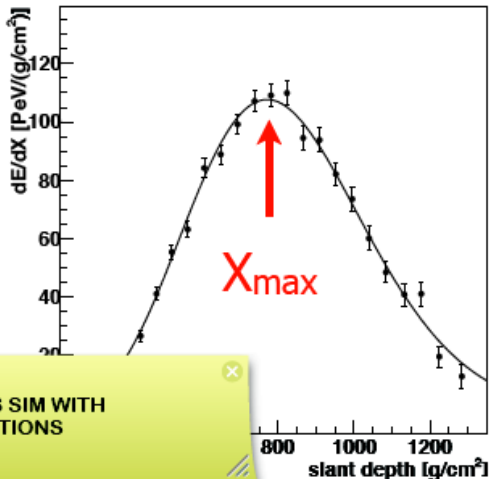
#709: Garcia Pinto



Muon Production Depth
from timing differences



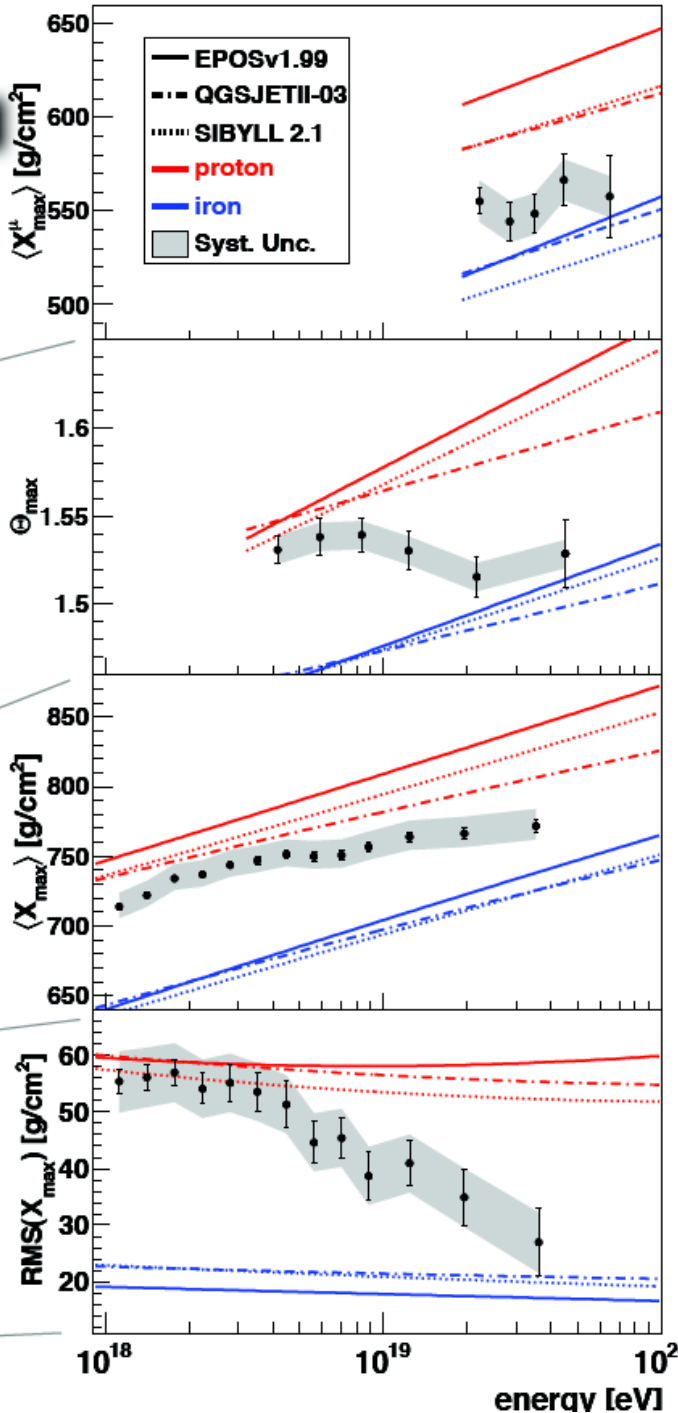
Shower Maximum from
asymmetry of rise times



PERHAPS SIM WITH
FLUCTUATIONS

X_{max} from FD

RMS(X_{max}) from FD



Results

- Energy spectrum
- Mass composition
- **Hadronic Interactions**
- Astrophysics
- Search for photons and neutrinos

Measurement of the p-air cross-section

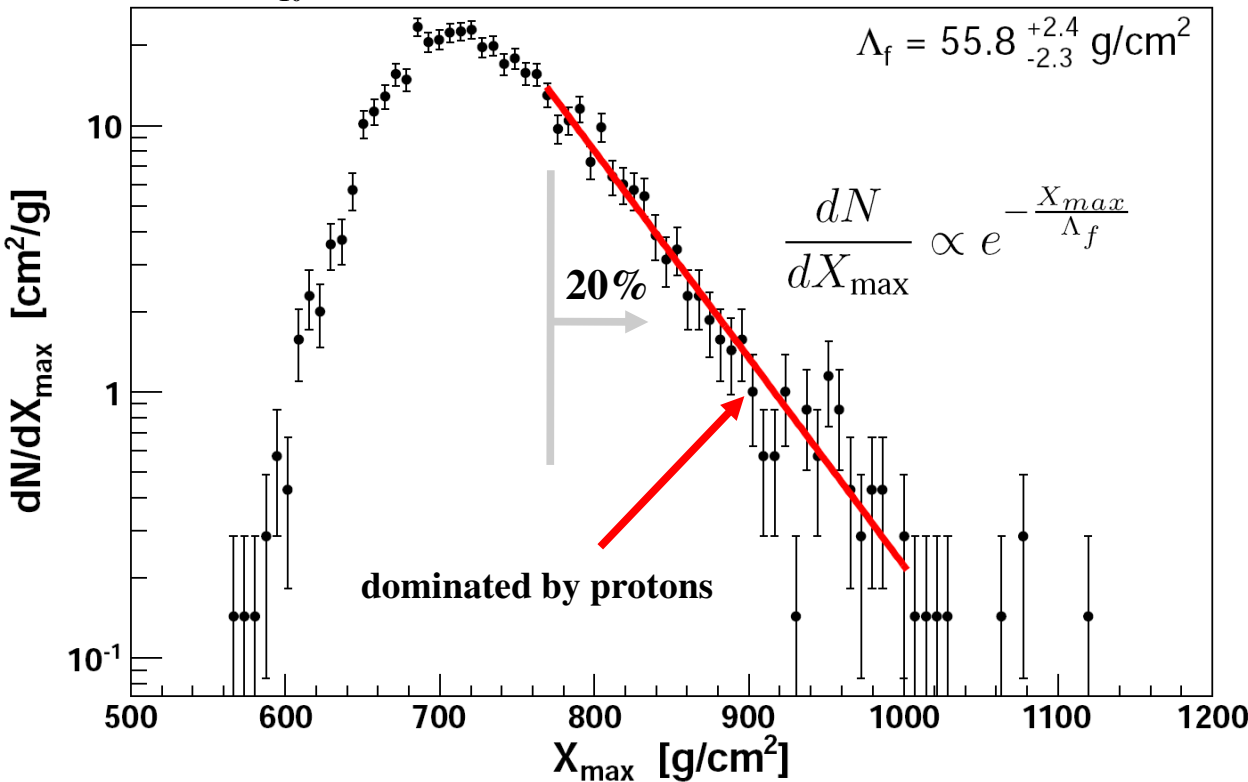
Tail of the distribution of $\langle X_{\max} \rangle$ sensitive to cross-section

Ellsworth et al. Phys. Rev. D26 (1982) 336

Fly's Eye →

Baltrusaitis et al. Phys. Rev. Lett. 52 (1984) 1380

$$18 < \log_{10}(E/eV) < 18.5$$



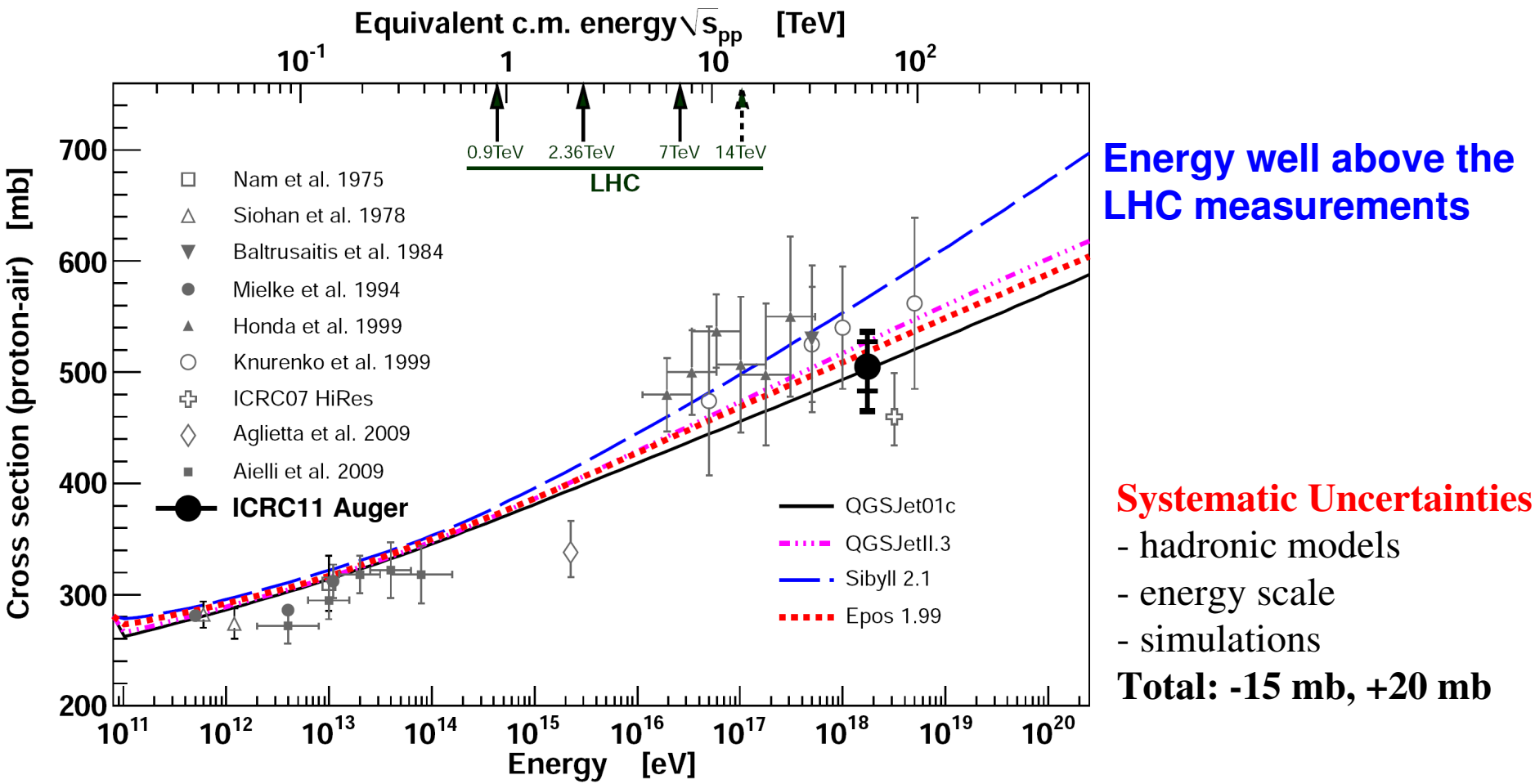
Dedicated analysis to select a proton-enriched data sample

Why 20%?

15% helium contamination produces a bias at the level of the statistical uncertainties

Use simulations to correlate Λ_f^{MC} with cross-sections

Λ_f^{MC} adjusted to reproduce the measured Λ_f



$$\langle E \rangle \sim 1.7 \text{ EeV} \quad \sqrt{s} = 57 \text{ TeV}$$

$$\sigma_{\text{p-air}} = (505 \pm 22_{\text{stat}}^{+26}_{-34} \text{syst}) \text{ mb}$$

Additional Uncertainties due to diverse contaminations:

- photon fraction 0.5% +10 mb
- helium fraction 10% -12 mb
- helium fraction 25% -30 mb

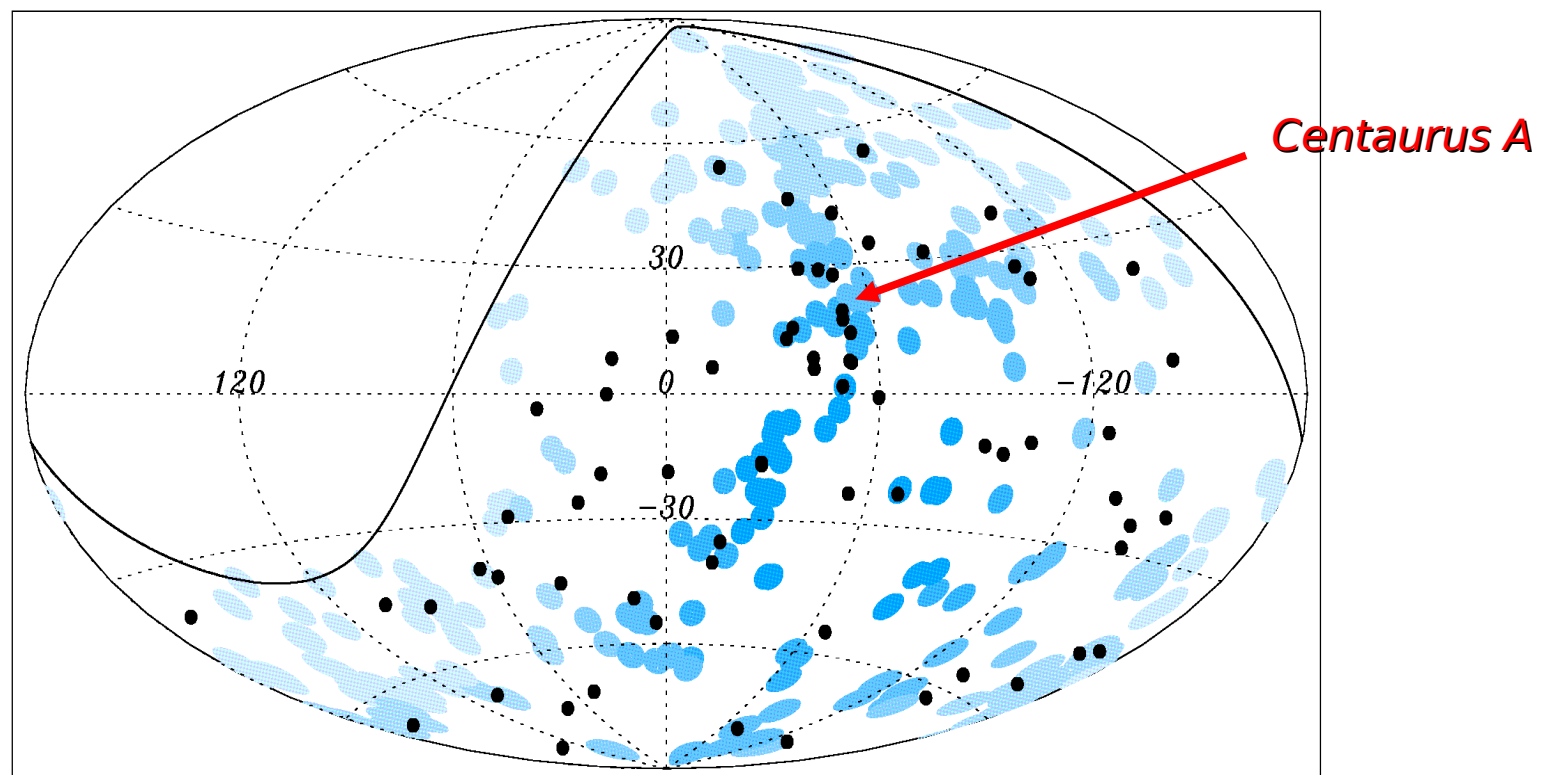
Results

- Energy spectrum
- Mass composition
- Hadronic Interactions
- **Astrophysics**
- Search for photons and neutrinos

Anisotropy at the highest energy

Astropart. Phys. 34 (2010) 314

Jan 2004
Dec 2009



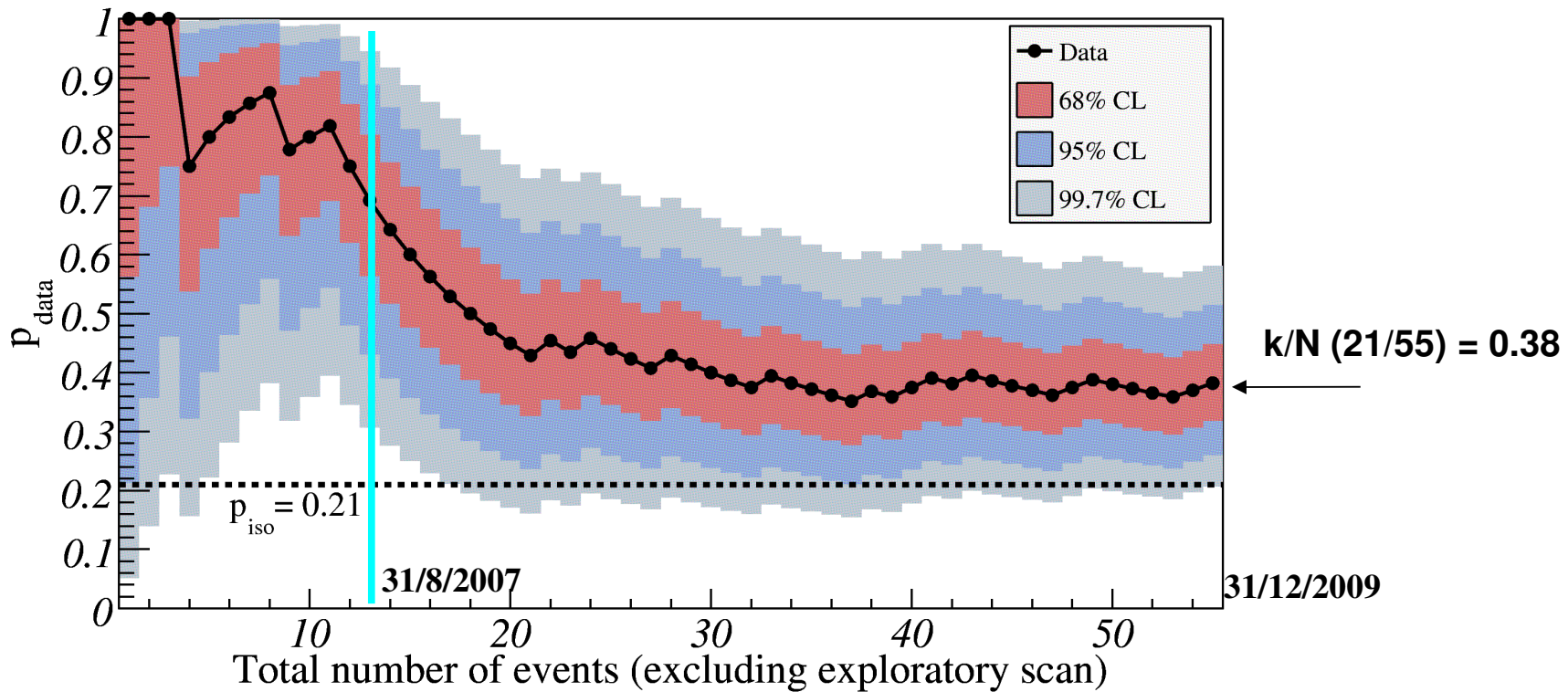
The 69 events with Energy > 55 EeV detected by the Pierre Auger Observatory

Blue circles of radius 3.1° centered at the positions of the 318 AGNs < 75 Mpc in the VCV catalog. The exposure-weighted fraction of the sky covered by the blue circles is 21% (fraction of correlating events under the hypothesis of isotropy)

Limitations of the catalogue: incomplete and inhomogeneous

Degree of correlation

Astropart. Phys. 34 (2010) 314



Degree of correlation $p_{\text{data}} = k/N$ vs total number of time-ordered events:

the 68%, 95% and 99.7% confidence level intervals around the most likely value are shaded.
The isotropic value is $p_{\text{iso}} = 0.21$. The current estimate of the signal is $0.38 (+0.07, -0.06)$.

Facts and open issues

- the degree of correlation has decreased (from 69% to 38%)
- probability from an isotropic distribution $\sim 3 \cdot 10^{-3}$
- with the current degree of correlation about four years of new data are required for a 5σ significance

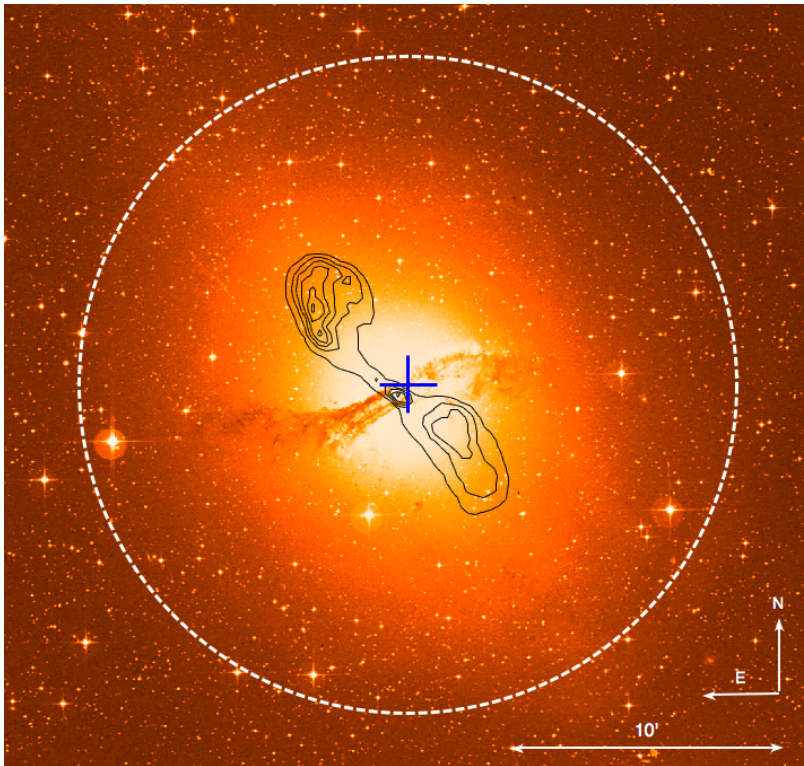
Anisotropy consistent with a proton based composition

Xmax measurement suggest mixed composition (though not measured for $E > 55$ EeV)

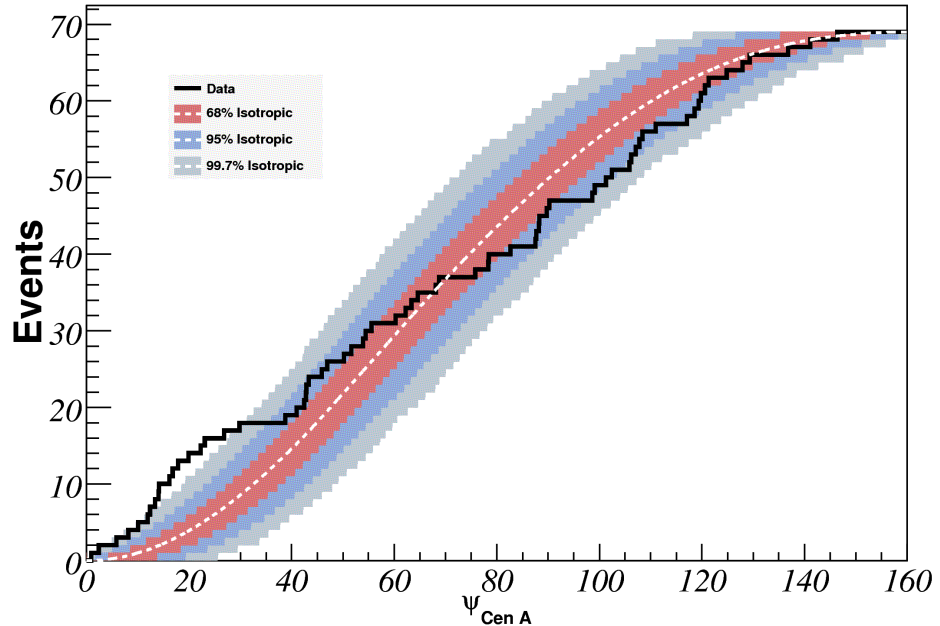
Anisotropy not confirmed by HiRes (lower statistics, northern Hemisphere)

Centaurus A

Astropart. Phys. 34 (2010) 314



CEN A: optical image, radio contours (VLA),
VHE best fit position and 95% C.L. (HESS).
From <http://arxiv.org/pdf/0903.1582v1>



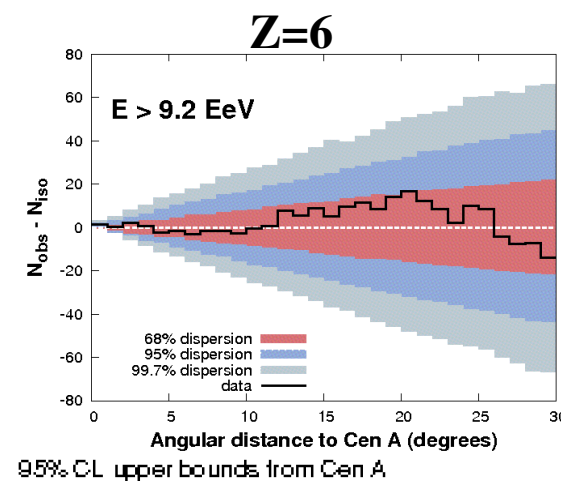
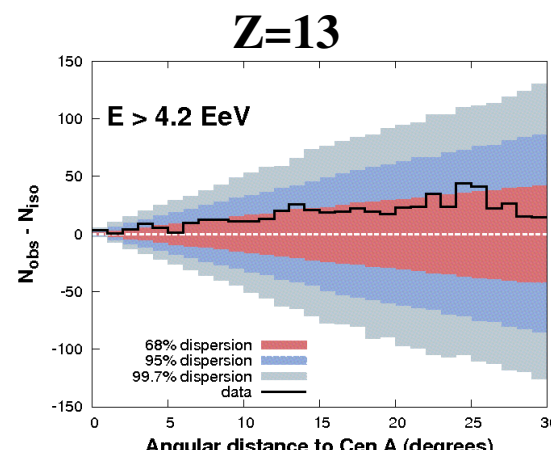
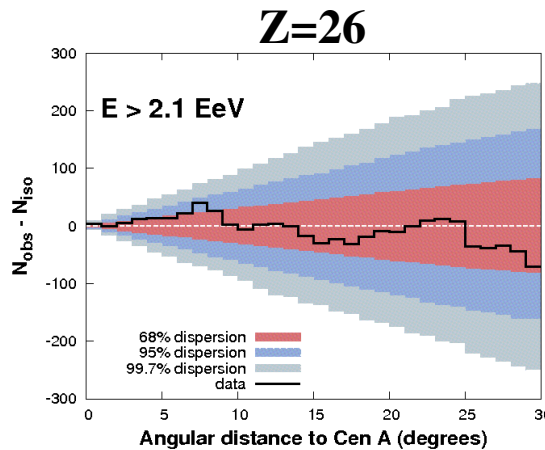
Cumulative number of events with energy $E \geq 55$ EeV as a function of angular distance from the direction of Cen A.

The bands correspond to the 68%, 95%, and 99.7% dispersion expected for an isotropic flux. 13 events fall in this area (18°) vs. 3.2 expected from isotropic flux.

Anisotropy and chemical composition

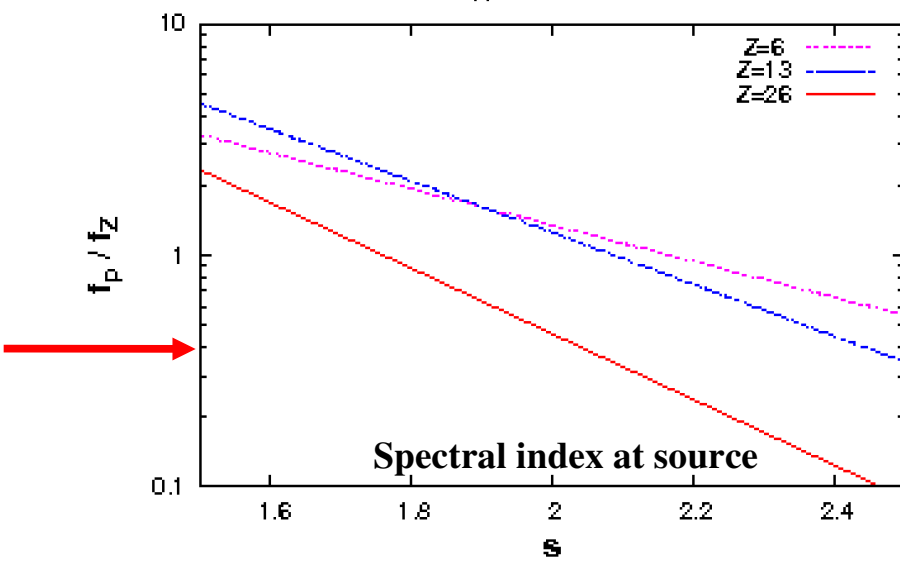
If the excess at $E_{\text{thres}} > 55 \text{ EeV}$ is due to nuclei (Z), the proton counterpart should be observed at energy above E_{thres}/Z

Lemoine & Waxman JCAP 11 (2009) 009



No excess observed from CEN A at lower energies

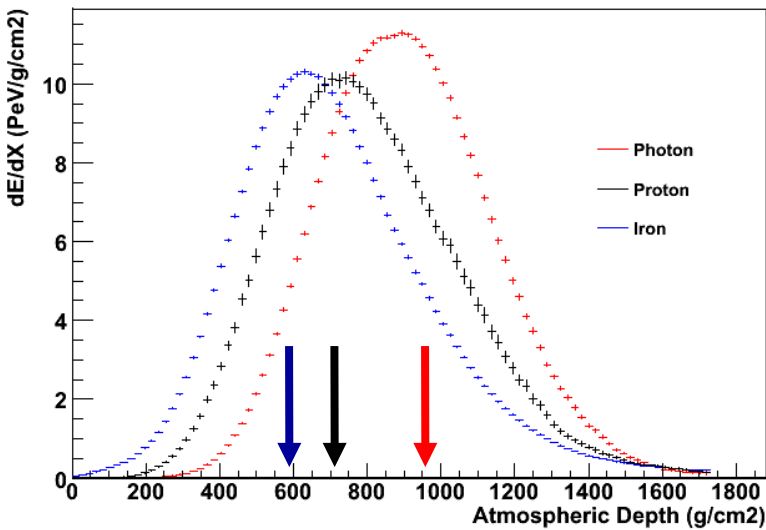
Upper limit to the proton fraction at the source (within the model assumption)



Results

- Energy spectrum
- Mass composition
- Hadronic Interactions
- Astrophysics
- **Search for photons and neutrinos**

Search for photon primaries

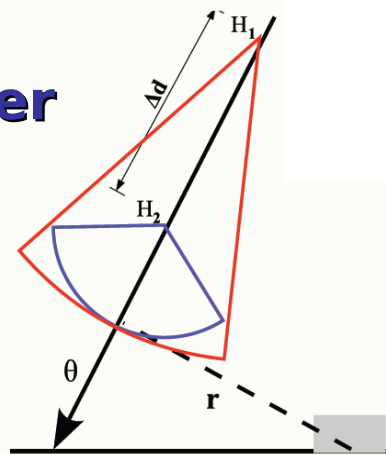


Photon showers develop deeper in the atmosphere

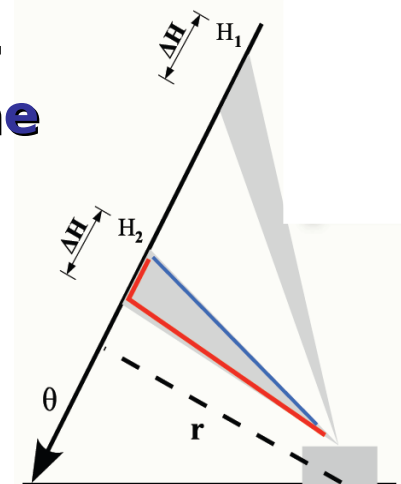
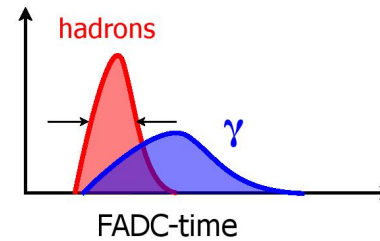
FD: search for events with deep X_{max}

SD: search based on signal time structure

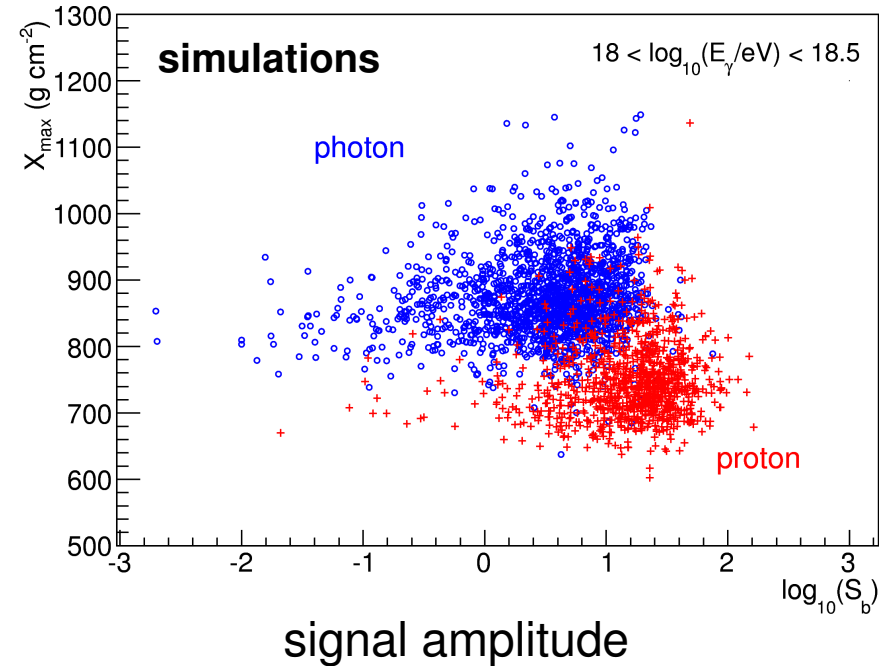
Deeper
showers larger
curvature



Slower signal,
longer risetime



(hybrid) photon/hadron separation



Realistic and time dependent

actual DAQ and atmospheric conditions
taken into account (same approach used
for the hybrid spectrum)



Proton background less than 1%

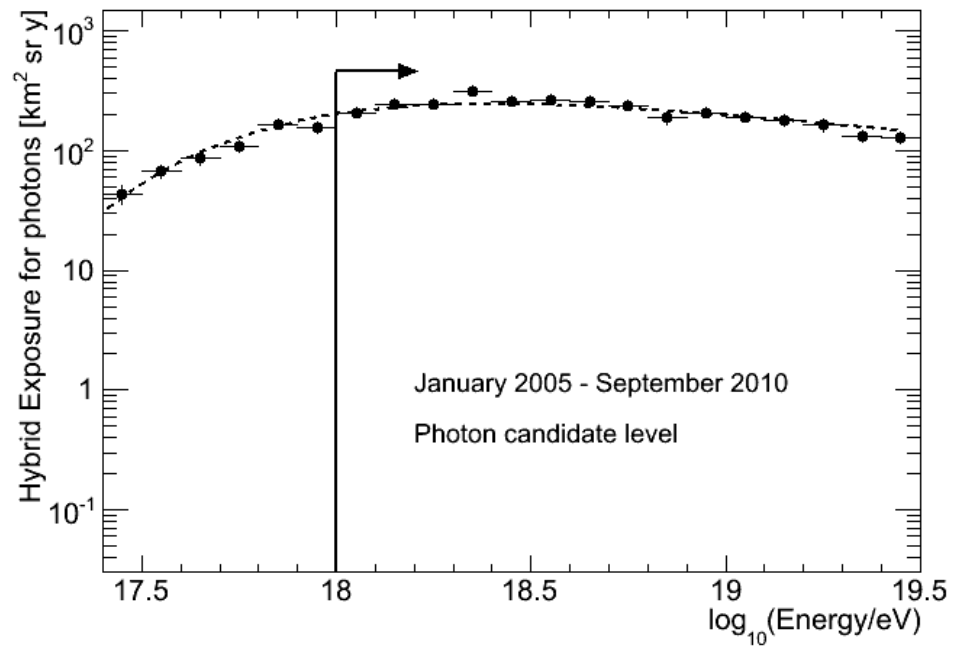
- deep shower

large X_{\max} (from FD)

- structure of the LDF

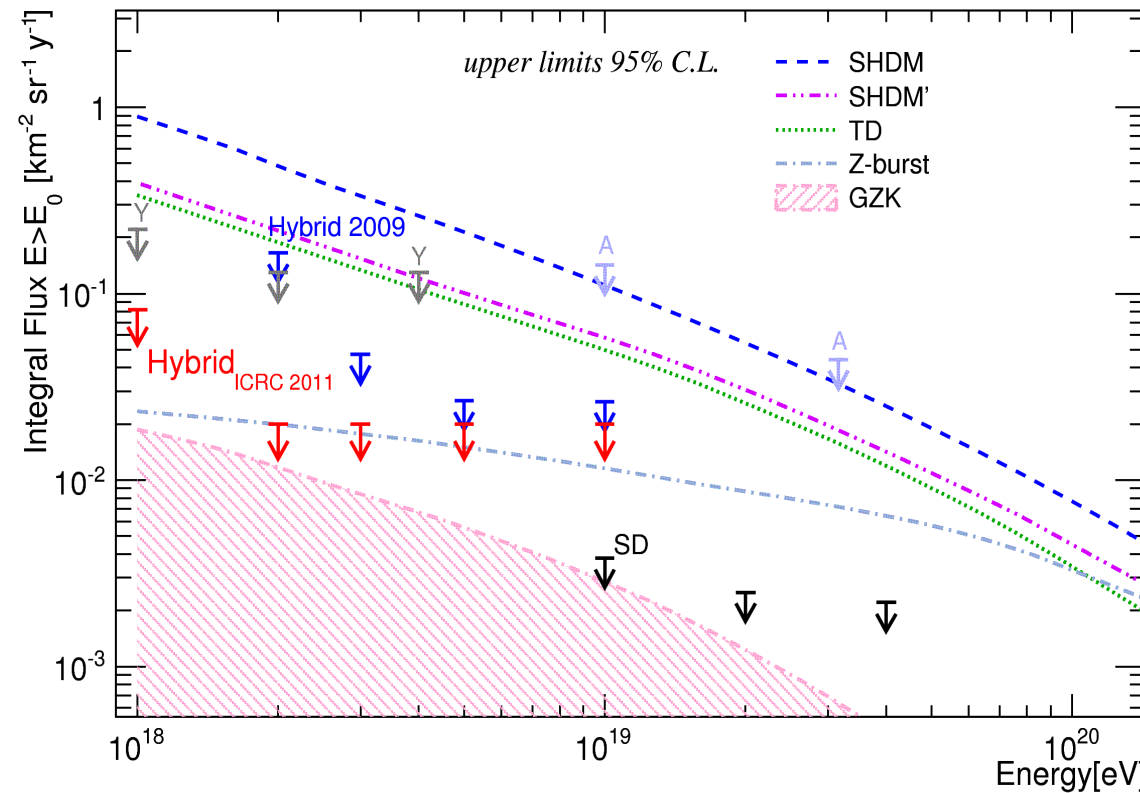
different time structure and smaller
signal (from SD)

Hybrid Exposure for photons



Upper limit to the integral photon flux

M. Settimi @ ICRC 2011



Upper limits to the integral photon fraction assuming the Auger Spectrum

0.4%, 0.5%, 1.0%, 2.6% and 8.9% for $E > 1, 2, 3, 5$ and 10 EeV

Number of candidates
6, 0, 0, 0, and 0 for $E > 1, 2, 3, 5$ and 10 EeV

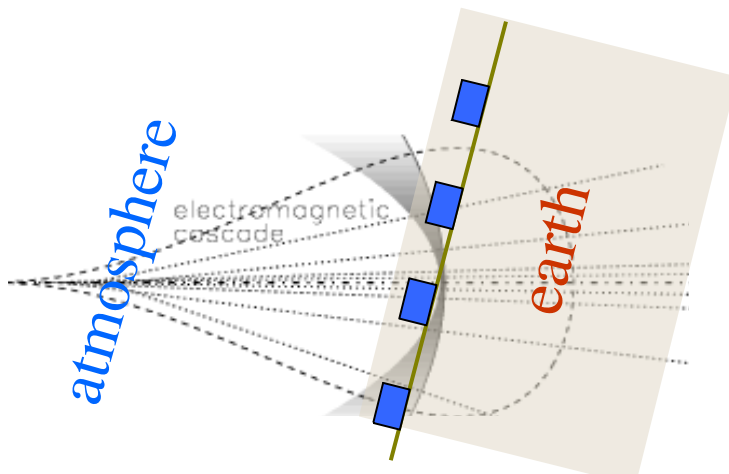
flux and fraction upper limits
down to the EeV region

**top-down models
severely constrained**

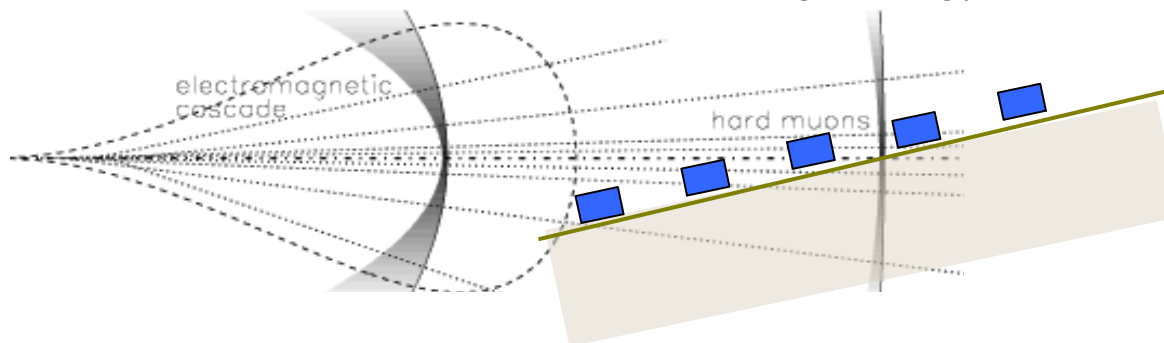
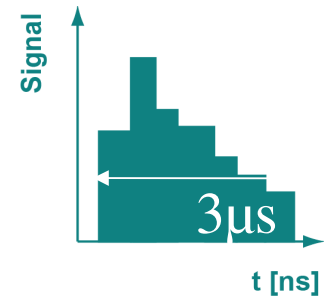
- favour astrophysical origin of UHECR
- reduce systematics in measurements of energy spectrum, p-air cross section, mass composition

**GZK region within reach
in the next years**

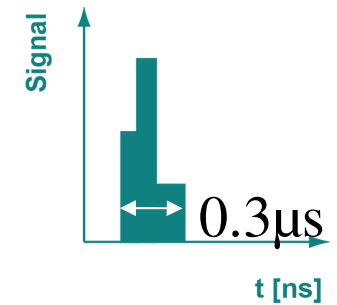
Search for neutrinos



Almost vertical
muons + electromagnetic



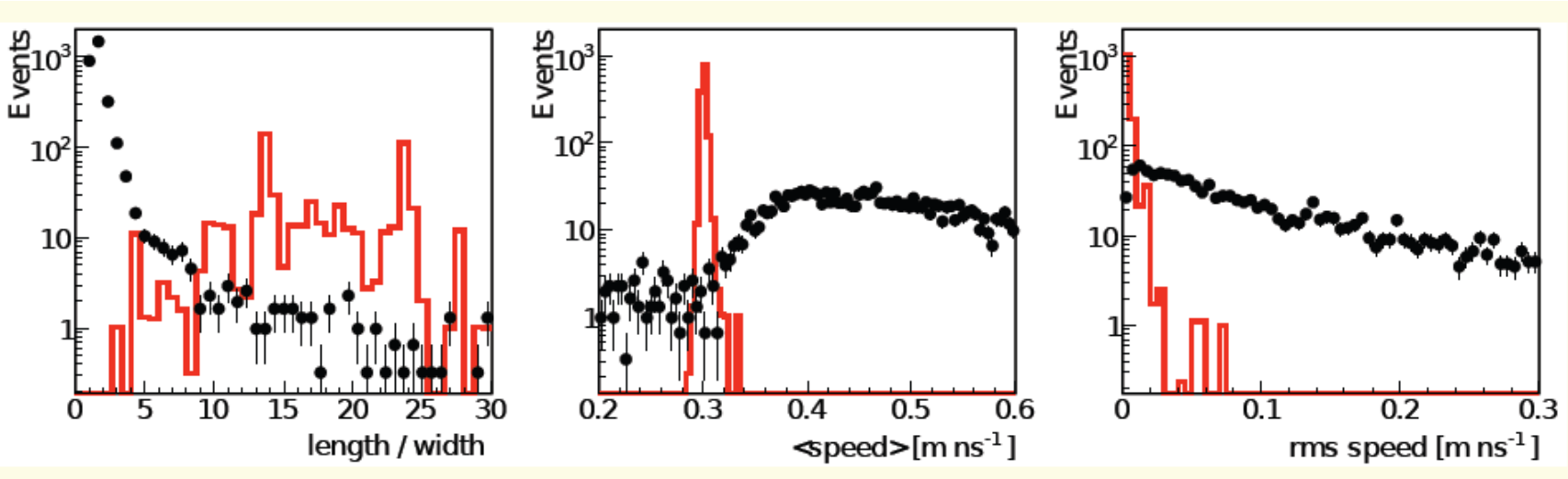
Very inclined, thin flat front
high energy muons



Important for neutrino detection: observable only if almost horizontal

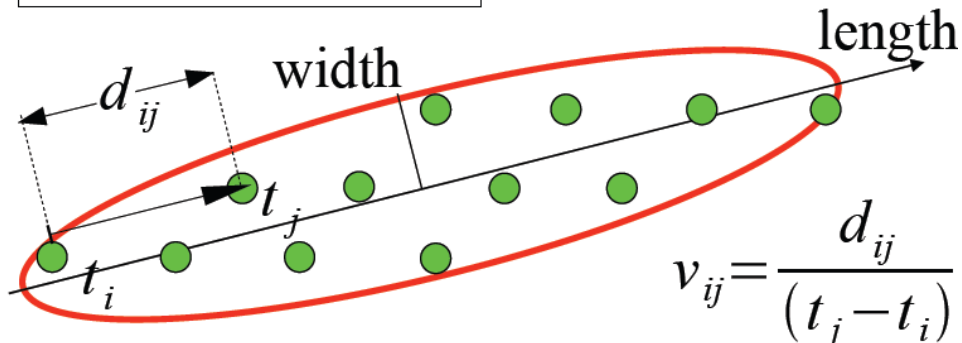
Neutrino signature: an inclined shower with large electromagnetic component

Neutrino-like event selection



Data

Inclined Showers



Simulated
neutrino signal

Earth-skimming

Length/width > 5

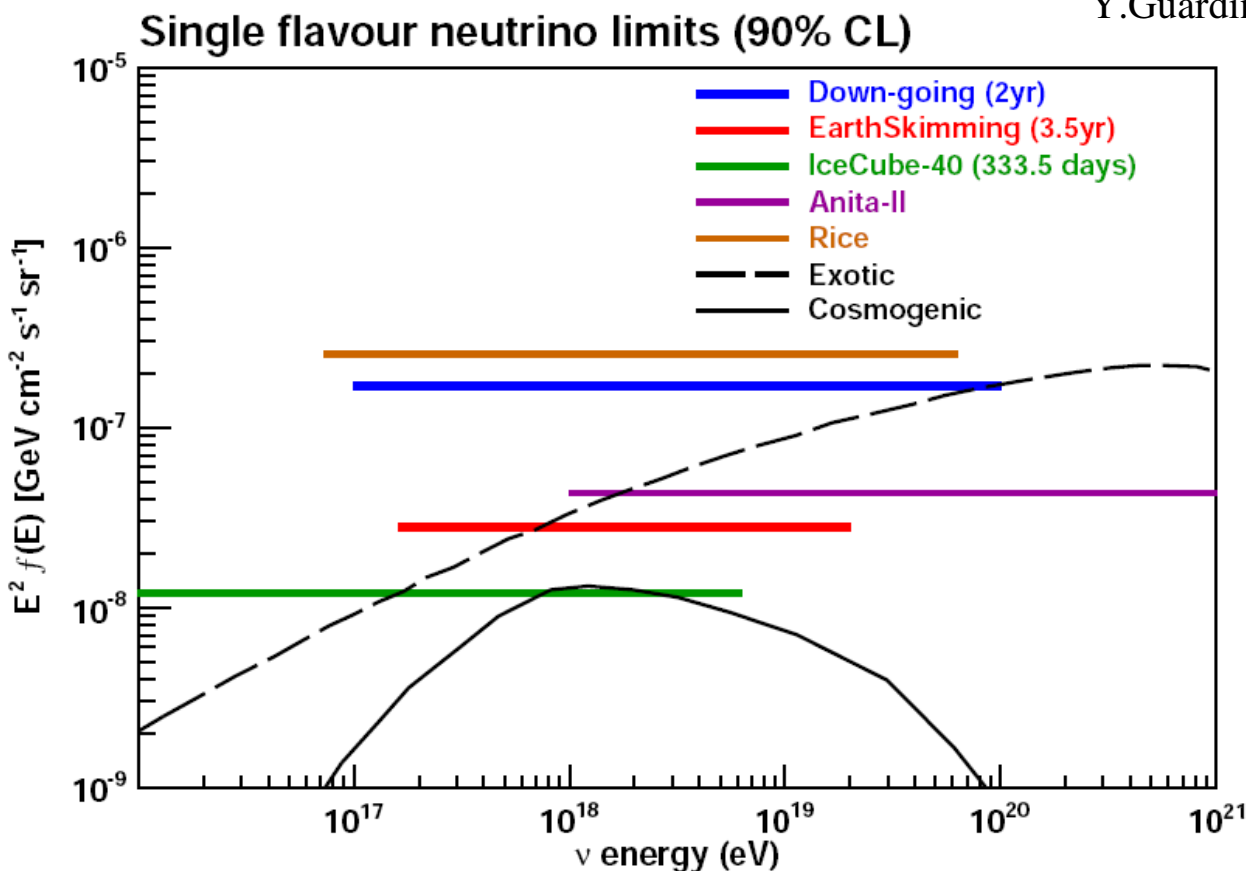
0.29 < speed < 0.31 m/ns

rms < 0.08 m/ns

Similar selection rules for down-going

Upper limit on the diffuse neutrino flux

Y.Guardincerri @ ICRC 2011



$k < 2.8 \times 10^{-8} \text{ GeV cm}^{-2} \text{s}^{-1} \text{sr}^{-1}$ in $1.6 \times 10^{17} \text{ eV} < E < 2.0 \times 10^{19} \text{ eV}$

$k < 1.7 \times 10^{-7} \text{ GeV cm}^{-2} \text{s}^{-1} \text{sr}^{-1}$ in $1 \times 10^{17} \text{ eV} < E < 1 \times 10^{20} \text{ eV}$

Enhancements and future plans

Extension towards the lower energies

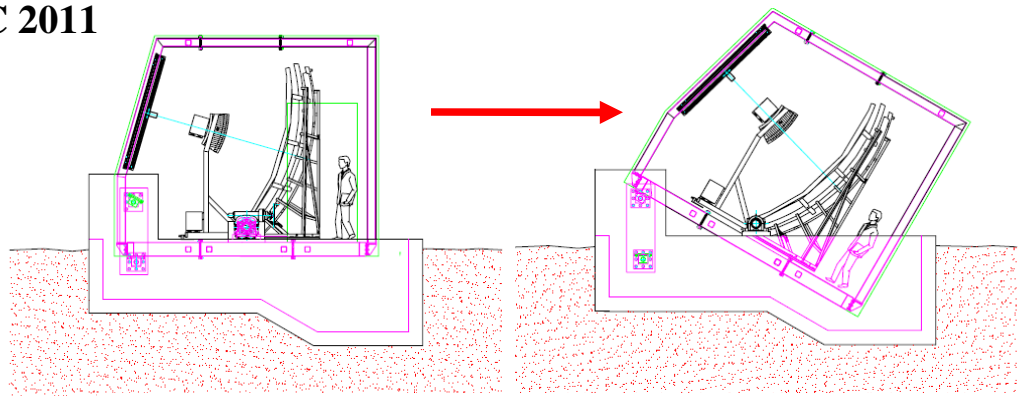
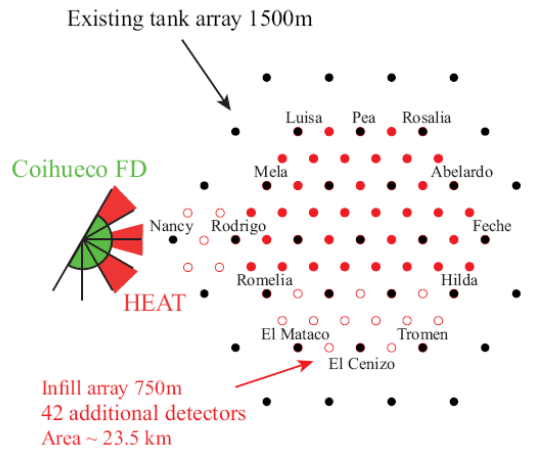
- improve detector performance at the transition to extragalactic component between $\sim 10^{17}$ and 10^{18} eV (HEAT and AMIGA)
- cross calibration with other experiments

The Pierre Auger Observatory as an ideal site to test and develop new detection techniques

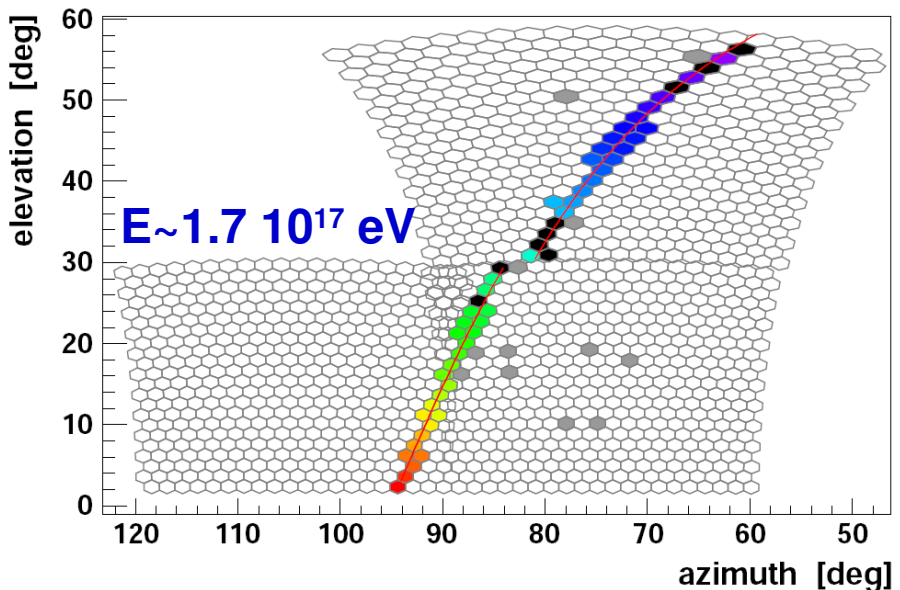
- Radio detection (AERA)
- Microwave detection (several projects)

FD Auger enhancement: HEAT

H-J Mathes @ ICRC 2011



3 telescopes nearby Coihueco
30° up to 60° elevation

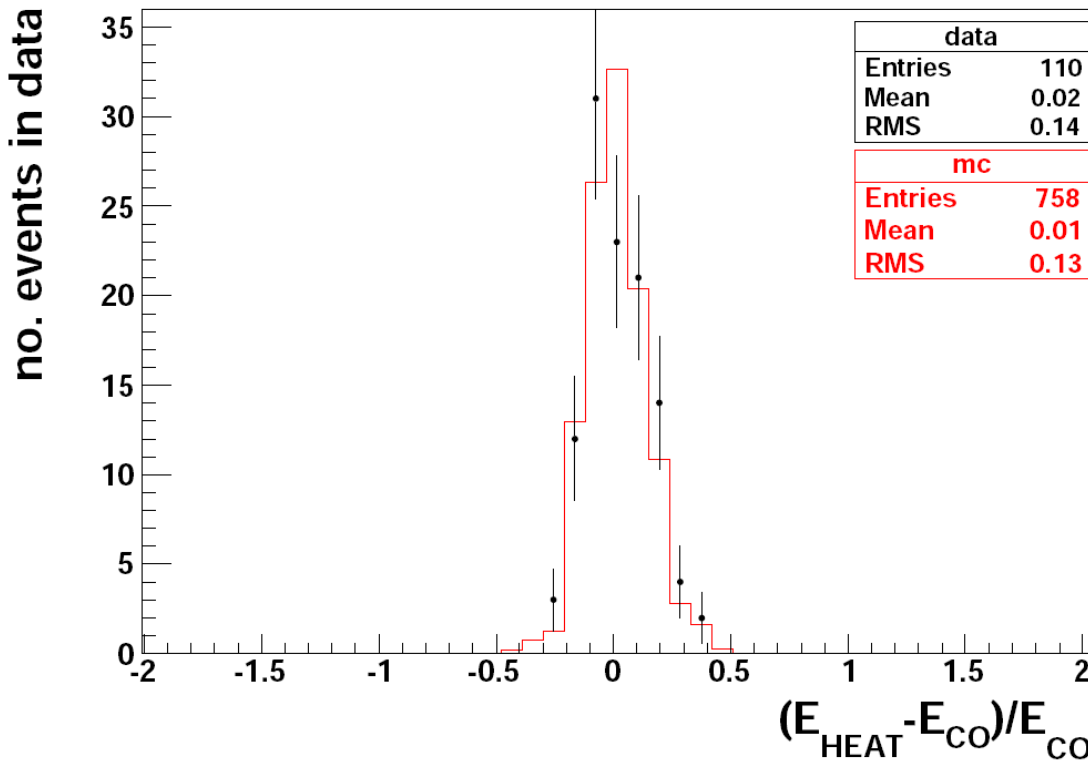


Higher elevation

lower energies ($\sim 10^{17}$ eV) unbiased observation of longitudinal profile

Taking data since Sept. 2009

First data used for alignment and calibration



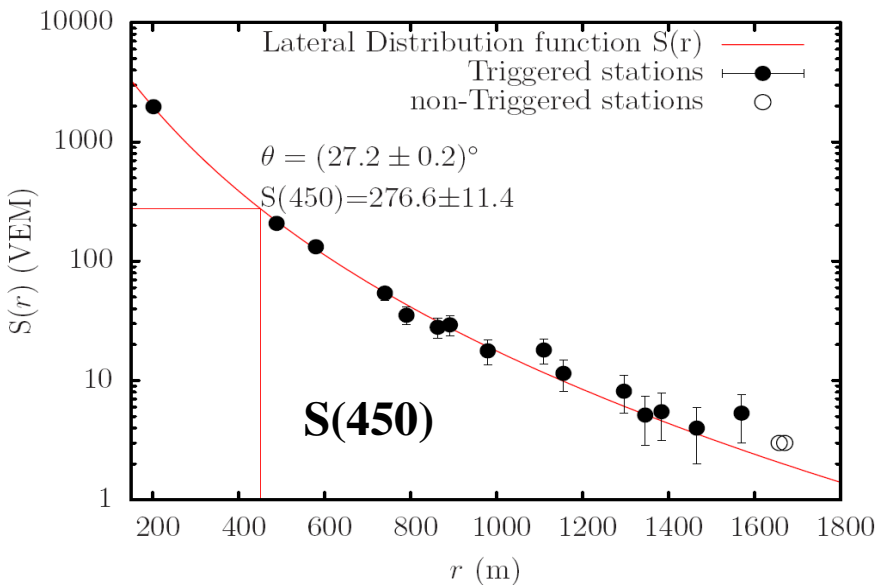
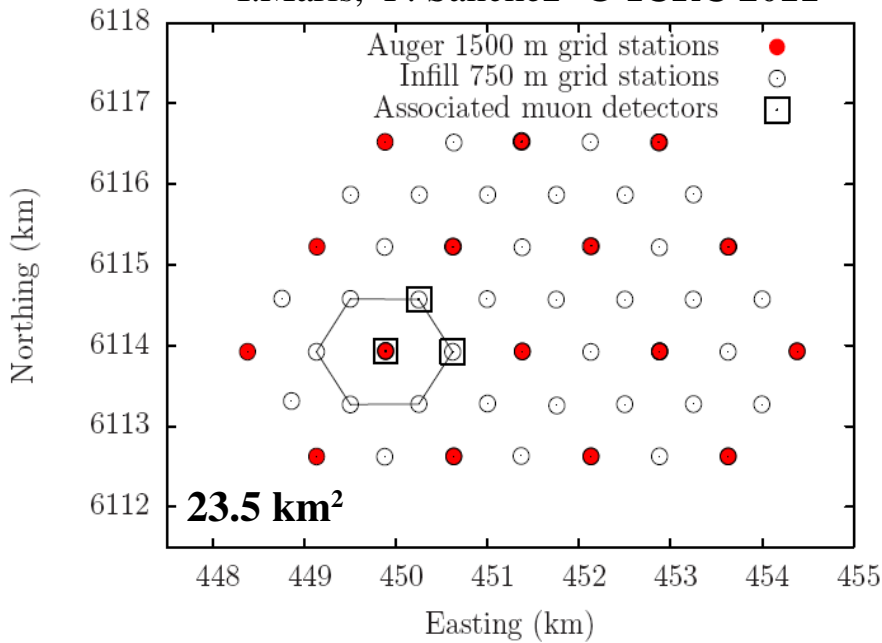
Energy reconstruction

- cross-calibration of HEAT (working in downward mode) and Coihueco
- agreement with simulations

Plenty of new high-quality data are being collected

SD Auger enhancement: AMIGA

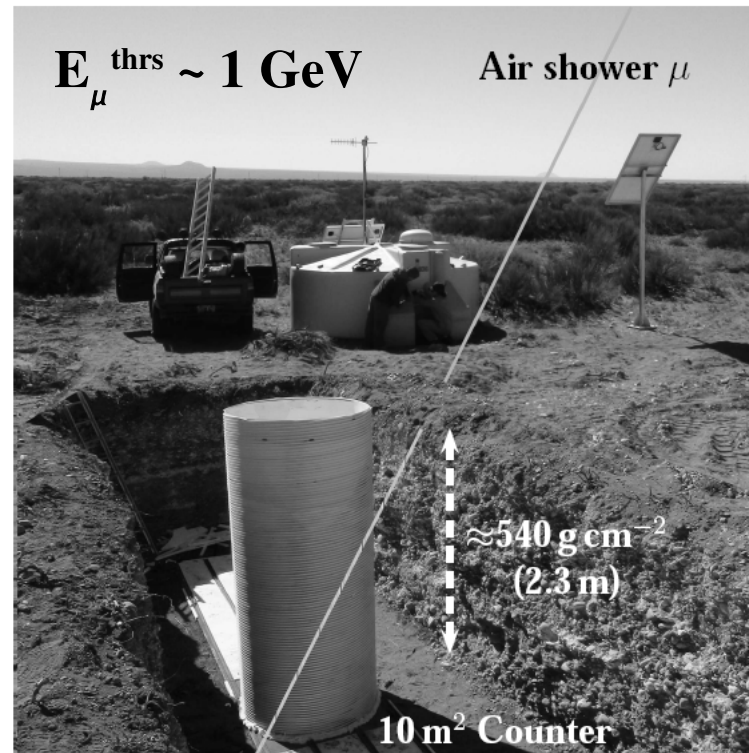
I.Maris, F.Sanchez @ ICRC 2011



INFILL array (Cherenkov stations) and Muon detectors (scintillators)

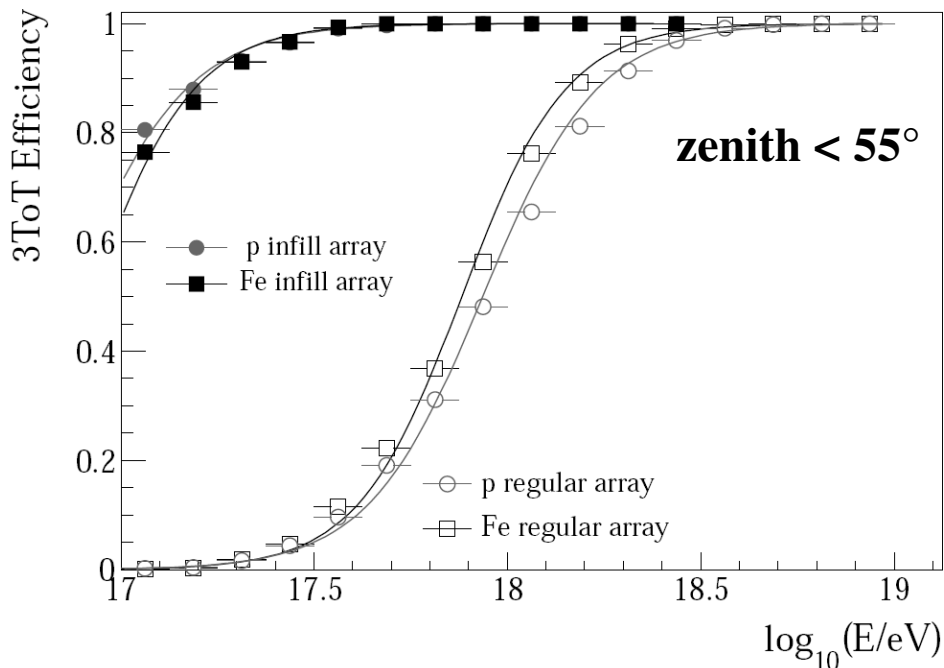
- 53 station with spacing 750 m deployed
- 4 buried scintillator modules installed

Exposure: $(26.4 \pm 1.3) \text{ km}^2 \text{ sr yr}$



700 (20, 4) events/ month $E > 10^{17.5} (18, 18.5) \text{ eV}$

Infill array performance



$S(450)$ → particle density at 450 m
- S_{35} corrected for the zenith angle dependence
- 22% (13%) uncertainty at 3 (10)VEM

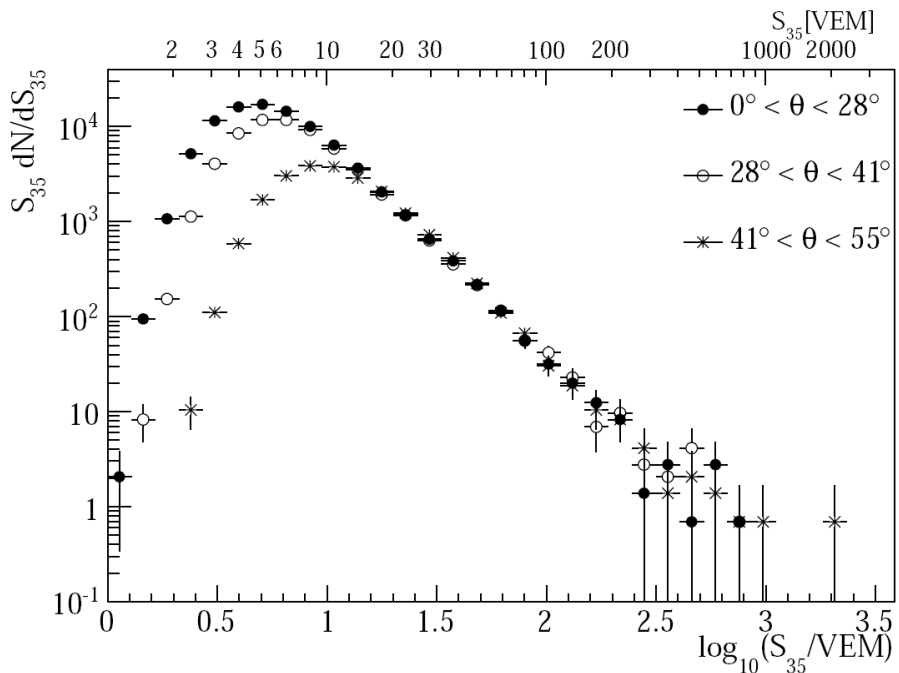
Imminent result:
the energy spectrum down to $3 \cdot 10^{17}$ eV

Full Efficiency above $3 \cdot 10^{17}$ eV

Angular resolution

1.3° for at least four stations
1° for at least six stations

About 200.000 fiducial events collected

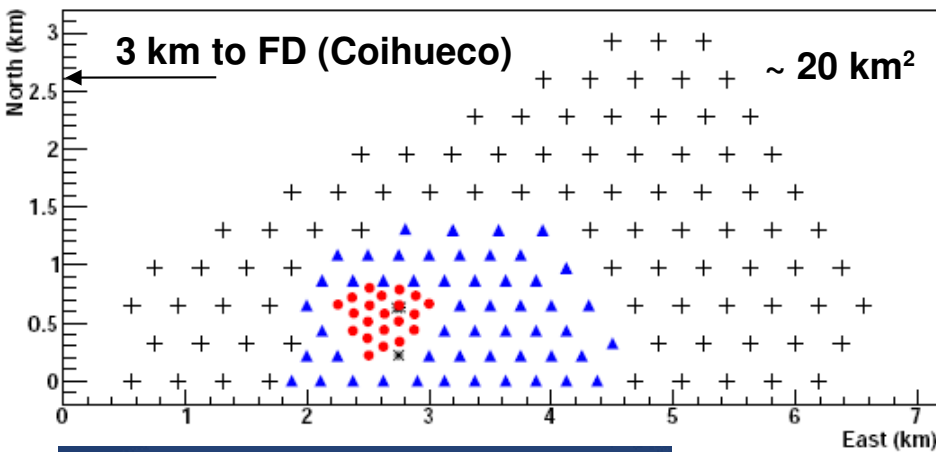


AERA: Radio detection

B. Revenu, J.L Kelley @ ICRC 2011

Observation of radio emission from electromagnetic cascade

- geomagnetic field
- charge separation



VHF band 10-100 MHz

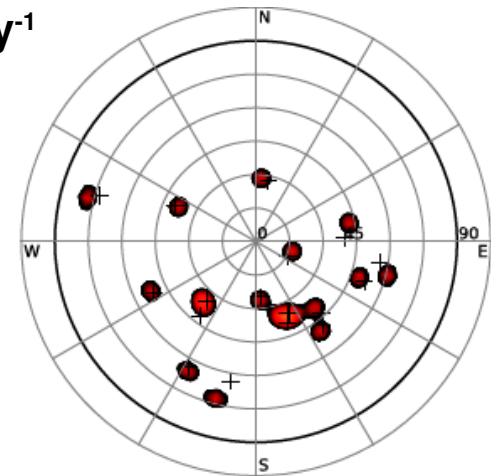
Deployed in 2010 (21 Radio stations, 150m)
stage 2 (250 m)
stage 3 (350 m)

First physical radio-hybrid events

Radio/SD 0.5 day⁻¹

$$E_{\text{thres}} \sim 10^{17} \text{ eV}$$

Logarithmic
periodic dipole
antenna (two
polarizations)



Polar plot, SD and radio reconstruction

First Radio/FD/SD super hybrid event observed

Microwave detection

Observation of microwave emission from electromagnetic cascade

Molecular Bremsstrahlung isotropic emission

Signal $\propto N_e^2$ quadratic scaling

Signal $\propto N_e$ linear scaling

P. Gorham et al., Phys. Rev. D, 2008, 78: 032007

~100% duty cycle – negligible atmospheric absorption

P. S Allison @ ICRC 2011

Radiometers in coincidence with SD



2.4 m off-axis parabola
C Band: 3.4 - 4.2 GHz
ku band: 10.95 14.5 GHz
Total FoV 7°x 7°
First test at Hawaii, then shipped to Argentina
Collecting first data



GhZ Antenna
C Band: 3.4 - 4.2 GHz
Total FoV 60° to zenith
First test at Paris, then shipped to Argentina
Collecting first data

Self-trigger same logic as FD

Observation of the longitudinal profile

4.5 parabolic reflector with a 53 pixel camera
Total FoV 20°x 10°
C Band: 3.4 - 4.2 GHz
Data collected at Chicago, then shipped to Argentina



$E_{\text{thrs}} \sim 2 \cdot 10^{18} \text{ eV}$ (quadratic scaling)
 $E_{\text{thrs}} \sim 1 \cdot 10^{19} \text{ eV}$ (linear scaling)

All operating (or very close to) at the Auger Site

Summary of results

Spectrum	<ul style="list-style-type: none">- flux suppression established ($E > 4 \cdot 10^{19}$ eV)- ankle observed at about $4 \cdot 10^{18}$ eV
Composition	<ul style="list-style-type: none">- mixed scenario: light dominated at low energies, heavier with increasing energy (interpretation is model dependent)
Hadronic interactions	<ul style="list-style-type: none">- first measurement at $\sqrt{s} = 57$ TeV
Arrival directions	<ul style="list-style-type: none">- the degree of correlation with VCV catalog has decreased- definitive conclusions must await additional data
Photons and neutrinos	<ul style="list-style-type: none">- flux photon limits above 1 EeV (top-down model disfavored)- updated limits on the diffuse flux

Outlook and future

The Pierre Auger Observatory takes data smoothly since 2004

- construction completed in 2008

Extensions towards the lower energies (HEAT and AMIGA)
ready to deliver new measurements -> ICRC 2011

- study the transition from galactic to extragalactic CR component
- allow cross-calibration with other experiments

The Pierre Auger Observatory for new detection techniques

Radio detection (AERA), radio hybrid events collected

Microwave detection, several detectors being installed

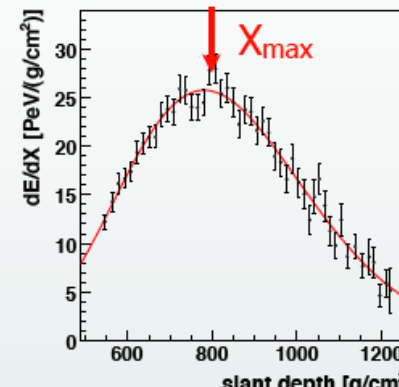
“In order to make further progress, particularly in the field of cosmic rays, it will be necessary to apply all our resources and apparatus simultaneously and side-by-side.”

V.H.Hess, Nobel Lecture, December 1936

Back-up slides

From the Fluorescence Detector:

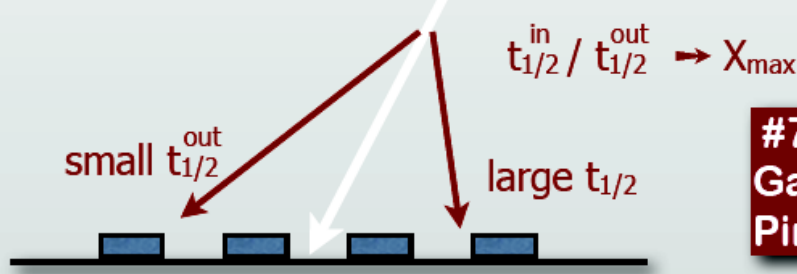
- $\langle X_{\max} \rangle$
- full X_{\max} -distribution
- RMS(X_{\max})



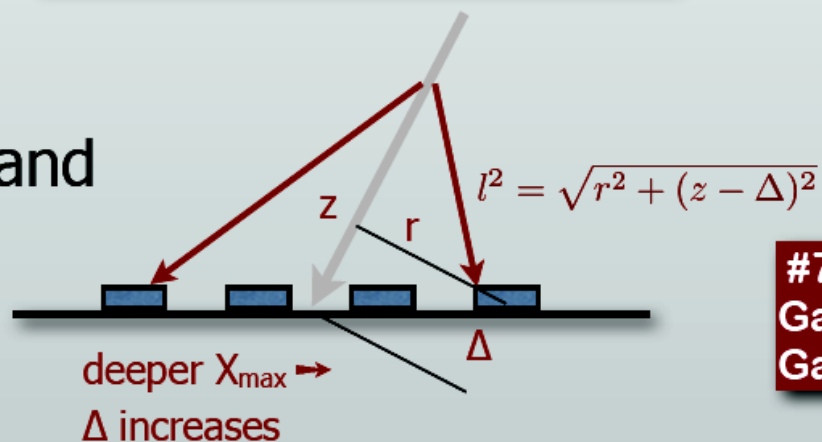
#725:
Facal

From the Surface Detector:

- azimuthal asymmetry of the signal risetime: Θ_{\max}
- time difference between μ and shower plane $\rightarrow \langle X_{\max}^{\mu} \rangle$



#709:
Garcia
Pinto



#735:
Garcia
Gamez

Anisotropy at the highest energy

Data Set

01/01/2004 –

31/08/2007

27 high energy events

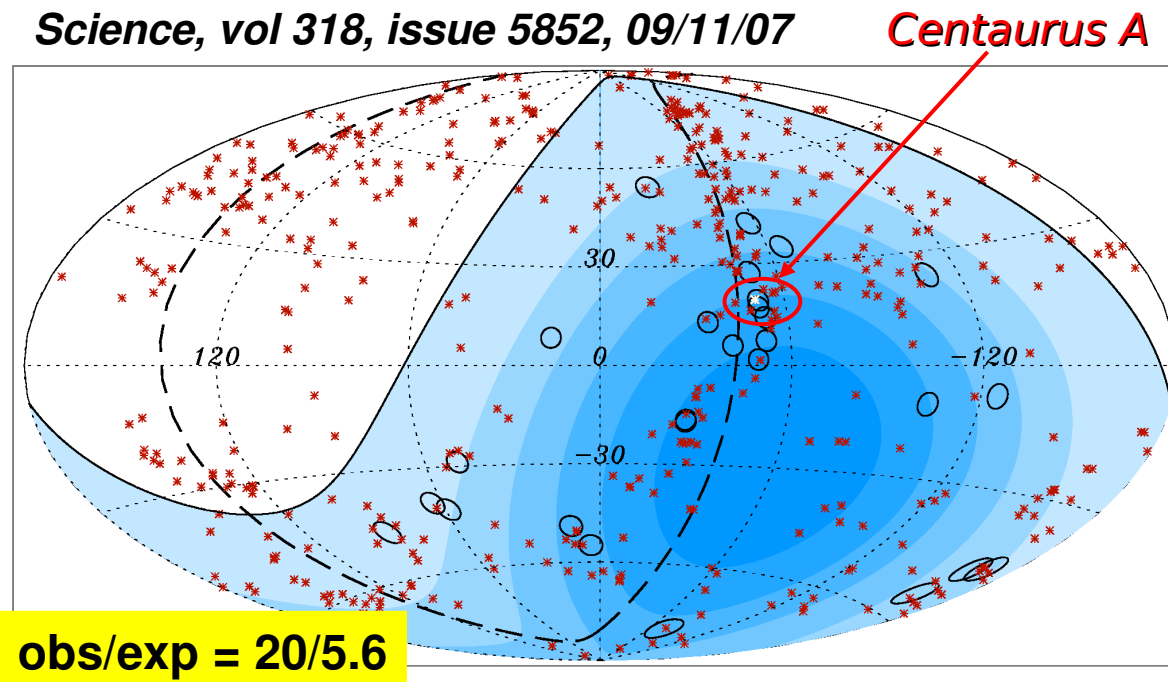
E>57 EeV

Angular radius of 3.1°

Dmax=75 Mpc

Taking as reference the catalog by Véron-Cetty and Véron (2006)

20/27 events correlate with nearby AGN



○ events with $E > 57$ EeV, angular radius $\psi = 3.1^\circ$,
✖ 472 AGN within $D_{max} = 75$ Mpc (318 in the Auger FOV)

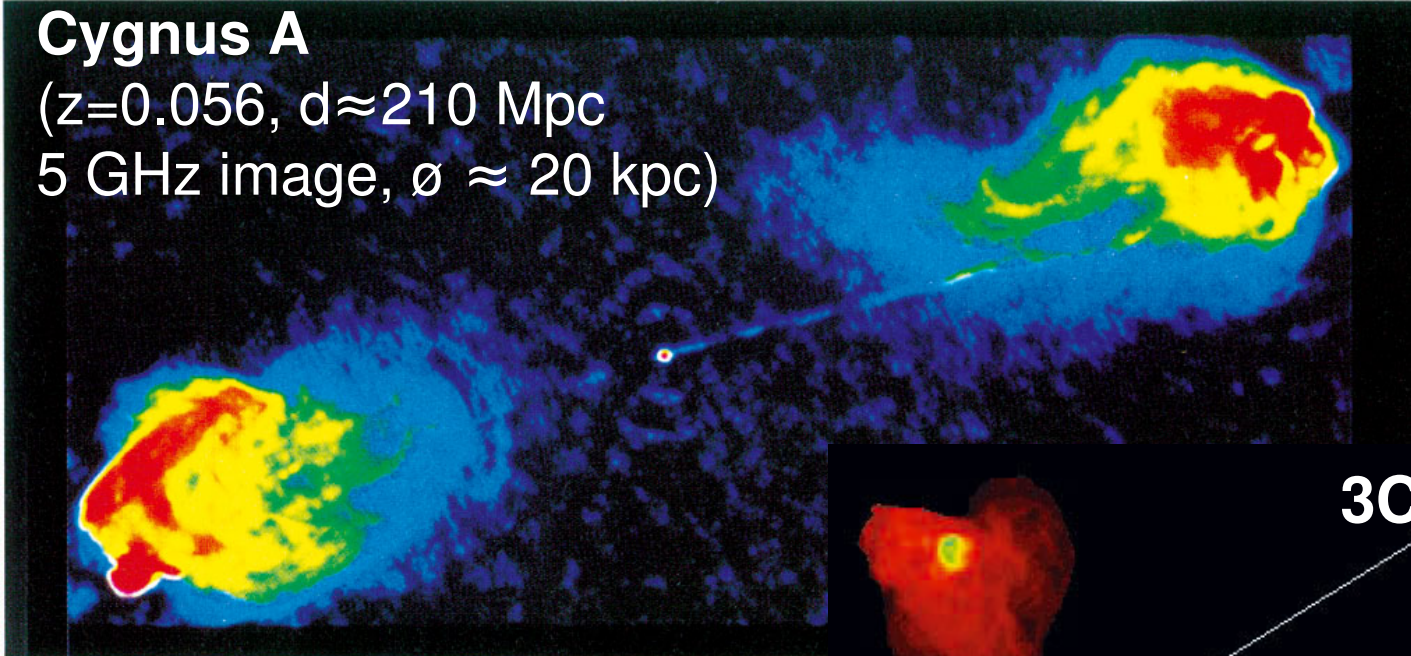
Isotropic chance probability < 1%

Limitations of the catalogue: incomplete and inhomogeneous

Cosmic Rays: astrophysical sources

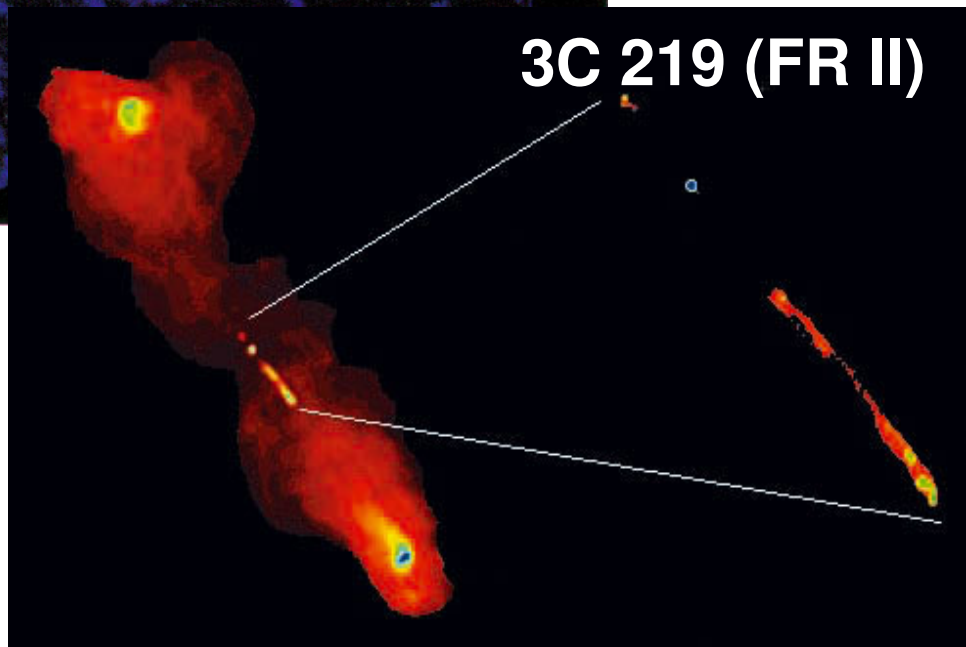
Cygnus A

($z=0.056$, $d \approx 210$ Mpc
5 GHz image, $\phi \approx 20$ kpc)

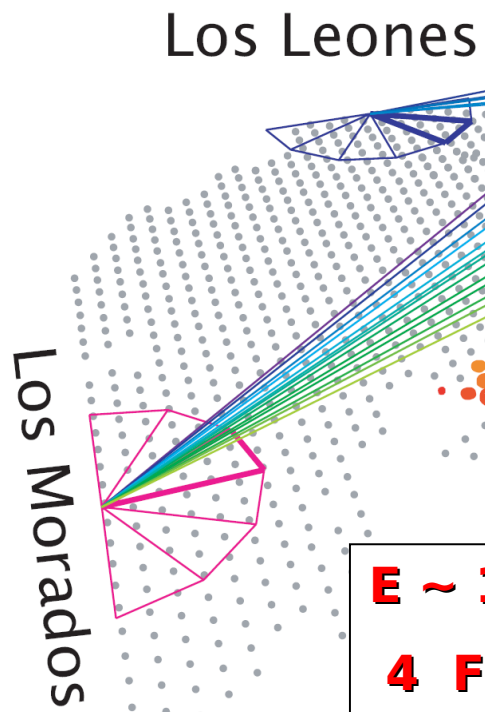
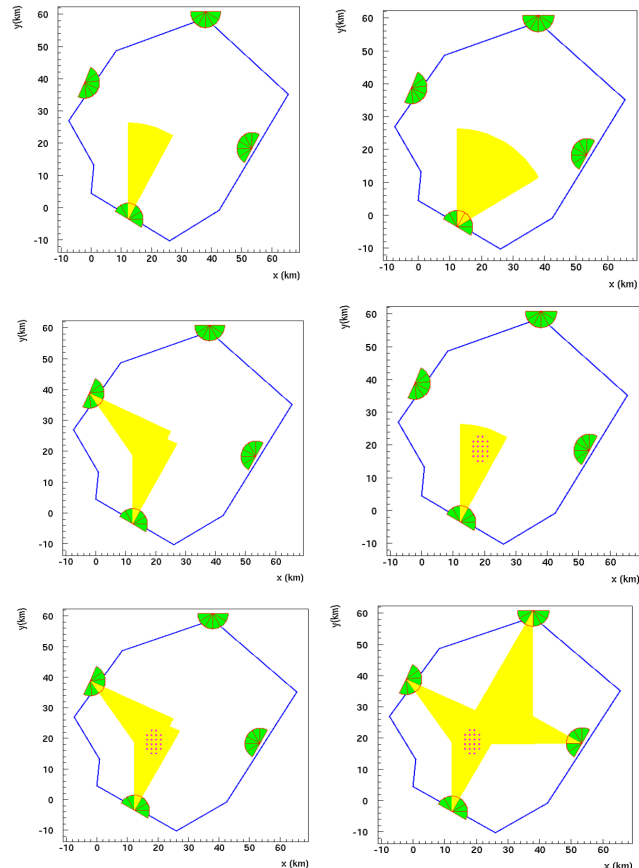


AGN radio-lobes:
(Rachen&Biermann, 1993)
AGN Jets:
(Norman et al., 1995)

3C 219 (FR II)



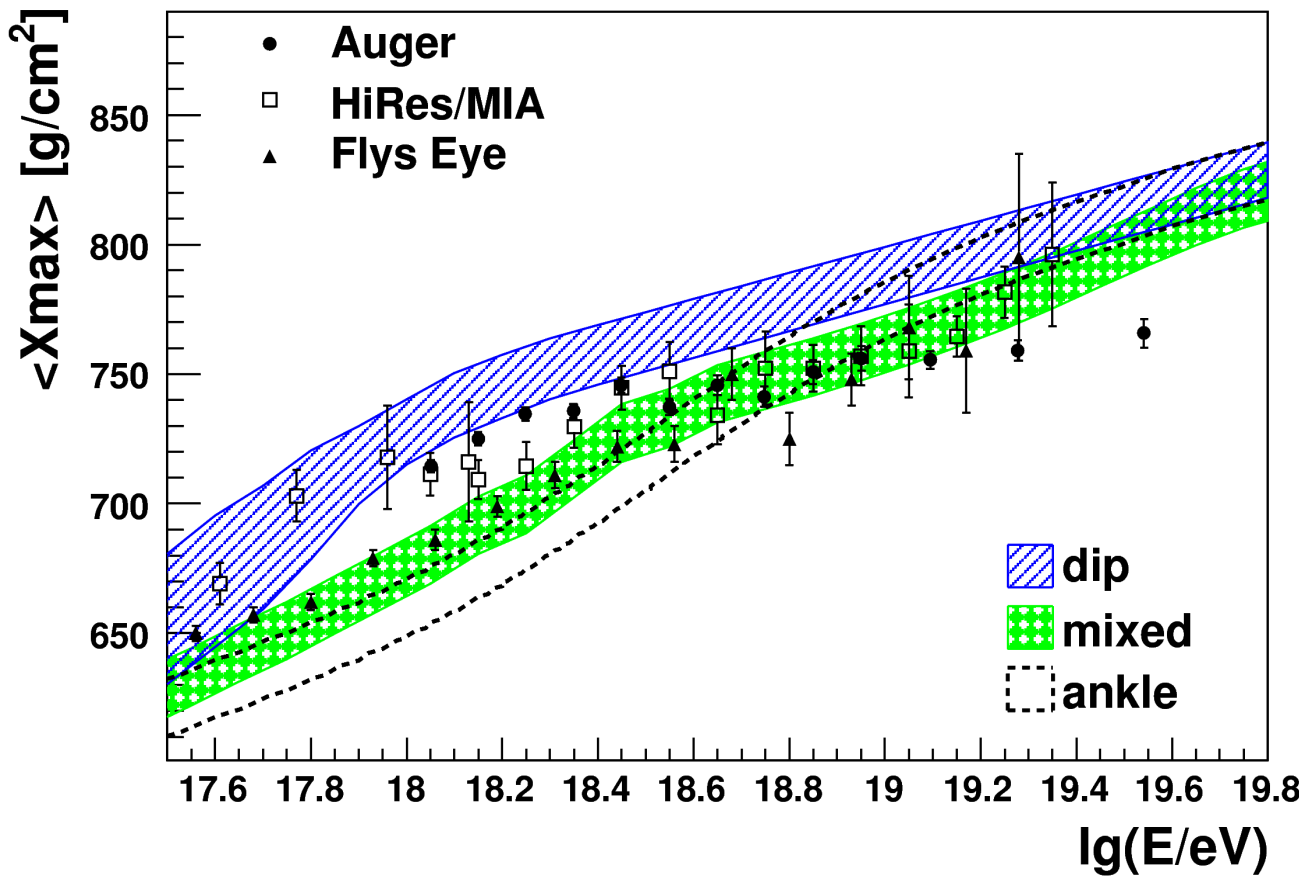
Event topologies



$E \sim 10^{19}$ eV
4 FD eyes
15 stations

~ 50 km

Data compared to models

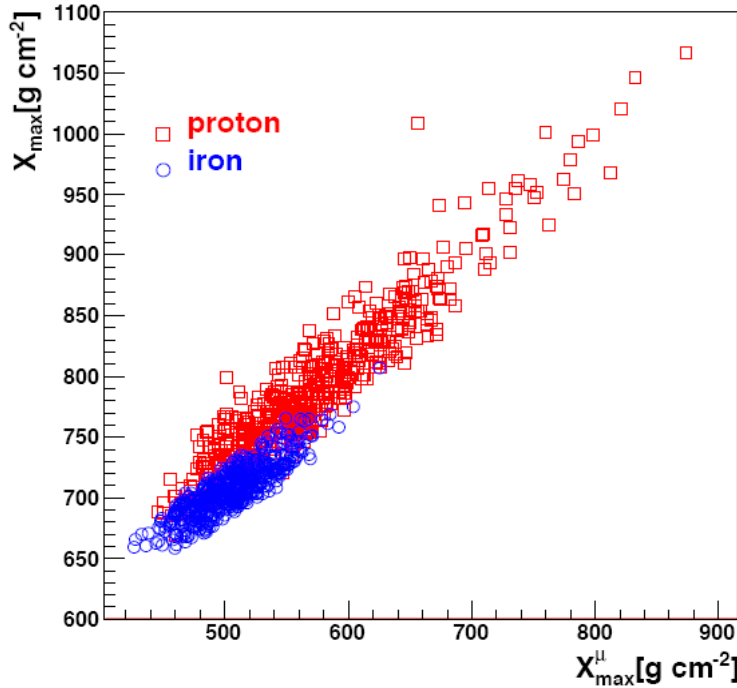


Courtesy of Michal Unger

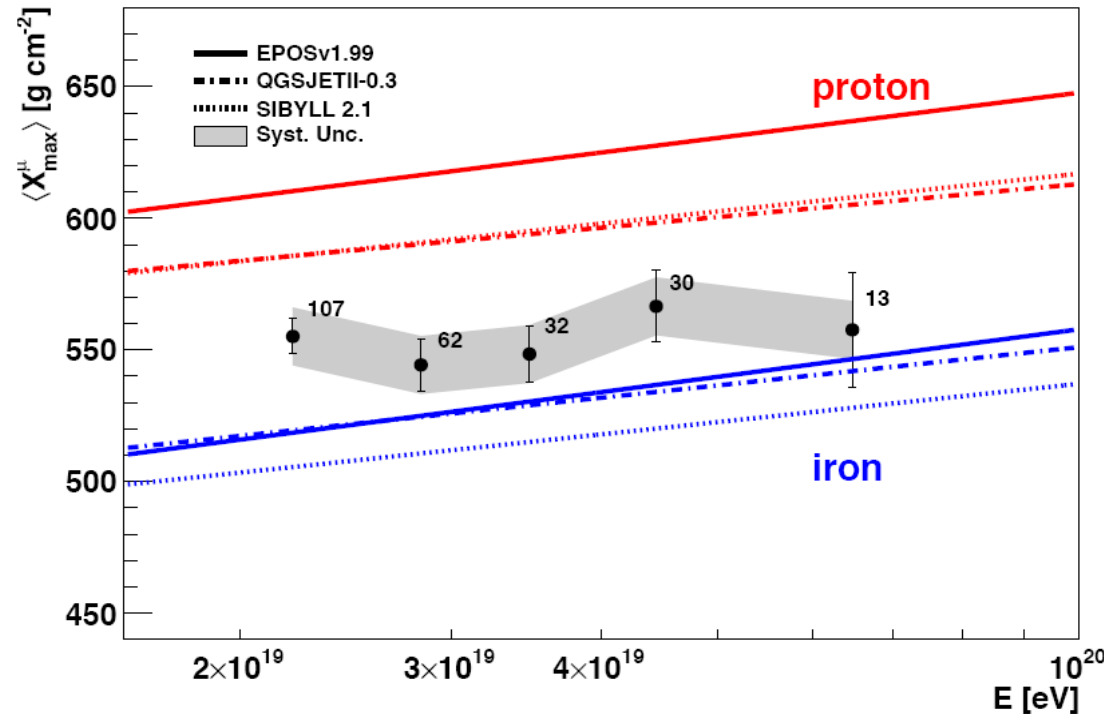
none of the model satisfactorily explains data yet (shape, absolute value)
→ constraints by studying X_{\max} distribution (known syst. unc.)

Mass Composition: X_{\max}^{μ}

X_{\max}^{μ} vs X_{\max}



$\langle X_{\max}^{\mu} \rangle$ vs E

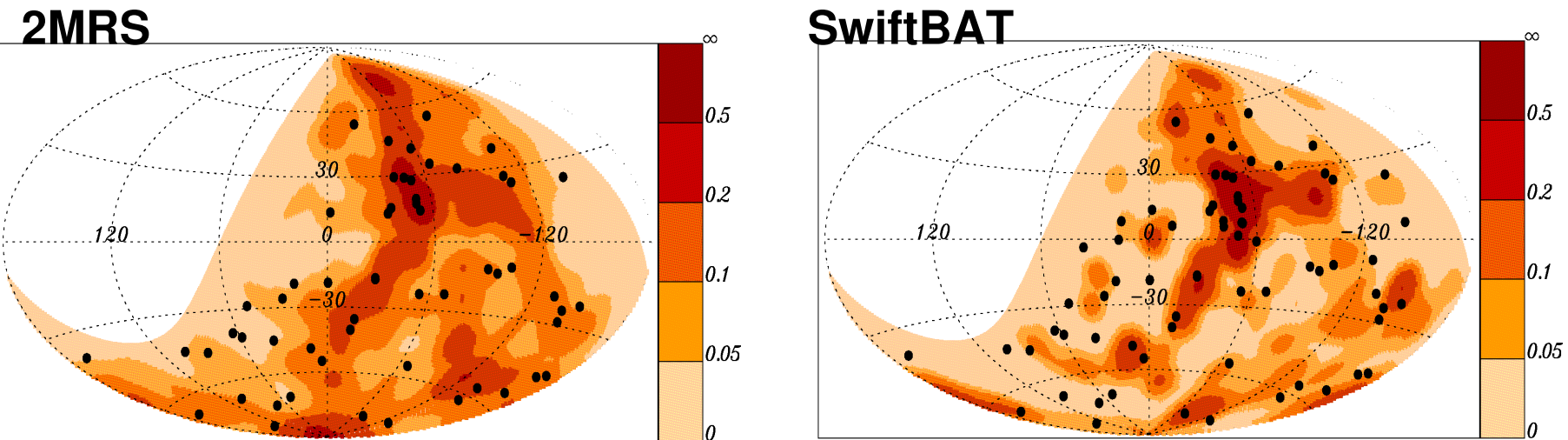


- MC hybrid events
- Correlation with X_{\max}

- 244 SD events (Jan 2004 – Dec 2010)
- $E > 20$ EeV $55^\circ < \theta < 65^\circ$

A posteriori searches

Astropart. Phys. 34 (2010) 314



5 σ detection requires more data (165 for $P=6 \times 10^{-7}$)
→ tests on other catalogues: 2MRS (IR) & SwiftBAT (X-rays)

Not only muons hit the tank!!!!



**Bird droppings
together with dry
weather degrade
solar panels.**



**Bird nests behind
solar panels
sometimes catch
fire.**